UNIVERSITI TEKNOLOGI MARA

PARAMETERS SCREENING AND KINETIC STUDY OF AMOXICILLIN BIODEGRADATION BY *ASPERGILLUS TAMARII*

MUHAMMAD ZAFRI BIN ZAMRI

MSc

June 2026

UNIVERSITI TEKNOLOGI MARA

PARAMETERS SCREENING AND KINETIC STUDY OF AMOXICILLIN BIODEGRADATION BY *ASPERGILLUS TAMARII*

MUHAMMAD ZAFRI BIN ZAMRI

Thesis submitted in fulfilment
of the requirements for the degree of
Master of Science
(Molecular Biology)

Faculty of Applied Sciences

June 2026

CONFIRMATION BY PANEL OF EXAMINERS

I certify that a Panel of Examiners has met on the 7th November 2025 to conduct the final examination of Muhammad Zafri Bin Zamri on his Master of Science thesis entitled "Parameters Screening and Kinetic Study of Amoxicillin Biodegradation by *Aspergillus tamarii*" in accordance with Universiti Teknologi MARA Act 1976 (Akta 173). The Panel of Examiners recommends that the student be awarded the relevant degree. The Panel of Examiners were as follows:

Hamizah Mohd Zaki, PhD
Associate Professor
Faculty of Applied Sciences
Universiti Teknologi MARA
(Chairman)

Wan Razarinah Wan Abdul Razak, PhD
Associate Professor
Faculty of Applied Sciences
Universiti Teknologi MARA
(Internal Examiner)

Kamarul Zaman Zarkasi, PhD
Senior Lecturer
School of Biological Sciences
Universiti Sains Malaysia
(External Examiner)

PROFESSOR DR HJH ZURAEDA IBRAHIM
Dean
Institute of Postgraduates Studies
Universiti Teknologi MARA
Date: 11 June 2026

AUTHOR'S DECLARATION

I declare that the work in this thesis was carried out in accordance with the regulations of Universiti Teknologi MARA. It is original and is the results of my own work, unless otherwise indicated or acknowledged as referenced work. This thesis has not been submitted to any other academic institution or non-academic institution for any degree or qualification.

I, hereby, acknowledge that I have been supplied with the Academic Rules and Regulations for Postgraduate, Universiti Teknologi MARA, regulating the conduct of my study and research.

Name of Student	:	Muhammad Zafri Bin Zamri
Student I.D. No.	:	2022726817
Programme	:	Master of Science (Molecular Biology) – AS753
Faculty	:	Applied Sciences
Thesis Title	:	Parameters Screening And Kinetic Study Of Amoxicillin Biodegradation By *Aspergillus tamarii*
Signature of Student	:	
Date	:	June 2026

ABSTRACT

Amoxicillin (AMX) is a semisynthetic β-lactam antibiotic classified known as aminopenicillin due to an extra amine group. It is commonly used against bacterial infections in both humans and animals. However, AMX is abused and is consumed in large amounts globally. A significant amount of amoxicillin residue in water bodies is difficult to remove and will negatively affect the environment by increasing the bacterial resistance towards amoxicillin. This will simultaneously harm the aquatic ecosystem in the environment due to the genotoxic effect of AMX residues. Other existing methods are costly, may have fouling problems, are too complex in real field operations and consume a high amount of energy causing the technology inaccessible to developing countries. Biodegradation is a studied method which is low risk, low cost, environmentally friendly and easy to control. The fungus, *Aspergillus tamarii* was observed in a previous study to exhibit degradation ability against AMX in submerged fermentation. This study screened the significant parameters: initial pH, agitation speed, incubation time, and inoculum level using the fractional factorial with a 2^{4-1} design, with the percentage amoxicillin biodegradation (AMX%) as a response. It was discovered that the main effects including incubation time , initial pH , agitation speed and inoculum size were found to be significant ($p < 0.05$) to the biodegradation process. Using the significant parameters obtained, the process achieved maximal biodegradation of 81.18 ± 2.5% (mean±SD). Using the parameters obtained, this study also evaluates the fermentation profiles and kinetics of *A. tamarii* with the presence and absence of AMX in shake flasks. Results showed that AMX presence had minimal impact on *A. tamarii*'s growth, glucose consumption and protein production. Kinetic models demonstrated strong agreement between simulated and experimental data. Further experiments were conducted in a stirred tank reactor (STR) at 250, 500 and 770 rpm impeller speeds to investigate its large scale potential. Among the tested speeds, 770 rpm showed the highest efficiency, yielding the lowest residual glucose concentration (3.94 g/L) and the highest protein production (0.071 g/L). AMX degradation data fitted well with the second-order polynomial regression model, with high R^2 values at 250 rpm (0.98) and 770 rpm (0.94). In conclusion, the significant conditions were successfully screened, and the process was enhanced using fractional factorial design (FFD) with live fungal biomass for amoxicillin biodegradation. *A. tamarii* exhibits potential degradation abilities against pollutants like AMX, as the antibiotic did not affect its metabolism according to the kinetic studies. Upscaling processes is complicated, thus requiring stringent control of operational parameters to ensure efficient and predictable biodegradation.

ACKNOWLEDGEMENT

I would like to express my heartfelt gratitude to my parents and siblings for their unwavering support, encouragement, and belief in me throughout my masters' journey. I am also deeply thankful to my supervisors, Associate Professor Dr Zaidah Zainal Ariffin and Dr Muhammad Naziz Saat, for their invaluable guidance, expertise and mentorship, not to mention, assuring me in times of worry. These were instrumental in the successful completion of this journey. Their support has been a cornerstone to my academic and personal growth. Therefore, I am forever grateful. I would also like to thank the laboratory assistants at the Faculty of Applied Sciences who sincerely helped to ease my lab work, their generosity and kindness will not be forgotten. My appreciation also goes to my postgraduate friends who shared for only a semester with me due to different mode of study, helped to make the laboratory lively with both laughters and serious discussions that made the experience meaningful. I am also very thankful to my partner who were there for me, to motivate and help me face every problems and struggles throughout the journey. Lastly, I am thankful to Allah SWT for granting me the resilience, perseverance and strength to witness this journey until the end. Alhamdulillah.

TABLE OF CONTENTS

LIST OF TABLES

LIST OF FIGURES

LIST OF SYMBOLS

Symbols

%	Percentage
˚C	Degree Celsius
CFU	Colony-forming Unit
cm	Centimeter
g	Gram
L	Litre
M	Molar
mg	Milligram
mL	Millimeter
m_s	Maintenance Coefficient
nm	Nanometers
P	Protein Concentration
ppm	Parts per Million
rpm	Revolutions per Minute
S	Glucose Concentration
t	Time
v/v	Volume Over Volume
X	Biomass Concentration
Y_G	Biomass Yield Coefficient Over a Substrate
α	Alpha
β	Beta
µL	Microlitre

LIST OF ABBREVIATIONS

Abbreviations

ACN	Acetonitrile
AMX	Amoxicillin
AMX%	Amoxicillin Biodegradation Percentage
ANOVA	Analysis of Variance
CCD	Central Composite Design
DMSO	Dimethyl Sulfoxide
DNA	Deoxyribonucleic Acid
DNS	3,5-Dinitrosalicylic Acid
FFD	Fractional Factorial Design
HPLC	High-Performance Liquid Chromatography
LLE	Liquid-Liquid Extraction
LMPOs	Lytic Polysaccharide Monooxygenases
MLP	Modified Leudeking-Piret
MnP2	Manganese Peroxidase
PDA	Potato Dextrose Agar
PDB	Potato Dextrose Broth
PTFE	Polytetrafluoroethylene
SD	Sabouraud Dextrose
SPE	Solid Phase Extraction
STR	Stirred-Tank Reactor
UTI	Urinary Tract Infection

CHAPTER 1
INTRODUCTION

1.1 Background of Study

β-lactam antibiotics such as carbapenems, penicillin and cephalosporins are one of the most widely consumed antibiotics globally. Approximately 200,000 tons of antibiotics are consumed annually and 50-70% are categorized under β-lactams (Li *et al.*, 2022). This class of antibiotics is characterized by the presence of β-lactam ring which demonstrated antimicrobial activity when consumed at appropriate concentrations, however causes side effects to allergic patients (Shaw, 2015; Fu *et al.*, 2017). Amoxicillin is derived from semisynthetic penicillin and is known as aminopenicillin due to an extra amine group (Papich, 2013). This antibiotic is commonly used to treat various bacterial infections in humans and several in animals such as sheep, goats, cattle, dogs and cats. It was found that β-lactams antibiotics are potent against Gram-positive and Gram-negative microorganisms by inhibiting the synthesis of the bacterial cell wall (İstifli & Topaktaş, 2010; de Sousa *et al.*, 2019). According to Papich (2016), AMX has been used for a wide range of infections in all species including urinary tract infections (UTI), pneumonia and soft tissue infections. However, most Gram-negative bacilli of the Enterobacteriaceae are usually resistant to the antibiotic, so it is suggested that frequent consumption of AMX for treatment is required.

Amoxicillin was chosen for this study as it is the most consumed antibiotic by humans and animals. According to Sodhi *et al.* (2021), amoxicillin consumption is higher than that of other antibiotics, which are in the range of 750-2250 mg/day. Due to the low metabolic degradation rate, most antibiotic molecules are secreted into the environment. The residues were discovered in different water bodies worldwide, including Italy, the UK, Australia and Spain (Elizalde Velazquez *et al.*, 2016). Moreover, most of the countries in the Asian region have reported that manufacturing factories discharge a huge amount of antibiotics into water systems (Bielen *et al.*, 2017). The excessive discharge of antibiotics in the environment has contributed to the

destruction of the natural aquatic ecosystem due to the increase of bacterial resistance towards antibiotics. The evolution of bacteria to gain antibiotic-resistant genes is induced by antibiotic residues in water bodies and is detrimental not only to the aquatic ecosystem but also to human health (Verma & Haritash, 2020). For example, Chowdhury *et al.* (2020) found that the amoxicillin residues were harmful to zebrafish genetically by damaging and breaking the DNA which disrupted the development of embryos. The evidence above proves that a large amount of amoxicillin residues in the environment is a major problem. Sustainable and effective degradation of the residues must be developed to solve these issues.

Biodegradation is defined as the disintegration or breakdown of materials by biological process, including the use of microorganisms using an organic substance as their carbon and energy source. Microorganisms such as fungi play an important role in the environment by treating water and soil, in addition to food and agricultural products preservation (Poznyak *et al.*, 2019). Fungi have been demonstrated in previous research to effectively degrade concerned pollutants, including dyes, pharmaceutical compounds, oil and hydrocarbons (Kamaruddin *et al.*, 2022; Zain ul Arifeen *et al.*, 2022; Ademakinwa *et al.*, 2025; Fayyaz *et al.*, 2025). Several fungal species have also been explored for their ability to degrade AMX. However, research on *A. tamarii*'s potential remains limited (Mohammadi *et al.*, 2021; Cai *et al.*, 2023). In this study, a fungus *Aspergillus tamarii* is chosen due to its significant potential. A previous study has reported that *A. tamarii* isolate 58 is capable of degrading AMX by 49.0% in 96 hours using suboptimized conditions (Abd Hamid *et al.*, 2023). For decades, this fungus has been well-known for various human infections such as eyelid infection, wound infection, nasal polyposis and invasive nasosinusal aspergillosis. Despite that, *A. tamarii* can be utilised in the food and fermentation industries (Ferreira *et al.*, 1999; Homa *et al.*, 2019).

1.2 Problem Statement

The abuse of amoxicillin usage occurs all over the world from various sources such as pharmaceutical factories, animal husbandry and human consumption (Rodriguez-Mozaz et al., 2020, as cited in, Pratiwi & Baihaqi, 2024). The concentration of AMX detected in surface water samples worldwide ranges from 7.81 ngL^{-1} in Malaysia to 13300 ngL^{-1} in Nigeria (Praveena *et al.*, 2018; Ebele *et al.*, 2020). Nearly

95% of that amoxicillin is difficult to degrade (Wahyuni *et al.*, 2024). As a result, it could harm the environment by producing antibiotic-resistant bacteria and cause carcinogenic and genotoxic effects on both humans and animals. If not treated, then the damage would be irreversible. Other existing methods such as advanced oxidation process, coagulation, and membrane separation are high cost, may have fouling problems, are too complex in real field operations, and have high energy consumption. In addition, the technology may not be easily accessible to developing countries. Therefore, we resort to biodegradation which is low risk, low cost, environmentally friendly and easy to control. However, there is a lack of studies on utilising *A. tamarii* to biodegrade pollutants like amoxicillin and how it performs when exposed to the pollutant despite its potential in biodegradation based on a previous study. The conventional method of using trial and error method to screen significant parameters that influence the degradation process is costly and time-consuming. A large number of experiments would be produced from this method. Fractional factorial design is utilized to screen the significant parameters efficiently with less experimental runs compared to conventional method. Furthermore, improving the AMX biodegradation requires a clear and accurate representation through kinetic behavior. The absence of kinetic model limits the ability to analyze system performance which translates into identifying and predicting growth-product relationships and biodegradation trends. Applying suitable kinetic models such as Verhulst-Pearl logistic growth model and Leudeking-Piret model for protein production may provide a better understanding of these processes, in addition to improve the ability to predict the bioprocesses whether in shake flask or bioreactor.

1.3 Significance of Study

This research investigates the significant parameters affecting amoxicillin degradation by *A. tamarii*. since the conditions diverge and differ between various organisms and enzymes, screening the parameters affecting the response should be investigated. Proving its biodegrading ability might even open up possibilities to degrade other pollutants. Furthermore, utilizing the kinetic modelling to study the fungal biomass weight, glucose utilization and protein production of cultures with and without amoxicillin will allow evaluation of the fungus's performance and predicting its successful use in biodegradation. Then, analyze the biodegradation of amoxicillin

using a stirred-tank reactor and provide foundational data that will assist in clearing up pollution in large-scale applications for future research. Biodegradation is an effective method to remove amoxicillin pollution due to its low risk, low cost, being environmentally friendly and easy to control. Since amoxicillin is manufactured and consumed worldwide, including in countries lacking technology, biodegradation by *A. tamarii* would be one of the solutions to treat this pollution. Simultaneously, studying *A. tamarii*'s potential in producing enzymes for biodegradation or commercial products.

1.4 Scope and Limitations

This study specifically focuses on the use of fractional factorial design to obtain the main conditions for amoxicillin biodegradation by *Aspergillus tamarii*. The scope of this research focuses on fungal biodegradation in a shake flask with selected biodegradation parameters to scale up the application. Then, kinetic modelling was used to investigate the biomass weight, glucose utilization and protein production. Lastly, the biodegradation of amoxicillin is further experimented in a stirred-tank bioreactor. However, due to restrictions in materials and time, the fungal biomass in a stirred-tank bioreactor was not collected. Commercial amoxicillin is utilized as a source of antibiotics for the biodegradation process.

1.5 Objectives

1. To determine selected parameters (pH, agitation speed, incubation time and inoculum size) on the percentage biodegradation of amoxicillin by *Aspergillus tamarii* using Fractional Factorial Design (FFD) in shake flask.

2. To investigate the performance of *A. tamarii* based on biomass weight, glucose utilisation and protein production using screened parameters with and without AMX in a shake flask.

3. To assess the effect of impeller speed on the percentage biodegradation of amoxicillin, glucose consumption and protein production profiles by *A. tamarii* using a stirred-tank reactor.

CHAPTER 2
LITERATURE REVIEW

2.1 Antibiotic

Antibiotic is a compound that can be utilized as an agent against microorganisms such as bacteria, fungi and protozoa. However, back in the 19th century, it was referred to as a molecule that exhibits antibacterial or bacteriostatic activity (Thakare *et al.*, 2020). Antibiotic was used way back in ancient Egypt, and they used filamentous fungi which grew on bread to treat wounds and burns. In China and Greece, healers in the Middle Ages would treat various diseases using mould (Durand *et al.*, 2019). According to Clardy *et al.* (2009), in 1941, Selman Waksman described an antibiotic as a molecule produced by a microbe that inhibits the growth of other microbes. Later from 1945 to 1955, penicillin, streptomycin, chloramphenicol and tetracycline were produced by fungi and soil bacteria leading to the antibiotic age.

Antibiotics can be grouped based on their molecular targets, function and chemical class. Compared to other medicinal areas, antibiotics target poor, resistrcted to cell membrane, protein and nucleic acid synthesis, and peptidoglycan biosynthesis which is the component of the cell wall. The cell wall of microorganisms is unique making it a high-value target for antibiotics. In addition, the structure and function of protein and nucleic acid synthesis is detailed which makes them different to animal cells, however can be similar in terms of general mechanism (Abbas *et al.*, 2024).

Vardanyan and Hruby (2016) explained that there are 7 main groups of antibiotics: β-Lactams, tetracyclines, macrolides, aminoglycosides, peptides, lincosamides and streptogramins. These antibiotics were classified based on their chemical structures as shown in Table 2.1. Most macrolide and aminoglycoside antibiotics are synthesized through traditional bio-fermentation methods, on the other hand production of sulfonamide and quinolone antibiotics by chemical synthesis (Lewis, 2020). Other antibiotics such as β-lactam and tetracycline are produced semi or even full synthesis due to advancements in medicine and molecular chemistry. Before such advancements are utilized, these antibiotics were mainly produced by bio-fermentation (El-Gamal *et al.*, 2017).

Table 2.1
Main classes of antibiotics with their unique structure and examples.

Antibiotic	Main Structure	Example
β-Lactams		Oxacillin (Bush, 2010) 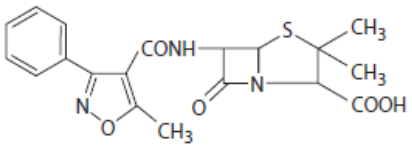
Tetracyclines	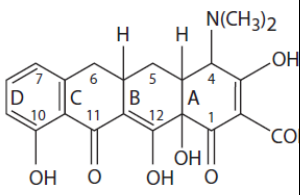	Chlortetracycline (Chopra, 2010) 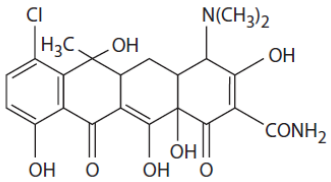
Macrolide	Macrolactone Ring (two sugars and one amino sugar attached)	Erythromycin (Bryskier, 2010) 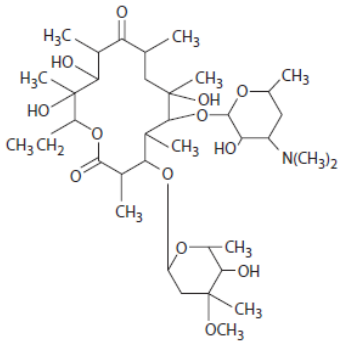
Aminoglycoside	Six-membered ring with amino group substituents (Leggett, 2017)	Streptomycin (Sharma *et al.*, 2021)

		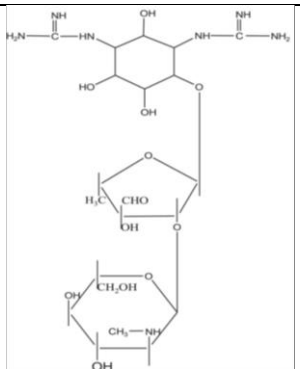
Peptide	No standard classification system yet (Vardanyan & Hruby, 2016)	
Lincosamides	Amino acid and sugar moieties are connected by an amide bond (Kwon, 2017; Spížek & Řezanka, 2017)	Lincomycin (J. Zhang *et al.*, 2020) 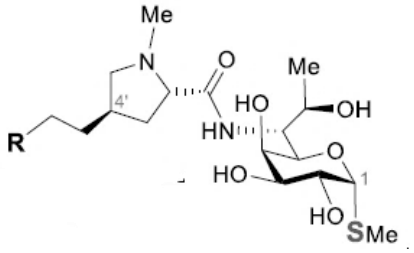
Streptogramins	A group: polyunsaturated mactolactones	Pristinamycin (Mast & Wohlleben, 2014) A type: 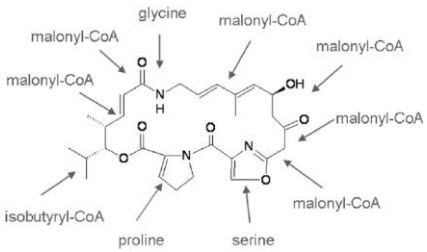

	B group: cyclic hexadepsipeptides	B type: 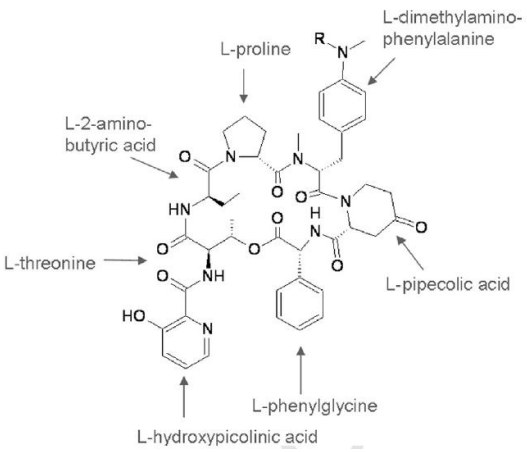

The fermentation of actinomycetes yield derivation of aminoglycoside and macrolide. Some examples include neomycin and tylosin which are synthesized by the fermentation of *Streptomyces Fradiae*, gentamicin by *Micromonospora purpurea*, and erythromycin by *Saccharopolyspora erythraea* (Dowling et al., 2025). In an effort to enhance the stability and oral bioavailability of these antibiotics, semi-synthetic approaches have become common. Clarithromycin and azithromycin, for example, are derivatives of erythromycin A, synthesized through relatively short chemical modification pathways involving four to six steps (Dinos, 2017).

Furthermore, macrolides antibiotics have given rise to ketolide derivatives in the 21st century, such as telithromycin. Figure 2.1 shows macrolide antibiotics with different number of of atoms on macrolactone ring: 14-membered, 16-membered, 23-membered and 36-membered. These are developed by replacing the cladinose sugar with a keto group, introducing fluorine atoms, or appending arylalkul-substituted carbamate chains at specific positions to enhance potency. However, their clinical use remains limited due to hepatotoxicity (Fernandes *et al.*, 2019). Fortunately, recent innovations in total chemical synthesis have now made it possible to manufacture almost all macrolide structures, although this is primarily applied in research settings rather than in large-scale production (Seiple *et al.*, 2016).

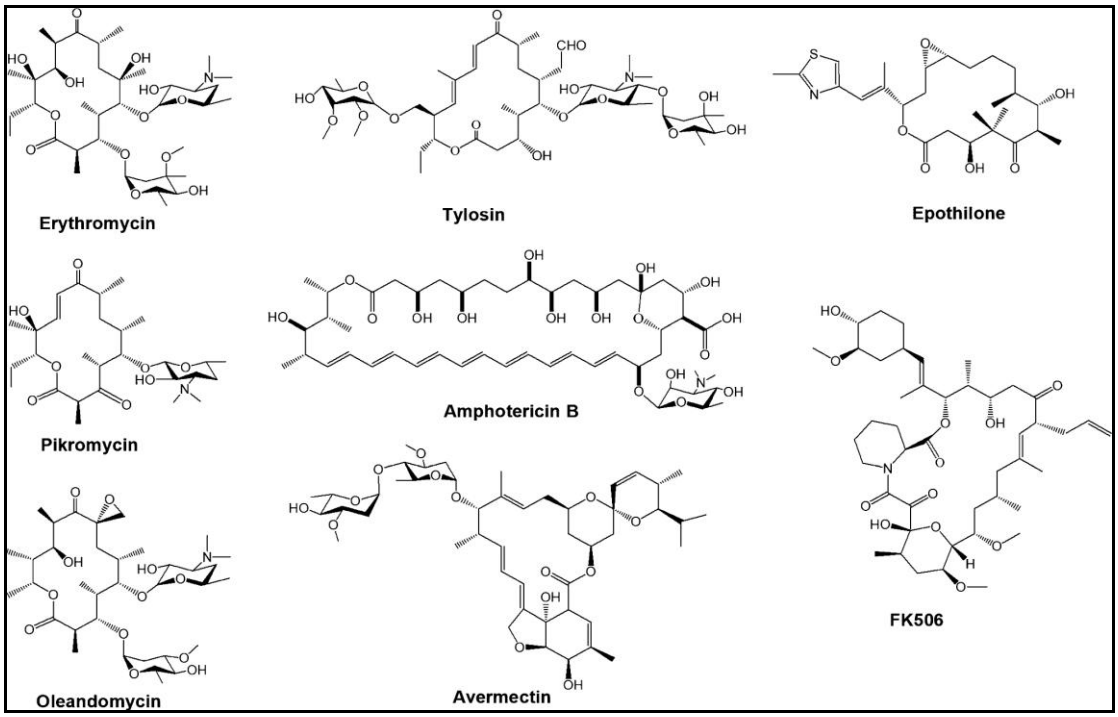

Figure 2.1: Examples of macrolides according to the number of atoms on macrolactone ring: 14-membered, 16-membered, 23-membered and 36-membered (Park *et al.*, 2010).

Sulfonamides and quinolones are entirely synthetic in origin. Sulfonamides were among the first synthetic antibiotics developed and are characterized by the common sulfonamide functional group (A-SO_2NHR). Figure 2.2 shows some examples of sulfonamide antibiotics. Their synthesis typically involves a nucleophilic reaction between amino-containing compounds and sulfonyl chlorides in the presence of a base, followed by functional group modifications (Mondal & Malakar, 2020). Quinolones, first commercialized in 1961, are based on either a 2-quinolone or 4-quinolones core structure (Kealey *et al.*, 2017). Altering these cores with various substituents enables the creation of structurally diverse antibiotics with varying antimicrobial potencies (Dhiman *et al.*, 2019).

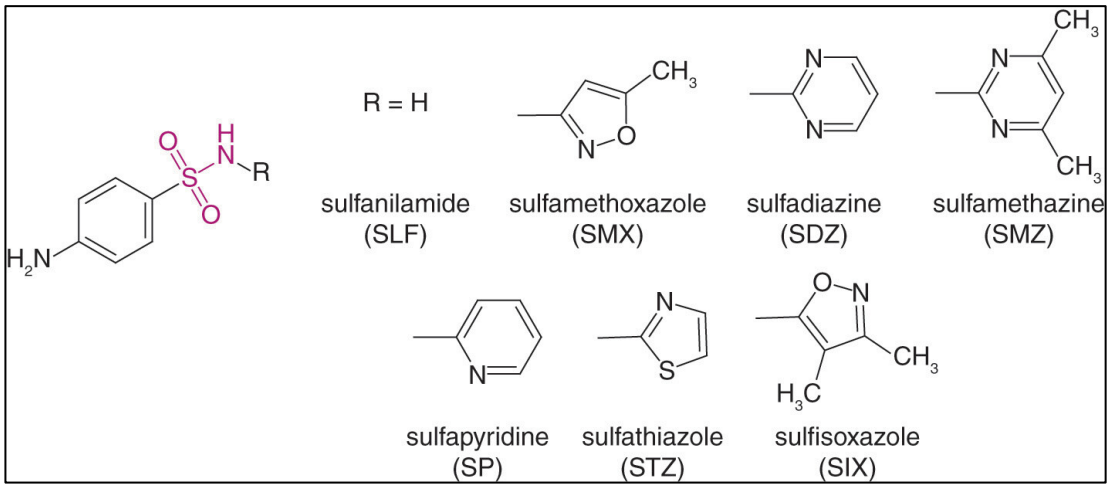

Figure 2.2: Examples of sulfonamides
(Krátký, 2024)

β-lactam antibiotics, a class to which amoxicillin belongs, are further classified into subgroups such as penicillins, carbapenems, and cephalosporins based on their structural features. While early β-lactam antibiotics like thienamycin, cephalosporin C, and penicillin were obtained through fermentation, many modern β-lactam are produced using semi-synthetic strategies. Penicillin G, for example, is chemically deacylated to produce 6-aminopenicillanic acid (6-APA) or 7-aminocephalosporanic acid (7-ACA), which serve as precursors for the synthesis of various β-lactam antibiotics via enzyme-mediated acylation with different side chains (Elander, 2003).

Tetracycline antibiotics, another important class, are biosynthesized by actinomycetes. Chemical modifications of tetracycline molecules have led to the development of numerous second and third-generation antibiotics, enhancing their spectrum and stability.

2.1.1 Antibiotic Usage in Human and Veterinary

Antibiotics are metabolic compounds produced by microorganisms that process antimicrobial properties and are capable of inhibiting the growth of other microbes. They are widely utilized in both humans and animals to prevent and treat infectious diseases and also employed in livestock industry as growth enhancers to improve weight gain in animals (Zhou *et al.*, 2013). Human exposure to antibiotics occurs through several pathways, primarily via medical treatment, but also through dermal contact, inhalation and dietary intake of contaminated food and water (Sarahroodi & Mikaili, 2012; Paul *et al.*, 2019). It was found that high concentration of antibiotics have been

detected in human urine, often exceeding 3000ng/mL for antibiotics such as tetracycline, norfloxacin, ofloxacin, and azithromycin (Wang *et al.*, 2018). This is likely due to recent therapeutic use. According to Klein *et al.* (2018), in 2015, global antibiotic consumption in humans reached approximately 34.8 billion defined daily doses (DDDs), and this figure is projected to surge to 84 billion DDDs by 2030. Furthermore, antibiotic usage in animal agriculture was reported at 63,151 tonnes in 2010 and is anticipated to increase by 67% by the year 2030 (Van Boeckel *et al.*, 2015). These unmetabolized antibiotics enter the aquatic environment through improper discarding of unused or expired medications, excretion of these antibiotics by humans and animals, discharges from agricultural fields and veterinary facilities, and wastewater treatment plants that are not facilitated to remove antibiotics (Freitas & Radis-Baptista, 2021; Cherian *et al.*, 2023). These will cause a rise in antibiotic-resistant bacteria, disruption of aquatic ecosystems and the ability to harm human health through exposure to contaminated water (Rajak *et al.*, 2025).

2.1.2 Antibiotic Production Methods

Antibiotics originate from three distinct manufacturing processes which includes fermentation, chemical synthesis and semi-synthesis. Each of these processes not only contributes to the global supply of antibiotics but also generates wastewater with distinct compositions and treatment challenges.

Fermentation remains the most widely used technique in antibiotic production due to its cost-effectiveness and simplicity. Usually, it involves cultivating microorganisms, such as Streptomyces species, under controlled conditions to biosynthesize antibiotic compounds (Mohr, 2016). During the fermentation process, large volumes of wastewater are produced, especially during stages such as biomass separation, solvent extraction, and compound purification (Xiang *et al.*, 2009). The fermenters themselves contribute the majority of wastewater volumes. This wastewater typically contains antibiotic residues, fungal mycelia, metabolic by-products, organic solvents, and remnants of the culture medium. These constituents make fermentation wastewater highly biodegradable but also prone to rapid decay and strong odors if not treated properly (Wang *et al.*, 2024).

Chemical synthesis of antibiotics involves converting organic or inorganic raw materials into pharmacologically active compounds through a series of chemical reactions. Notable examples include sulfonamides and quinolones, which are fully synthetic and produced without microbial involvement. Chemical synthesis was the earliest method used in antibiotic manufacturing, predating even the discovery of penicillin, and although partially replaced by bio-fermentation, it continues to play a pivotal role, especially with advances in molecular and synthetic biology (Durand *et al.*, 2019; Hutchings *et al.*, 2019). However, this method also causes pollution which typically originates from crystallization, rinsing, and recovery stages. Hazardous substances such as catalysts, resins, adsorbents, organic solvents, intermediates, and antibiotic by-products, would be present in the wastewater (Lukacs & Ohno, 2012).

Semi synthetic antibiotic production on the other hand, represents a hybrid of biological and chemical processes. It generally begins with fermentation to obtain precursor molecules like 6-aminopenicillanic acid (6-APA) or 7-aminocephalosporanic acid (7-ACA), which are then chemically modified to improve therapeutic activity or pharmacokinetic stability. This method is especially common in β-lactam antibiotic production, where a diverse range of penicillins and cephalosproins are created from a limited set of core structures. Such modifications are also made to prevent bacterial resistance (Segura *et al.*, 2013).

2.1.3 Artificial Intelligence in Antibiotic Discovery

The utilization of A.I is to replicate key elements of human intelligence, such as planning, reasoning, language understanding, and perception. Therefore, it offers a promising approach for tackling complex challenges like antimicrobial resistance (AMR). It includes a broad range of quantitative methods, ranging from basic models such as logistic regression to advanced approaches including deep learning and generative A.I (Howard *et al.*, 2025).

Conventional microbiology methods have clarified the fundamental mechanisms underlying bacterial dormancy and tolerance, the development of effective strategies to eliminate persister cells remains highly challenging. The incorporation of A.I and machine learning (ML) offers new approach to address this limitation. AI-based predictive models enable the interpretation of complex omics datasets to predict persister cell formation and uncover potential therapeutic targets. In antibiotic

discovery, AI-driven deep learning models including GANs and graph-based networks, enable the design and screening of novel development of precision biologics that enhance targeted immune clearance, extending beyond the capabilities of traditional antibiotics. Overall, AI-driven frameworks represent a promising shift toward more effective strategies against persistent and recurrent infections (Yakobi & Nwodo, 2025).

2.2 β-Lactam Antibiotic

Alexander Fleming was the first researcher to discover *Penicillium notatum* as an antibacterial agent. The *Staphylococcus* colonies' growth was inhibited and *P. notatum* was able to release an antibacterial compound. However, the discovery of *Penicillium* mould by Alexander Fleming in 1928, which could prevent bacterial growth in culture was not enough without being subjected to human tests. In 1941, Florey, Chain and Abraham have conducted the first study of penicillin treatment in patients and since then, penicillin has been produced on an industrial scale (Watkins & Bonomo, 2017; Lima *et al.*, 2020). According to Gidijala *et al.* (2010), the penicillin biosynthesis pathway which occurs in *A. nidulans* as shown in Figure 2.3. This process needs compartmentalization of enzymes. In the cytosol, the non-ribosomal peptide synthetase ACVS (AVCS-OH) is initiated by a dedicated PPTase into the active form ACVS-SH, which can synthesize ACV from the three precursor molecules AAA, L-cysteine and L-valine. The enzymes IPNS will then converts ACV into the β-lactam IPN. This compound is delivered into peroxisomes. In this organelle, phenoxyacetic acid (POA) is activated by PCL into phenoxyacetyl CoA (POA-CoA), and utilized by the NTN hydrolase AatA (IAT) to synthesize Penicillin V. Penicillin V subsequently transported from the organelle and ultimately secreted to extracellular environment. Traditionally, the production of β-Lactam is done by fermentation, in which the biological activities of the microorganism are artificially controlled, and then the intermediate products are separated and purified to produce crystalline products (Hu *et al.*, 2022).

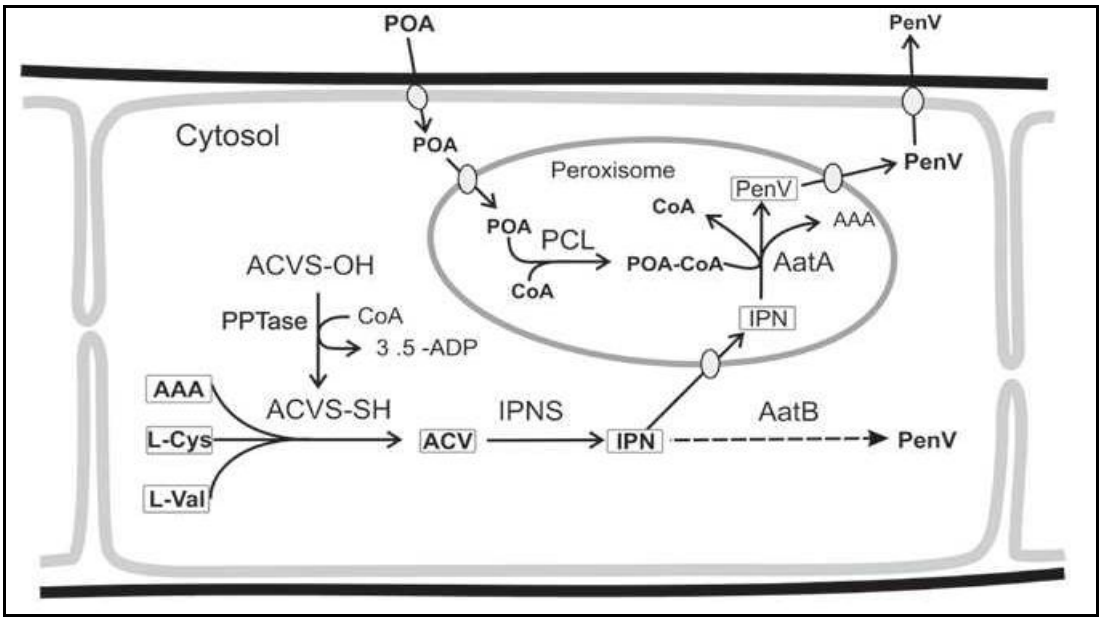

Figure 2.3: Penicillin V biosynthesis pathway and the enzymes involved in filamentous fungi
(Gidijala *et al.*, 2010).

Nowadays, many β-Lactam antibiotics have been discovered including natural, synthetic and semi-synthetic. Figure 2.4 shows the β-Lactam family and its chemical structure. These β-Lactam antibiotics are considered highly effective, low cost, easy to administer and have only slight side effects. For medical purposes, the antibiotics have been prioritized compared to other classes of antibiotics due to their effectiveness in causing cell lysis, which leads to cell death due to their wide spectrum of infections (Wilke *et al.*, 2005; Llarrull *et al.*, 2010; Lobritz *et al.*, 2022). By inhibiting the transpeptidases of bacteria known as penicillin-binding proteins, the peptidoglycan structure of the cell wall could be altered due to disruption of the enzyme involved in cell wall biosynthesis and restructuring. Such reaction is irreversible and effectively inactivates the enzyme (Rodriguez-Herrera *et al.*, 2019).

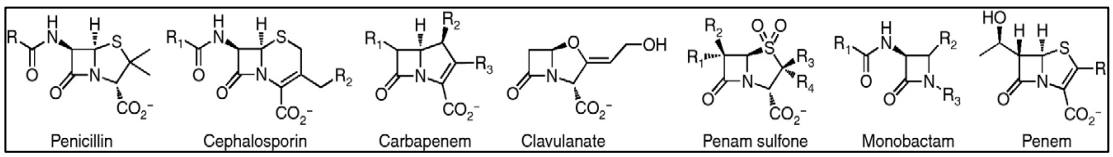

Figure 2.4 The β-Lactam family and their chemical structure
(Llarrull *et al.*, 2010)

2.3 Penicillin

The penicillin was announced as a chemotherapeutic agent in the 24 August 1940 issue and has been used to treat people with bacterial infection (Lalchhandama, 2021). Penicillin is one of the most consumed antibiotics in the whole world and has saved tens of millions of people worldwide since World War II (Ligon, 2004). It is effective against bacteria and free of toxins for humans. Its ability to eradicate a wide variety of bacteria-causing infections made it well-known as the most successful natural product in chemotherapy (Kardos & Demain, 2011). The penicillin was highly effective against infections which include Gram-positive cocci, Gram-positive rods, most anaerobes, and Gram-negative cocci. However, few species of bacteria developed resistance towards the antibiotics and since then penicillin has been paired with other antibiotics to effectively treat infections (Yip & Gerriets, 2020).

A significant part of penicillin was the discovery of 6-aminopenicillanic acid (6-APA) which is located at penicillin's nucleus. Figure 2.5 shows the core structure of penicillin which functions to eradicate the bacterial cell walls.

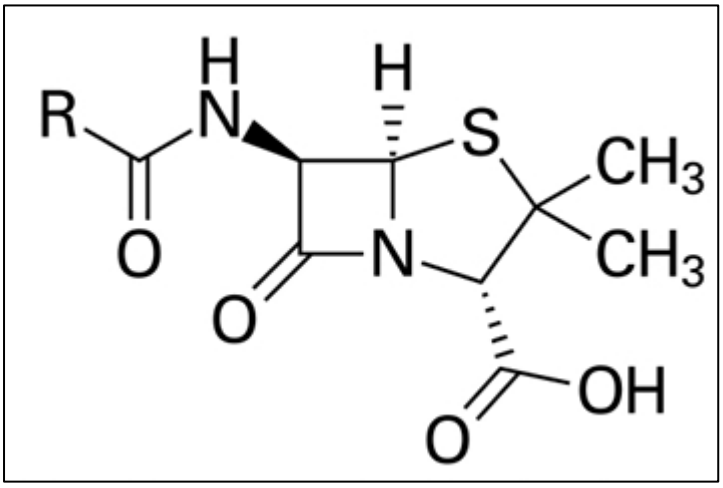

Figure 2.5. The core structure of penicillin. The central structure is known as the β-lactam ring
(Lalchhandama, 2021).

The demand for antibiotics and bacterial resistance towards antibiotic caused scientists to produce and develop derivatives from penicillin (Pichichero & Zagursky, 2014). The side chain R enabled possibilities of modifications which can alter the properties and abilities of the antibiotics as shown in Figure 2.6.

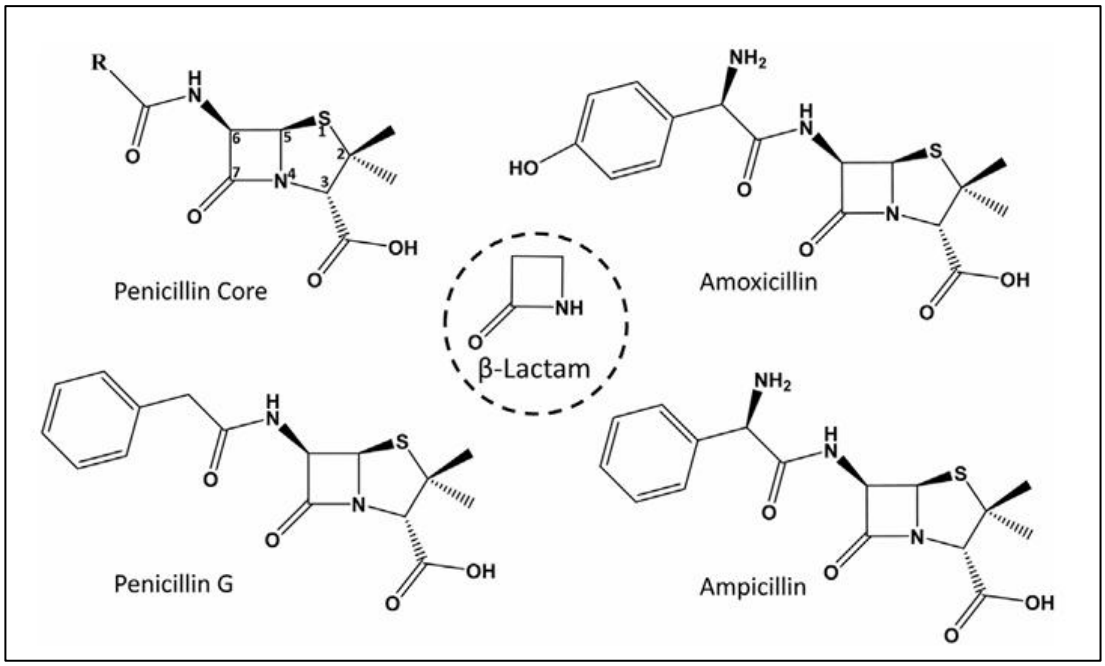

Figure 2.6. From the core structure of the β-lactam ring, other varieties of penicillin antibiotics can be developed proving the ability of the R-side chain (Pichichero & Zagursky, 2014).

2.4 Amoxicillin

Amoxicillin is a semi-synthetic penicillin belonging to the β-lactam antibiotic class with a chemical name of 6-[D(-)β-amino-p-hydroxyphenyl-acetamido.] penicillanic acid. The unique chemical structure of this antibiotic is the presence of the hydroxyl group in the *para* position of the benzene side chain (Roy, 2011; Doi & Chambers, 2015; Liu *et al.*, 2022). The chemical structure of amoxicillin is illustrated in Figure 2.7 below.

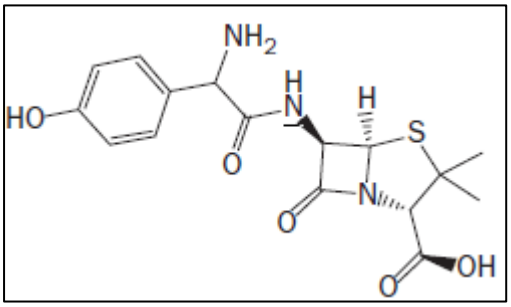

Figure 2.7. 2D chemical structure of amoxicillin (Roy, 2011)

This antibiotic is known for its effectiveness in a wide range of bacterial infections both Gram-positive and Gram-negative. It is frequently utilized as a primary

treatment against gastrointestinal, skin, respiratory and urinary infections in animals and humans (Guncum *et al.*, 2021). Furthermore, it comes in various dosage forms, including tablets, injections, suspensions and capsules (Purohit *et al.*, 2021).

2.4.1 Mechanism of Antibacterial Activity by Amoxicillin

The mechanism of action of amoxicillin is similar to that of its β-Lactam family. The peptidoglycan synthesis, which is a significant element in the bacterial cell wall of both Gram-positive and Gram-negative bacteria, is disrupted. The transpeptidases (penicillin-binding proteins) will facilitate the last step of transpeptidation in the peptidoglycan layer synthesis. However, when the penicillin-binding proteins permanently bind to the β-Lactam nucleus, it prevents and inhibits the final transpeptidation step or the crosslinking between linear peptidoglycan polymer chains. This will interfere with the cell wall structure and simultaneously activate the autolytic enzymes in the cell wall of bacteria. Finally, the process will promote cell lysis and the eradication of bacterial cells, thus causing cell death (Weber *et al.*, 1984; Salvo *et al.*, 2009; Kohanski *et al.*, 2010). Figure 2.8 below illustrates the mechanism of amoxicillin antibiotic for both Gram-positive and Gram-negative bacteria.

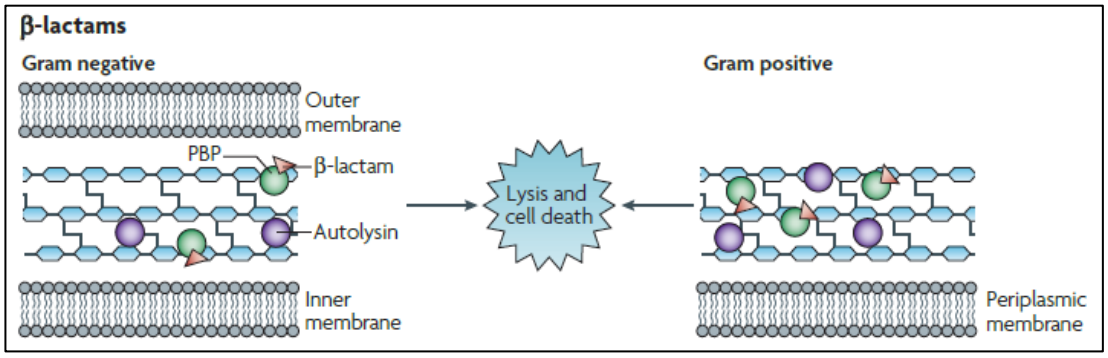

Figure 2.8 Mechanism of action of amoxicillin towards both Gram-positive and Gram-negative bacteria
(Kohanski *et al.*, 2010)

2.4.2 Amoxicillin Pollution in the Environment

Due to amoxicillin's effectiveness against Gram-positive and some Gram-negative bacteria, it has been a popular choice compared to its parent, penicillin. Despite that, an issue that emerged from the extensive usage of amoxicillin. This antibiotic is degraded between 80% and 90% which the residues are considered pollution to the

aqueous environment (Cela-Dablanca *et al.*, 2022). Treating high concentrations of amoxicillin in wastewater is very challenging, as it amounts to dozens to hundreds milligrams per litre (Wang *et al.*, 2019). Furthermore, the inability to treat this pollution may promote antibiotic-resistant genes in human and animal pathogens, which causes antibiotics to become useless against bacterial infections. This not only applies to a specific strain, but to numerous species in the environment. Consequently, this may increase the mortality rate due to the lack of antibiotics to effectively combat life-threatening bacterial infections unless a more effective antibiotic is discovered. In addition, amoxicillin pollution can also lead to carcinogenic, gene toxicity and other health risks (Inyinbor *et al.*, 2018). Therefore, an effective treatment such as bioremediation must be proposed to reverse the damage to the environment.

The exposure of amoxicillin towards the aquatic ecosystems directly impacts the phytoplankton populations. These single-celled algal species are significant to the ecosystem and are commonly used as bioindicators in ecotoxicology. Stress responses were found at different levels of biological organization (Broccoli *et al.*, 2021). Using risk quotients to measure the ecotoxicological risks of antibiotics, amoxicillin had a maximum risk quotient of 32.2 compared to other antibiotics tested (Lei *et al.*, 2019)This indicates that amoxicillin poses a risk to algae. Algae's role as an energy and food base for all organisms in the ecosystem may also harm other aquatic ecosystems.

It is important to note that amoxicillin, which is the pollutant in this study, can undergo hydrolysis through the opening of the β-lactam ring. It may act as a the preliminary step to improve degradation efficiency for the next reaction. Pérez-Parada *et al.* (2011) found that amoxicillin could achieve complete degradation in 24 hours in alkaline media compared to acidic media, in which residues could still be found after 5 days. Hydrolysis was also found at a pH of 8 due to the free lone pair of electrons on the amine group allowing nucleophilic attack on the carbonyl group to produce the diketopiperazine ring (Gozlan *et al.*, 2013). Moreover, another study discovered similar findings in which amoxicillin could undergo hydrolysis at pH 11 producing amoxicillin penicilloic acid, amoxicillin 2',5'-diketopiperazine, amoxicillin penilloic acid and 3-(4-hydroxyphenyl)pyrazinol (Busto *et al.*, 2020).

2.4.3 Development of Amoxicillin Resistance

Antibiotic resistance is a challenging issue for public health, and understanding the crisis in a deeper and comprehensive manner will surely assist in mitigating this global concern. Antibiotics are consumed globally against infections, and the increase in usage has caused an increase in antibiotic resistance.

Microbes produce antibiotic materials, so possessing self-protection abilities against the antibiotic comes naturally. The antibiotic biosynthesis gene clusters (BGCs) consist of both biosynthetic assembly for antibiotics and self-protection mechanisms (Wencewicz, 2019). Thus, when exposed to antibiotics, the microbes develop resistance to defend themselves. These microbes evolved rendering antibiotics useless against them causing infections that are untreatable. It was found that the spontaneous mutations which happen during replication of the chromosome can induce resistance towards antibiotics by altering the cellular targets of antibiotics (MacLean & San Millan, 2019)This mutation can occur with or without contact with a drug, and transferring it to other bacterial species is impossible due to the mutation occurring in the chromosome.

Resistance built on exposure towards antibiotics can spread and transfer to the rest of the population, increasing their survival rate. Studies have shown that bacteria can acquire foreign DNA which encodes for antibiotic resistance known as horizontal gene transfer (HGT) (Urban-Chmiel *et al.*, 2022). The HGT constitutes transformation, transposition and conjugation. The transformation is the process where the bacterium receives extracellular donor DNA containing resistant genes. The bacterium infected by a bacteriophage which has a donor DNA containing resistance towards antibiotics is known as transduction. Lastly, in conjugation, through mating, the bacterium transfers DNA to another bacterium (Mancuso *et al.*, 2021).

The abuse of AMX administration will cause rapid transformation of resistance genes and allowing bacteria to modulate new pathogenicity (Adamus-Białek *et al.*, 2019). One of the modes of AMX resistance in bacteria are point mutations in genes coding for PBP. This led to a decreased affinity for the antibiotic as it targets PBP to inhibit cell wall synthesis causing cell lysis (Tran *et al.*, 2022). A research has found that alterations to penicillin binding protein Pbp2x, Pbp2b, and Pbp1a, and another protein responsible for cell wall synthesis called MurM are important for AMX resistance (Gibson *et al.*, 2022). On the other hand, *Staphylococcus aureus* produces β-

lactamase enzymes, mediated by plasmids to hydrolyze and inhibit the bactericidal structure of β-lactam antibiotic and reduce its effectiveness. (Keshri *et al.*, 2018).

2.4.4 Efforts for Amoxicillin Pollution Treatment

2.4.4.1 Advanced Oxidation Process

Oxidation-based degradation has been widely used to degrade pollutants around the globe including amoxicillin (Souza *et al.*, 2018; Rahdar & Ahmadi, 2019; Carvalho & Moraes, 2021). The advanced oxidation process utilizes various oxidation agents which are strong enough to degrade pollutants such as hydroxyl radical (·OH), ozone (O_3) and superoxide radical (O_2^-) (Essawy *et al.*, 2020; H. Zhang *et al.*, 2020; Asghar *et al.*, 2022). These agents can be produced through different ways such as Fenton, photocatalytic, electrochemical oxidation and many more (Wang & Zhuan, 2020). Unlike membrane processes, one of the main advantages of these technologies over conventional technology is their ability to degrade recalcitrant components efficiently without producing a secondary waste stream. Furthermore, such technology usually limit the formation of hazardous species in the effluent. This is particularly beneficial compared to competing technologies like chlorine oxidation of organics, which synthesizes a significant amount of organo-chlorinated species (Dewil *et al.*, 2017).

2.4.4.2 Coagulation

Coagulation is one of the wastewater treatment methods which has been proven to effectively remove pollutants including amoxicillin (Alidadi *et al.*, 2018; Oulebsir *et al.*, 2020). Coagulation is the process of agglomeration of fine particle colloids into larger particles, thereby reducing turbidity, natural organic matter, and other soluble organic and inorganic pollutants in wastewater (Teh *et al.*, 2016). Generally, the coagulation process involves four steps: charge neutralization, sweep coagulation, bridging and patch flocculation. During the process of coagulation, colloidal particles, which are negatively charged, cause repulsion. A coagulant is added to stabilize these colloidal particles and eliminate the repulsive forces. Normally, the added coagulant is a poly-electrolyte, which brings the zeta potential of the colloids close to zero. This step is known as the charge neutralization mechanism. Then, sweep coagulation is where the

addition of high concentrations of metal salts to the water leads to the precipitation of amorphous metal hydroxides, forming large lumps over time. Bridge flocculation produces very large flocs due to the adsorption of high molecular weight linear-chain compounds, often based on polyacrylamide. This process happens simultaneously across multiple particles. Lastly, patch flocculation occurs when the polymer adsorbs onto the particles, causing a local charge reversal. This results in an attractive force between particles (Sukmana *et al.*, 2021).

2.4.4.3 Membrane Separation

Previous studies have utilized membrane separation to treat amoxicillin pollution and yielded satisfactory results (Shahtalebi *et al.*, 2011; Derakhsheshpoor *et al.*, 2013; Homayoonfal & Mehrnia, 2014). Essentially, a membrane acts as a barrier that separates the two phases by selectively restricting the movement of certain components through it. based on their composition and structure, these membranes are classified as isotropic or anisotropic. Isotropic have uniform composition, either microporous or nonporous to allow high or low permeation fluxes, respectively. On the other hand, anisotropic membranes are non-uniform consisting of different layers with varying structures and composition (Obotey Ezugbe & Rathilal, 2020).

2.4.4.4 Biodegradation

Microorganisms have the ability to break down organic pollutants and this process is called biodegradation. It is one of the most important methods to remove pollutants such as antibiotics from the environment and has been proven to remove amoxicillin residues (Baghapour *et al.*, 2014; Cheng *et al.*, 2018; Yang *et al.*, 2020; Sathya *et al.*, 2023). The ability to exhibit structural changes or degradation of pollutants makes microorganisms an effective in removing dangerous compounds from the environment (Pinto *et al.*, 2020). Moreover, compared to other methods of removing organic pollutants, biodegradation is low-cost, easy to control and optimize, has low side effects and can be used for a variety of antibiotic pollutants (Aldas-Vargas *et al.*, 2021; Chen *et al.*, 2022).

One of the commonly used microorganisms for biodegradation is fungi due to their ability to produce enzymes and degrade organic pollutants into harmless products.

The fungi possess the ability to secrete enzymes to degrade a wide variety of substrates in the environment. The small molecules of degraded substrates will then be absorbed and metabolized by their cells for growth (Ferreira *et al.*, 2020; Benguenab & Chibani, 2021). Some examples of enzymes that are produced include amylase, protease, lipase, nuclease, etc., which help them to degrade chemicals, metals, metalloids, radionuclides and biomass residues. The process of biodegradation by fungi is illustrated in Figure 2.9. In addition, the fungi do not require any supplementation of nutrients other than the pollutants for their survival. Hence, it strengthens the significance of utilizing fungi in removing organic or metal pollutants in soil, water and air (R. K. Singh *et al.*, 2020).

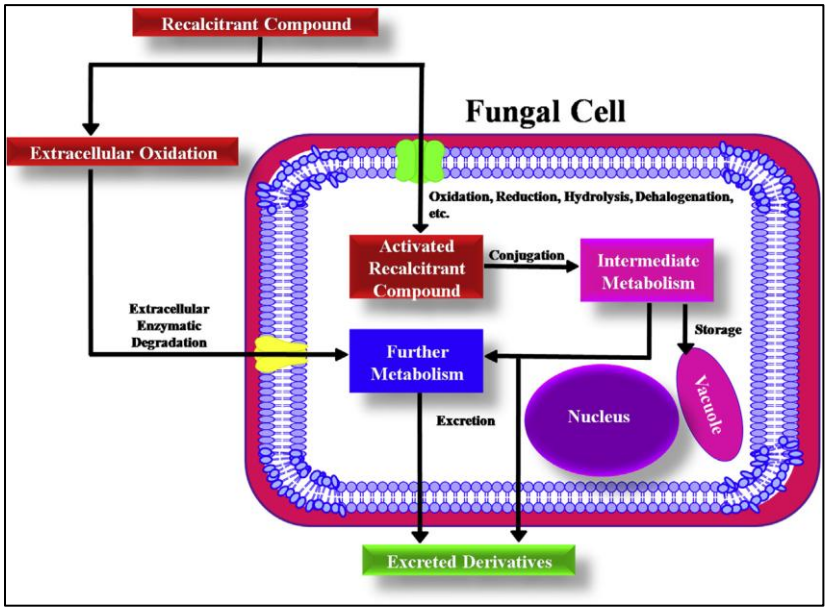

Figure 2.9 Biodegradation process of pollutants in the environment by fungi (R. K. Singh *et al.*, 2020)

According to a previous study, biodegradation by activated sludge eradicated the β-lactam ring. However, the phenolic hydroxyl group and aromatic rings maintained the same (Wang *et al.*, 2019). Another research by Muthukumar Sathya *et al.* (2023) found that when AMX is exposed to β-lactamase enzyme producing bacteria, the β-lactam ring is broken down, producing highly polar AMX penicilloic acid. The compound reacts with AMX as a precursor molecule to form AMX diketopiperazine, which is a stable six-membered ring compound (Busto *et al.*, 2020). The amide bonds in diketopiperazine is reduced by coenzymes, followed by double dehydration to form phenol hydroxypyrazine (Dogan & Kidak, 2016). Fragmentation of peptide bonds, decarboxylation and rearrangement of the azole ring will cause the formation of low

molecular weight compounds and will break down further to yield water, carbon dioxide, and ammonia as end products.

2.5 Fungi

Fungi is a kingdom containing around 90,000 species and every year, approximately thousands are discovered and described. It is estimated that there are more than one million species worldwide making them one of the most significant in the tree of life. Fungi come in various forms including both macroscopic and microscopic organisms. Despite that, a common characteristic is shared such as non-motile heterotrophic eukaryotes with a cell wall surrounding the cell mainly made of chitin. Furthermore, to reproduce, fungi can either be sexual or asexual (Zaragoza, 2017). The Fungi kingdom is grouped into five major phyla according to their structure of sexual reproduction: Chytridiomycota, Zygomycota, Glomeromycota, Ascomycota and Basidiomycota. These fungi may be both beneficial and harmful to humans. There are various ways to benefit from fungi and some of the examples are using yeast for baking and brewing, antibiotic production, steroids and hormones, organic acid production and Stone-washed jeans. On the other hand, these fungi may also cause diseases to humans, plants and animals, contamination and rotting of food, and lastly damage manufactured goods, except for some pesticides and plastics (Volk, 2013).

2.5.1 Aspergillus sp.

The *Aspergillus* was first discovered by Micheli in 1729 who found the similarity between the shape of an aspergillum used to sprinkle holy water and the head of an *Aspergillus* with spores (Balajee *et al.*, 2007). The morphological structure of *Aspergillus spp.* consists of an aspergillium-like spore-bearing structure with a conidial head shape. This species can be found in various ecosystems worldwide, such as soil, salterns, agroecosystems, polar, living plants, animals, stones, water, fossil records and humans (Abdel-Azeem *et al.*, 2016). *Aspergillus spp.* are commonly discovered in diverse habitats and utilized for medical, food fermentation and factory-scale enzyme production. Extracellular enzymes can be secreted by these fungi, which are used commercially in food processing, such as cellulases, pectinases, amylases and many other enzymes which could degrade complex polysaccharides (Ma *et al.*, 2021).

2.5.1.1 Aspergillus in Industry and Wastewater Treatment

The genus Aspergillus has become a cornerstone in the industry of biotechnology, especially in the production of enzymes and recombinant proteins. Its growing prominence stems from several biological and physiological features such as its ability to secrete large amounts of proteins, broad variety of substrate utilization and efficient post-translational modifications (Wakai *et al.*, 2017). In addition, several *Aspergillus* species like *A. niger*, *A. oryzae* and *A. nidulans* have been granted GRAS (Generally Recognized As Safe) status by the U.S Food and Drug Administration (FDA), allowing their widespread application in food, pharmaceutical, and enzyme production industries.

One of the most prominent applications of *Aspergillus* is the production of industrial enzymes such as cellulases, amylases, proteases, and lipases. These enzymes are vital for numerous industrial sectors including food and beverage, textile, paper, and biofuel production. *A. niger, A. flavus, A. fumingatus,* and *A. oryzae* are among the most utilized species due to their extracellular enzyme production capabilities and well-characterized fermentation profiles (Xiao *et al.*, 2012; Ajayi & Lateef, 2025; Honfoga *et al.*, 2025; Mu *et al.*, 2025).

In wastewater treatment, *Aspergillus* possess the capabilities to produce extracellular enzymes of a broad array including laccases, peroxidases, and hydrolases, which are commonly use in the degradation of various organic pollutants such as dyes, phenols, and pharmaceuticals. These enzymes allow the fungus to break down recalcitrant compounds that are often resistant to conventional bacterial treatment, making *Aspergillus* an attractive agent for advanced bioremediation strategies (Feng *et al.*, 2025). The degradation mechanisms employed by *Aspergillus* species are largely synergistic, involving complex interactions between enzymatic activity, organic acid production, redox mediators, and biosurfactants. A significant role is played by non-specific oxidases including lignin modifying enzymes like laccase and peroxidases. These enzymes act via radical-based oxidation pathways (Mir-Tutusaus *et al.*, 2018). Among the pollutants, oil sector often secretes oils and greases which can severely impact aquatic environments if not properly treated (Feng *et al.*, 2021). Lipase enzymes can hydrolyze ester bonds in tryglycerides. Notably, *A. oryzae* is a significant microbial source of lipase utilized in wastewater treatment. When immobilized on α-alumina membranes, lipase from *A. oryzae* not only enhanced the breakdown of oily

components, but also improved membrane antifouling and self-cleaning capabilities (Mulinari *et al.*, 2023). Furthermore, the production of fungal redox mediators which are small molecules that generate free radicals, allows *Aspergillus* to oxidize substrates that are structurally hindered. These mediators serve as electron shuttles and enhance the range of degradable pollutants, particularly under conditions where direct enzyme-substrate interaction is limited (K Chaurasia *et al.*, 2015). Biosurfactants produced by the fungi contribute to the overall biodegradation process by enhancing the solubility and bioavailability of hydrophobic compounds. These biosurfactants either emulsify non-polar substances or alter the surface properties of fungal mycelia to promote greater substrate affinity and uptake (Al-Hawash *et al.*, 2019).

The global market for industrial enzymes was valued at approximately USD 6.2 billion in 2020 and is growing steadily, underlining the need for robust and efficient protein expression platforms (Meghwanshi *et al.*, 2020). Among the wide variety of available fungi, *Aspergillus* stands out due to its strong protein secretion capacity. Nevertheless, its development as a protein production system has faced bottlenecks, particularly in the areas of genetic manipulation and inconsistent expression levels between homologous and heterologous proteins (Li *et al.*, 2020). As an example, homologous proteins in *A. niger* have been recorded at expression levels as high as 28.91 g/L in shake flasks. On the other hand, heterologous proteins might reach only 70 mg/L.

2.5.1.2 Aspergillus tamarii

The *Aspergillus tamarii* is widely used for its enzyme production. It was reported by Gonçalves *et al.* (2013) that *A. tamarii* produced a high level of β-glucosidase and xylanase in wheat bran among 36 other microorganisms tested that can be utilized in the production industry. Siddiquee (2018) also stated that *A. tamarii* produces metabolites such as kojic acid which is utilized in food and cosmetic industries for color preservation. Another research also found that the fungus can produce pectinolytic enzymes that can be used as a bio-agent in the development of green process technology (Shanmugavel *et al.*, 2018). When it comes to biodegradation, it produced laccase when grown with polypropylene as the only carbon source, demonstrating its ability to induce oxidative degradation of synthetic polymers (Ong *et al.*, 2024). The laccase enzyme was also discovered to effectively decolorize dyes such

as Remazol Black B as found in a research by Ayu and Kasiamdari (2022). Despite the benefits, Siddiquee (2018) mentioned that this fungus may produce aflatoxin and cyclopiazonic acid. Aflatoxin can cause significant damage to the economy and health worldwide due to its carcinogenicity to both humans and animals, while cyclopiazonic acid can spoil agricultural goods and animal food (Vulić *et al.*, 2021; Rajaura *et al.*, 2023). Furthermore, Bibashi *et al.* (2013) observed the morphology, which was branched sporangiophores along with a young sporangium under the microscope with a magnification scale bar of 100 μm as shown in Figure 2.10.

Figure 2.10**.** Branched sporangiophores with a young sporangium of *A. tamarii* under the microscope with a scale bar of 100 μm
(Bibashi *et al.*, 2013)

2.6 Parameters Affecting *A. tamarii* Growth and Enzyme Production

Microorganisms are highly affected by the pH of the medium. Their growth depends on the optimal pH, otherwise the population will not grow and degrade the pollutants effectively which may also influence other parameters (Khanpour-Alikelayeh *et al.*, 2020). According to the previous research, the conditions used were pH 5.5, 120 rpm, 96 hours and 100 μL of $1x10^6$ spore suspension, achieving amoxicillin biodegradation by 49% (Abd Hamid *et al.*, 2023). The biodegradation process is affected by various parameters which may increase or decrease the pollutant removal

efficiency. These parameters include the amount of pollutants, nutritional conditions, pH, temperature and other physiochemical factors. Optimizing these factors is significant in order to obtain the best conditions for biodegradation of the pollutant (Favier *et al.*, 2021).

2.6.1 pH level

Saravanan *et al.* (2020) have reported that the fungus grew well at pH 5.6 in Sabouraud Dextrose (SD) broth to yield pigments. These pigments exhibited antibacterial activity against *Streptococcus pyogenes* and *Escherichia coli,* and antifungal activity against *Chrysosporium keratinophilum* and *Candida albicans*. In addition, Sezhian and Bose (2019) have discovered that pH 5 showed maximum growth of *A. tamarii*, with total phenol and flavonoid content production of 163.59 mg/g and 78.73 mg/g respectively. This coincides with the fungi having minimum growth and metabolite production at a pH of 3 and 11. Maximum production of *A. tamarii* was recorded when pH 6.7 and able to shrink cotton fabric by 90% efficiency (Mohan *et al.*, 2019).

2.6.2 Agitation speed

An agitation speed of 135 rpm at 28 °C for 4 days in 100 mL of Czapek's medium, Ma *et al.* (2016) were able to extract 14 cyclic peptides from *A tamarii* isolated from roots of *Ficus carica.* These peptides exhibit strong antimicrobial properties and cytotoxic activities. Another study by Munir *et al.* (2020) found that *A. tamarii* grown using submerged fermentation with conditions of 1% (v/v) inoculum at pH 6, 200 rpm and 72 hours produced a maximum yield of polygalacturonase. This enzyme is widely used in food, fermentation and oil extraction industries. Furthermore, *A. tamarii* was also able to grow at 200 rpm for 48 hours to produce lytic polysaccharide monooxygenases (LMPOs) to degrade xyloglucan (Monclaro *et al.*, 2020). Based on previous reports, the suitable agitation speed was 200 rpm.

2.6.3 Incubation time

Maximum enzyme L-asparaginase activity by *A. tamarii* was recorded on the 7th day and dropped after the 9th day. The biomass production showed the highest after incubation for 7th days (Bedaiwy *et al.*, 2016). Furthermore, *A. tamarii* requires 24 hours of incubation to produce optimum magnetic nanoparticles (El-Sharkawy *et al.*, 2022). The lipase enzyme production by *A. tamarii* showed maximum yield after 7 days of incubation with lipase activity (2,32,500±192U/ml/min) using submerged fermentation (Das *et al.*, 2017).

2.6.4 Inoculum size

Previously, the *A. tamarii* was grown in basal broth medium at pH 9, inoculated with a 5.0 mL spore suspension, agitation speed of 180 rpm, incubated for 7 days (Anandan *et al.*, 2007). Premalatha *et al.* (2022) were able to produce higher activity of *α*-amylase (519.40 u/g) when using 2.5% (v/w) of inoculum level (containing 10^6 spores/ml). Furthermore, another research used 1 mL of *A. tamarii* spore suspension (10^6 spore/mL) where the maximum yield of β-Xylosidase was obtained after 120 hrs incubation (El-Gindy *et al.*, 2015).

2.7 Experimental Design for Screening Studies

Fractional Factorial Design (FFD) has been used to accomplish the main effects of the system, consisting of various variables while demanding less resource. Optimization studies require many factors to consider which may influence the biodegradation process. Performing the “one-factor-at-a-time” conventional method is highly inefficient as it is time-consuming and unable to detect the correlation among two or more factors. Therefore, the method mentioned above can surpass the limitations of single-variable optimization (Wu *et al.*, 2009; Colla *et al.*, 2016; Noormohamadi *et al.*, 2019; Favier *et al.*, 2021).

2.7.1 Factorial Design

A factorial design may either be full or fractional factorial. Factorial experiments normally employ two-level factorial designs and identify each factor’s

influence on the response. The influence of the factor is often measured by the change in response variable when the level of the factor is changed. This approach investigates all possible combinations of the factor levels (Durakovic, 2017). Factors in factorial are typically denoted by capital letters (A, B, C, etc.) along with their lower and higher levels represented as (-) or -1 and (+) or +1, respectively. When the middle level is present, it is designated as (0) (N. Politis *et al.*, 2017).

2.7.2 Full Factorial Design

Full factorial designs are orthogonal and balanced, enabling the estimation of all main effects and interaction factors (Yu *et al.*, 2018). These designs ensure that factors are completely independent of one another. Despite that, a large number of design points or samples are usually required to conduct such design. This design utilizes equation (2.1):

$$n = m^k \tag{2.1}$$

Where n represents the total number of samples, k denotes the number of factors and m indicates the number of levels for each factor.

Most experiments employ two levels in addition to a small number of factors, resulting in a 2^k design. Three-level factorial designs are more complex than two-level designs as the number of experimental runs becomes high to fully estimate the main and interaction effects.

2.7.2.1 Fractional Factorial Design

When the number of design variables is large, a fractional factorial design can be utilized instead of a full factorial design. This approach estimates only a subset of all possible variable combinations. This design called fractional factorial design is usually used for screening important variables (Yolmeh & Jafari, 2017). This design also reduces the size of the experiment while minimizing the loss of critical information that could result from not examining all possible combinations of factor levels (Gunst & Mason, 2009). Achieving this requires fractioning a full factorial 2^k design into a 2^{k-p} design, where p is the number of generators selected for design fractionation (Fukuda

et al., 2018). When a four-factor was taken as an example, a half-fraction factorial design is adopted as 2^{4-1} which equals to 8 experimental runs.

2.8 Kinetic Modelling

Numerous biological systems relevant to biotechnology which includes cell metabolism during fed-batch cultivation, stress responses at the cellular level, or regulatory mechanisms during the cell cycle. These are inherently dynamic and time dependent. In addition, these processes do not operate under steady-state conditions as their current responses often depend on their historical states. To represent the time-varying behaviors, researchers typically utilize mathematical models that describe the rates of biochemical reactions within the system. These reaction rates are then incorporated into mass balance equations, enabling the simulation of changes in the concentrations of biochemical components over time. This approach is known as kinetic modelling. However, literatures sometimes refers to these as dynamic models, with both terms being largely interchangeable in the context of modelling biological systems due to their shared and overlapping focus (Almquist *et al.*, 2014).

Additionally, kinetic models are not solely limited to simulate dynamic, non-steady state processes, they are equally applicable and informative in the analysis of quasi-steady-state or stationary systems. For example, during the exponential phase of microbial growth, the system may appear stable, yet underlying metabolic activities continue to follow definable kinetic patterns. In such situations, kinetic models offer a quantitative framework to relate observed steady-state behavior to the intrinsic rate constants and regulatory mechanisms of the biological system (Almquist *et al.*, 2014).

The Luedeking-Piret model is one of the most widely used kinetic models to describe product formation in microbial fermentation processes. It relates the rate of product formation to both the microbial growth rate and the biomass concentration as shown in equation (2.2).

$$\frac{dP}{dt} = \alpha \frac{dX}{dt} + \beta X \tag{2.2}$$

Where $\frac{dP}{dt}$ is the rate of product formation, $\frac{dX}{dt}$ is the rate of biomass formation, and X is the biomass concentration. The coefficients α and β represent growth-

associated and non-growth associated product formation, respectively (Nuñez *et al.*, 2016).

The Verhulst model, also known as the logistic growth model, is a foundational mathematical model used to describe population growth under resource-limited conditions. Unlike exponential models that assume unlimited growth, the Verhulst equation incorporates a carrying capacity to reflect the environmental limitations. The general equation of the Verhulst model is as stated in equation (2.3):

$$\frac{dN}{dt} = rN\left(1 - \frac{N}{K}\right) \tag{2.3}$$

where N is the population size or the biomass concentration, r is the intrinsic growth rate, K is the carrying capacity and $\frac{dN}{dt}$ represents the rate of change of the population over time (Ausloos, 2011).

The equation illustrates that when the population is small (N << K), the growth rate approximates exponential growth (rN). However, as N approaches K, growth slows down due to increasing competition for limited resources, eventually reaching a stationary phase where growth ceases ($\frac{dN}{dt} = 0\ when\ N = K$)(Ausloos, 2011).
The solution to the differential equation is as equation (2.4):

$$N(t) = \frac{K}{1 + \left(\frac{K - N_0}{N_0}\right)e^{-rt}} \tag{2.4}$$

where N_0 is the initial population at time t = 0. This sigmoidal (S-shaped) curve effectively models microbial growth in batch cultures, particularly during the lag, exponential and stationary phases.

In bioprocess engineering, the Verhulst model is widely used for simulating microbial growth kinetics, assessing bioreactor performance, and designing control strategies for biomass production (Robledo *et al.*, 2018; Robles-Morales *et al.*, 2021).

2.9 Bioreactor

A bioreactor is a vessel where a biological reaction or transformation occurs. The biological systems involved include enzymes, microorganisms, animal cells, plant

cells, and tissues. Designing an appropriate bioreactor for a specific bioprocess requires extensive studies on the biological system, which include cell growth, metabolism, genetic manipulation, and product expression, to understand the cell physical and chemical requirements. Furthermore, controlling bioreactor operating variables, such as dissolved oxygen concentration, pH, temperature, mixing, and nutrient supplementation, is essential to optimise the desired functions of the living cells or enzymes (Zhong, 2010).

Ensuring stable and optimal conditions during bioprocessing is vital to achieving the desired yields and product concentrations, regardless of the bioreactor design, microbial catalyst, or unexpected disturbances. Bioprocess control systems play an essential role by actively regulating critical operational parameters such as nutrient feed rate, temperature, pressure, agitation speed, pH, and dissolved oxygen levels (DO) (Murthy *et al.*, 2012). Without proper regulation, process deviations occur. Many researchers have extensively investigated strategies for bioreactor control and highlighted that small enhancements in system stability and efficiency can lead to significant economic improvements in industrial-scale production (Mitra & Murthy, 2022).

The selection of a suitable control strategy is largely influenced by the type of bioreactor employed. Conventional systems such as shaken flasks, stirred tank reactors (STRs), and bubble columns, often require minor adaptations based on specific bioprocess requirements. However, with the evolution of advanced biomanufacturing practices, including the emergence of single-use systems and micro-scale bioreactors, the demand for highly responsive and robust control mechanisms has grown to accommodate increasingly complex operations (Betts & Baganz, 2006).

Bioreactor design is closely aligned with the nature of the biological catalyst used. For instance, in animal cell culture processes, where cells exhibit shear sensitivity and limited proliferation rates, the use of high-density perfusion systems is common. These systems require precise environmental regulation to preserve cell vialbility. This is particularly relevant in regenerative medicine, where bioreactors must maintain stringent control conditions to ensure the integrity and therapeutic quality of the cultured cells and tissues, which themselves constitute the final product (Najafpour, 2007; Delavar & Wang, 2022).

2.9.1 Stirred-Tank Reactors (STRs) in Wastewater

Stirred tank bioreactor is the most commonly used bioreactor in the industry. This bioreactor fills 70-80% of the total volume with the medium. It consists of a cylindrical vessel with one or more agitators powered by an external motor. The ratio of the impeller diameter ratio to the tank diameter ranges from 0.3 to 0.6. The height of the bioreactor is typically two to three times the diameter of the bioreactor (Shokrkar *et al.*, 2018). Stirred tank bioreactors (STRs) have long served as a foundational system in industrial biotechnology, particularly within wastewater treatment applications. One of the most well-established uses of STRs is in the activated sludge process, an aerobic method used to treat industrial and municipal effluents. Despite its age, the activated sludge system remains widely adopted due to its relatively straightforward design, though it is not without operational and economic challenges.

In the conventional activated sludge process, wastewater is introduced into a large aerobic tank seeded with microbial biomass and this is typically a portion of recycled activated sludge. This tank acts as an STR, where the microbial community remains suspended and oxygen is supplied through sparging of compressed air at the base of the tank. Given the low solubility of oxygen in water, especially in large volumes, substantial energy input is required to deliver enough oxygen to meet the metabolic demands of the microbes. This reliance on large air compressors contributes significantly to operational costs, posing one of the primary limitations of the system (Narayanan & Narayan, 2019).

The main goal of the STR in this setup is the oxidation of organic matter into carbon dioxide and water, often accompanied by nitrogen removal processes. Ammonia in the wastewater is oxidized to nitrate in the aerobic tank (nitrification), while a secondary anoxic tank may be used for denitrification. Denitrification is where nitrate is reduced to nitrogen gas and released into the atmosphere. As this second phase does not require oxygen, aeration is unnecessary, making it more cost-effective (Narayanan & Narayan, 2019).

Over the years, the basic structure of the activated sludge process has been refined through numerous configurations. Most modifications still retain the use of STRs, either in series or in segmented compartments. In the classical setup, two STRs are connected in one sequence. The first is for aerobic treatment and nitrification, and the other for denitrification (Bhattacharya & Mazumder, 2021; Jain *et al.*, 2022). Post-

treatment, the effluent is passed into a sedimentation tank, where solid biomass settles. A portion of this sludge is then recycled to the initial aerobic tank to maintain the microbial population and ensure continued degradation performance (Augsburger *et al.*, 2021). Optimizing the recycle ratio is crucial, as excessive recycling may lead to microbial decay, while insufficient recycling can reduce biological oxygen demand (BOD) removal efficiency.

Among the enhanced designs, the Bardenpho process stands out (Tchobanoglus *et al.*, 2003). This approach utilizes four STRs in a specific sequence: initial denitrification, followed by aerobic treatment, a second denitrification tank, and a final aerobic polishing tank. This system is effective in achieving high levels of BOD, nitrogen, and phosphorus removal. However, its complexity and higher installation and operational costs make it suitable for large-scale applications where advanced treatment is necessary.

Alternative strategies to improve performance and reduce inefficiencies involve dividing a single large aerobic tank into multiple smaller, sequentially aerated compartments. This is a technique known as step aeration (Banti *et al.*, 2021). In this method, each compartment receives its own dose of compressed air, and wastewater flows sequentially through the compartments. This configuration enhances oxygen transfer, improves BOD degradation, and minimizes issues like dead zones or short-circuiting commonly found in large, single-tank systems. The compartmentalized design also better simulates the behavior of ideal continuous stirred tank reactors (CSTRs), ensuring more efficient contact between microbes and substrates (Banti *et al.*, 2021).

Furthermore advancements include serial-parallel configurations, which combine the benefits of step feeding and step aeration (Monaghan *et al.*, 2021). In this approach, raw wastewater is divided and introduced into multiple compartments, which each receiving both fresh influent and partially treated effluent from the previous compartment. Separate aeration systems are also used for each compartment. Separate aeration systems are also used for each compartment. This layout enhances the interaction between biomass and pollutants. In addition, this layout is recommended for high-volume industrial wastewater treatment plants. The system supports more consistent and controlled degradation processes and allows for flexible management of treatment parameters (Monaghan *et al.*, 2021).

CHAPTER 3
METHODOLOGY

3.1 Materials

3.1.1 Chemicals

Amoxicillin powder (Abcam, United Kingdom), Ethyl acetate (EAM, Malaysia), distilled water (dH_2O), glycerol stock solution (HmbG, Germany), Tween 80 (Merck, Germany), Potassium phosphate buffer (KH_2PO_4) (Bendosen, Norway), Methanol (EAM, Malaysia), Acetonitrile (ACN) (Chemiz, Malaysia), HPLC grade water (Chemiz, Malaysia), Dimethyl sulfoxide (DMSO) (Friendemann Schmidt, United Kingdom), dinitrosalicylic acid (DNS) reagent (Sigma-Aldrich Chemie, Germany), Bradford Dye reagent (LabServ, Thermo Fisher Scientific), Phenol (Chemiz, Malaysia), Sodium Sulfite (Bendosen, Norway), Sodium hydroxide (NaOH)(Emsure, Germany), Rochelle salt (Ajax Finechem Pty Ltd, Thermo Fisher Scientific), bovine serum albumin (BSA)(Sigma-Aldrich Chemie, Germany).

3.1.2 Media

Potato Dextrose Broth (PDB)(Oxoid, Thermo Fisher Scientific) and Potato Dextrose Agar (PDA)(Oxoid, Thermo Fisher Scientific).

3.2 Media Preparation

3.2.1 Potato Dextrose Broth (PDB)

PDB was prepared by dissolving 24 grams of PDB powder in 1.0 litre of distilled water. The mixture was subjected to preheating and stirred until homogenized. The homogenized PDB solution was sterilized in the autoclave at 121ºC for 15 minutes.

3.2.2 Potato Dextrose Agar (PDA)

PDA was prepared by dissolving 19.53 grams of PDA powder in 500 mL of pre-heated distilled water. The mixture was sterilized in the autoclave at 121°C for 15 minutes. Then, the mixture was cooled to a moderately warm temperature before pouring it into the petri dish.

3.3 Fungal Spore Suspension Preparation

3.3.1 Glycerol Stock Preparation

Approximately 10 mL of glycerol solution was added to 90.0 mL of distilled water. The mixture was sterilized by autoclaving and 1.0 mL of sterile glycerol solution was transferred into a 1.5 mL microcentrifuge tube. Fungal mycelium of 1.0 cm x 1.0 cm of *A. tamarii* was transferred into the microcentrifuge tube and stored at -20°C.

3.3.2 Preparation of Fungal Spores Suspension

A. tamarii was obtained from the Institute for Medical Research (IMR) Shah Alam, Selangor. The isolate is extracted from a patient's left nasal cavity tissue submitted by otolaryngologists clinic in Hospital Tengku Ampuan Rahimah Klang. This species was chosen due to its potential to degrade AMX based on previous research by Abd Hamid *et al.* (2023). Previous research have also supported *A. tamarii*'s ability to produce extracellular enzymes to degrade pollutants (Ayu & Kasiamdari, 2022; Ong *et al.*, 2024; Lawal *et al.*, 2025).

Glycerol stock of *A. tamarii* was cultured onto the PDA from the glycerol stock solution by using the inoculating loop apparatus. The plates were incubated at 25°C for 7 days.

The fungal plate was flooded with 20 mL of 0.1% Tween 80 and left for 3 minutes before scraping the culture medium's surface using micropipette tips. The solution was acquired by transferring the flooded plate into a 50 mL falcon tube and filling it with sterile distilled water until it reached 50 mL (Abd Hamid *et al.*, 2023).

3.3.3 Spore Suspension Concentration

In this step, the haemocytometer was used to calculate the concentration of the spore suspension, which was used as the culture inoculum. The haemocytometer and coverslip were sterilized using alcohol and rinsed with distilled water beforehand. The fungal spore suspension was pipetted into the haemocytometer slide groves at approximately 10.0 µL. Then, the slide was placed under the Olympus CX12 microscope. The number of spores in five large grid squares was calculated using the following equation equation (3.1) to obtain the concentration of spore suspension.

$$\text{Cell concentration per mL} = (n/5) \times 10^4 \quad (3.1)$$

where n is the average cell count per square, will be multiplied by 10,000 (10^4) which is a standard constant to determine the spores count per 1 mL suspension.

The stock solution will undergo dilution to 1 x 10^6 CFU/mL for biodegradation process usage.

3.4 Preparation of Amoxicillin Standard Solution

A weight of 2.5 g of amoxicillin powder was dissolved into 45 mL of sterile distilled water containing 5.0 mL of sodium hydroxide (NaOH). Thus, the final concentration of amoxicillin after preparation was 50.0 mg/mL (50,000 ppm). After that, the mixture was filtered using a 0.45 PTFE Minisart syringe filter (pore size of 0.45 µm). Then, the solution was wrapped with aluminium foil to prevent photolysis.

3.5 Biodegradation Assay in Shake Flask

The biodegradation experiment was conducted through a submerged fermentation technique indicated by Mohammad *et al.* (2018). Firstly, about 100.0 µL of 1.0 x 10^6 spore suspension of *A. tamarii* was inoculated into a 100.0 mL sterilized PDB medium in 250 mL Erlenmeyer flask culture under aseptic conditions. The broth containing fungal culture solely was used as biotic control while the one containing amoxicillin only as abiotic control. The sterilized cultured flasks were incubated for biodegradation studies. The fermentation parameters which include77,, initial pH,

agitation speed, incubation time and inoculum size, for biodegradation studies were carried out according to the experimental design indicated in Table 3.1.

Table 3.1 summarizes the range of selected parameters. The experimental runs were prepared and carried out according to the design matrix generated by the statistical software Minitab (Version 18).

Table 3.1.
Experimental runs for FFD with a range of selected parameters were designed using Minitab (Version 18).

RunOrder	pH	Incubation time (hrs)	Agitation Speed (rpm)	Inoculum size (uL)
1	4	24	120	100
2	4	96	200	100
3	8	96	120	100
4	4	24	200	1000
5	8	24	200	100
6	4	96	120	1000
7	8	24	120	1000
8	8	96	200	1000
9	4	24	120	100
10	4	96	200	100
11	8	96	120	100
12	4	24	200	1000
13	8	24	200	100
14	4	96	120	1000
15	8	24	120	1000
16	8	96	200	1000
17	4	24	120	100
18	4	96	200	100
19	8	96	120	100
20	4	24	200	1000
21	8	24	200	100
22	4	96	120	1000
23	8	24	120	1000
24	8	96	200	1000

After the first 72 hours of incubation, amoxicillin solution was inserted into the same culture broth with a final amoxicillin concentration of 100 ppm. The culture were then be further incubated according to the parameters. After that, the sample was subjected to HPLC (Agilent 1200) analysis on the biodegradation percentage of AMX (AMX%). Fermentation flasks were prepared for each 24-hour interval with triplicates for kinetic studies.

3.6 Biodegradation in Stirred Tank Reactor (STR)

3.6.1 Stirred-Tank Reactor (STR) Specifications

The amoxicillin biodegradation experiment was conducted in a 3.6-liter double-walled vessel with a working volume of 2.0 liters as shown in Figure 3.1. The borosilicate glass vessel was cylindrical with a round bottom and measured 37 cm in height and 11.5 cm in inner diameter. The experiment was carried out in a stirred-tank reactor equipped with a monitoring and control system for agitation, pH, aeration, temperature, and antifoam to ensure optimal conditions. However, due to a lack of funding, only the temperature was kept constant. The reactor utilized two Rushton impellers, each with six blades measuring 4.6 cm in diameter. A temperature of 30ºC was maintained using a Pt100 1/3 DIN-B sensor and heated through a vessel jacket. The initial pH was set to 4.3 and monitored using a gel-type electrolyte sensor and was not controlled during the entire 7-day fermentation process.

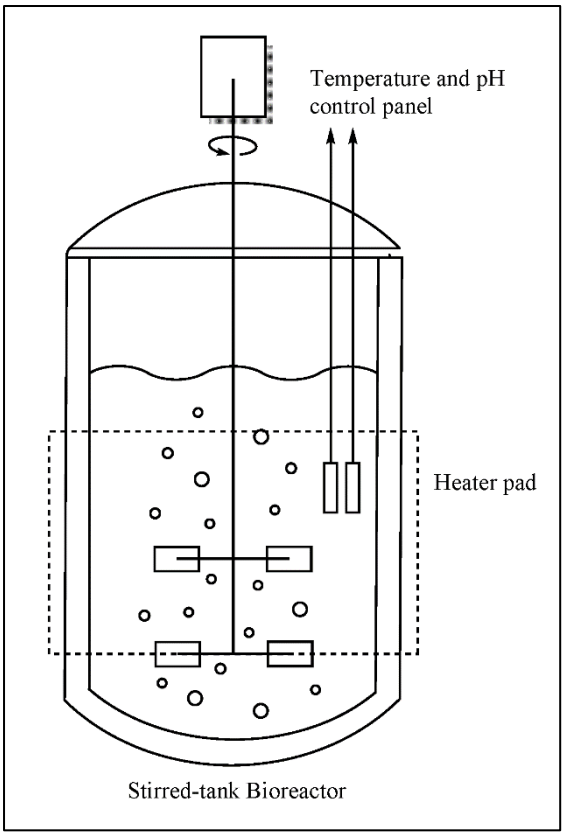

Figure 3.1. A Schematic Diagram of the Stirred-Tank Bioreactor (STR) Used for Amoxicillin Biodegradation Experiments.

3.6.2 Biodegradation Assay in Stirred-Tank Reactor (STR)

The biodegradation experiment in a stirred tank reactor (STR) was conducted through the submerged fermentation technique. Firstly, about 100.0 µL of 1.0 x 10^6 spore suspension of *A. tamarii* was inoculated into a 100.0 mL sterilized PDB medium in a 250 mL Erlenmeyer flask culture under aseptic conditions for 24 hours. After 24 hours, the content of the culture broth was fully transferred into the reactor for further fermentation. The process was conducted at three different agitation speeds: 250, 500 and 770 rpm, with two replicates for 168 hours. Previous research has found that these impeller speeds produced maximum enzyme activity such as β-glucosidase, endoglucanase, xylanase, and endoinulinase (Abdella *et al.*, 2020; Buffo, Esperança, Farinas*, et al.*, 2020; Maumela *et al.*, 2021; GARES *et al.*, 2023).

After the first 72 hours of fermentation, the amoxicillin solution was inserted into the same reactor culture broth with a final amoxicillin concentration of 100 ppm. The sample was collected at intervals of 24 hours and subjected to HPLC analysis for the residual amoxicillin concentration. Glucose was conducted using the DNS assay and protein concentration was determined using the Bradford reagent.

3.7 Screening of Significant Parameters Affecting Biodegradation of AMX by *A. tamarii*

3.7.1 Fractional Factorial Design (FFD)

FFD was carried out as designed by Saat and Annuar (2020) with slight modifications to find the four factors for *A. tamarii* to biodegrade amoxicillin. Each factor was tested at two levels of range, which were expressed as the maximum level (+) and minimum level (-). The four factors include initial pH (4.00 and 8.00), biodegradation time (24 and 96 hours), inoculum size (100 µL and 1000 µL) and agitation speed (120 and 200 rpm). The percentage of biodegradation was used as an experimental response for fractional factorial analysis. The design matrix for FFD was generated by Minitab (Version 18) as shown in Figure 3.1.

3.8 Cleaning Up and Extraction of AMX Residues Degraded by *A. tamarii*

3.8.1 Liquid-liquid Extraction (LLE)

The amoxicillin residues were treated with liquid-liquid extraction at 24-hour sample intervals of incubation according to Mohammad *et al.* (2018) and Seifollahi *et al.* (2019)-method with modifications. This experiment used ethyl acetate as the organic extracting solvent due to its low polarity.

This technique was executed in a separating funnel by mixing 50 mL of HPLC-grade water with 50 mL of ethyl acetate and 6 mL of fermentation broth. The separating funnel was positioned inverted, and the valve was opened periodically to release gas and pressure. Then, the mixture was allowed to settle for 10 minutes to allow the formation of two layers of solvents. Each layer was collected into a 50.0 mL falcon tube and concentrated with a rotary evaporator to reduce pressure. Concentrated amoxicillin was dissolved in 3.0 mL of DMSO. The amoxicillin residue was further purified in solid-phase extraction (SPE).

3.8.2 Solid Phase Extraction (SPE)

The residue was transferred into the C18 Hypersep SPE cartridge preparation for a further clean-up step. The method was based on C. Zhang *et al.* (2020) with slight modifications. Prior to extraction, a pre-conditioned SPE cartridge with 3.0 mL methanol and 3.0 mL of water was carried out. The sample volume of 4.0 mL was loaded into the column, allowing it to pass through by gravity. Then, the cartridge was washed with 2 mL of HPLC-grade water and eluted with 3 mL acetonitrile.

3.9 Quantitative Analysis of Amoxicillin Residues by High-Performance Liquid Chromatography (HPLC)

3.9.1 Preparation of Amoxicillin Standard Solution

The amoxicillin standard solution was prepared with a final concentration of 1000 ppm. The HPLC column (ZOBRAX SB-C18, 5 μm, 4.6 x 250 mm) was subjected to a column wash pre-calibrated to avoid noise in the HPLC baseline. Approximately 100 mg of amoxicillin powder was transferred into a 250 mL Erlenmeyer shake flask,

which contained 100 mL of 0.1 M KH_2PO_4 (pH 3.5). After that, the mixture was filtered with a 0.45 µm nylon syringe filter and transferred into a 50 mL falcon tube. As previously done, the tube was wrapped with aluminium foil to prevent photolysis.

3.9.2 Standard Curve of Amoxicillin Standard For Quantification Analysis

The amoxicillin stock was subjected to the serial dilution with different stock concentrations (ppm) ranging from 1 ppm to 100 ppm (Table 3). The standard was filtered using a 0.45 µm filter to remove any possible contaminants. The results were recorded, and the standard curve was plotted using the average area under the graph (mAU*s) versus the concentration of amoxicillin standards. Then, the curve was evaluated by the coefficient of determination (R^2). Table 3.2 below shows the preparation of the calibration solution from the stock.

Table 3.2
Preparation of amoxicillin standard solution

Concentration of standards (ppm)	100	50	40	20	10	5	1
Volume of antibiotic stock (µL)	200	100	80	40	20	10	2
Volume of diluent solvent (µL)	800	900	920	960	980	990	998
Total volume (µL)	1000	1000	1000	1000	1000	1000	1000

3.9.3 Percentage Recovery of Amoxicillin

The total amount of pure amoxicillin recovery after extraction and the cleaning-up process with the non-purified standard was compared by calculating the percentage recovery for both standards. Preparations must be made before hand by preparing 200 ppm of antibiotics each and labelling them as purified (LLE and SPE standard) and non-purified, respectively. Approximately 6 mL of standard solution is used in LLE and SPE, corresponding to the method in sections 3.7.1 and 3.7.2.

Subsequently, the purified and non-purified standards were filtered using 0.45 µm filter, and injected into the HPLC system. The percentage of amoxicillin recovery was calculated using the following equation (3.2) based on concentration:

$$\text{Percentage Recovery} = \left(\frac{a}{b}\right) \times 100\% \quad (3.2)$$

which, a = concentration of purified amoxicillin solution while b = concentration of non-purified amoxicillin solution.

3.9.4 High Performance Liquid Chromatography (HPLC)

The extraction was performed using a C18 Agilent analysis reverse phase column (ZOBRAX SB-C18, 5 μm, 4.6 x 250 mm). The contaminants in the column were washed and eluted out using HPLC-grade acetonitrile (60:40) for 10 minutes before the separation process.

The mobile phase solvent was made by using phosphate buffer (KH_2PO_4) and acetonitrile (ACN). Approximately 6.825 grams of KH_2PO_4 powder was dissolved in 500 mL of sterile distilled water to produce 0.1M KH_2PO_4. To ensure a pH of 3.5, 10% (v/v) phosphoric acid was added and measured using a pH meter. After that, a vacuum pump with a 0.45 μm filter was used to sterilize the phosphate buffer. The system was a constituent of 0.1 M phosphate buffer (pH 3.5) and acetonitrile (40:60).

Analytical High-Performance Liquid Chromatography (Agilent 1200) was used to analyze residues of amoxicillin after biodegradation. To produce a result of clear peaks with less noise, the isocratic elution was conducted.

3.10 Determination of Fungal Biomass Concentration

The fungal biomass concentration was measured via the gravimetric method as utilized by (Saat *et al.*, 2014). The entire fermentation medium (100 mL) was filtered through a pre-weighed Whatman No. 44 filter paper. The broth obtained will be used for glucose residual and protein production concentration. The biomass on the filter was rinsed with sterile distilled water to ensure purity. The filter paper with the biomass was then dried in an oven at 60ºC until reaching a consistent weight. Once dried, it was cooled to room temperature in a desiccator and weighed to obtain the final biomass measurement. The filtered biodegradation medium is further used for glucose and protein determination.

3.11 Determination of Glucose Residual Concentration

The 3,5-Dinitrosalicylic acid (DNS) method was used to determine the biodegradation medium's residual glucose. The filtered broth will be used to detect residual glucose concentration.

3.11.1 Preparation of DNS reagent

In order to prepare the DNS reagent, 1.0% (w/v) DNS, 0.2% (v/v) phenol, 0.05% (w/v) sodium sulfite, and 1.0% (w/v) NaOH were dissolved together. The sodium sulfite was not added during preparation and the reagents were stored in an amber bottle at 4°C. Moving on to the Rochelle salt solution, 400g of the salt was dissolved in 1.0 liter of distilled water to achieve a 40.0% (w/v) solution.

3.11.2 Glucose Standard Curve Preparation

In order to achieve precise outcomes, a series of known concentrations were produced by diluting the glucose stock solution. Each test tube was filled with 3.0 mL of DNS reagent, followed by 3.0 mL of the diluted glucose solution with a known concentration. After covering the tube with aluminium foil, the tube was placed in a hot water bath at 95°C for 10 minutes. Following removal from the water bath, 1.0 mL (40%) of Rochelle salt was added, and the absorbance of the solution was measured at 575 nm. This process was repeated for each known glucose concentration, with distilled water serving as a blank. Finally, a glucose standard calibration plot was established, and the linear regression equation was used to determine the actual glucose concentration of the sample. The samples were run using the same procedure and concentration of glucose residual was measured using the standard curve.

3.12 Protein Concentration using Bradford Assay

The filtered broth will be used to measure protein concentration produced by *A. tamarii*. The Bradford assay was selected to determine the concentration of residual protein. Prior to use, the Bradford reagent was filtered. Nine dilution series of bovine serum albumin (BSA) were prepared, and 3 mL of Bradford reagent was added to nine test tubes. Then, 0.06 mL of each diluted protein solution was added to the

corresponding test tubes containing Bradford reagent. The mixture was incubated for 5 minutes at room temperature. Following incubation, the absorbance of each protein standard was measured at 595 nm using a spectrophotometer. Based on these results, a protein standard curve was constructed. The same procedure was repeated with the biodegradation product (Saat *et al.*, 2014) to determine its concentration. The product's concentration was determined based on the curve plotted. The same procedure was applied for biodegradation samples, and the concentration of protein was determined using the standard curve.

3.13 Kinetic Modelling

Utilizing unstructured kinetic models, the batch fermentation profiles of glucose concentration (*S*), biomass concentration (*X*), and protein concentration (*P*) were simulated according to Saat *et al.* (2014)The measurements were carried out with respect to time (t). Polymath 6.0, a mathematical software, was used to determine all kinetic parameters. Each kinetic variable was determined through non-linear regression.

3.13.1 Kinetic of Fungal Growth

The Verhulst-Pearl logistic model was used to describe the kinetics of fungal growth as in equation (3.3):

$$\frac{dX}{dt} = \mu_{max}(X)\left(1 - \frac{X}{X_{max}}\right) \tag{3.3}$$

Where d*X*/d*t* is the rate of biomass production (g L^{-1} day^{-1}), *X* is the biomass concentration (g L^{-1}), μ_{max} is the maximum specific growth rate (day^{-1}) and X_{max} is the maximum attainable biomass concentration (g L^{-1}).

The Equation 3.3 is reorganized as shown:

$$\frac{dX}{X}\left(\frac{1}{1-\frac{X}{X_{max}}}\right) = \mu_{max}(dt) \tag{3.4}$$

Introduce a new variable, K:

$$K = \frac{X}{X_{max}} \tag{3.5}$$

$$X = K(X_{max}) \tag{3.6}$$

$$\frac{dK(X_{max})}{K(X_{max})}\left(\frac{1}{1-\frac{K(X_{max})}{X_{max}}}\right) = \mu_{max}(dt) \tag{3.7}$$

Cancelling constant factor and rearrange the equation:

$$dK\left(\frac{1}{K(1-K)}\right) = \mu_{max}(dt) \tag{3.8}$$

Partial Fraction Equation

The left side of Equation 3.34 can be expressed as partial fractions expansion where *A* and *B* are unknown constants:

$$\frac{1}{K(1-K)} = \frac{A}{K} + \frac{B}{(1-K)} \tag{3.9}$$

Multiply with $K(1-K)$:

$$1 = A(1-K) + B(K) \tag{3.10}$$

$$1 = A - A(K) + B(K) \tag{3.11}$$

$$1 = A + (B-A)K \tag{3.12}$$

$$1 + 0K = A + (B-A)K \tag{3.13}$$

From the polynomial form in the Equation, constants *A* and *B* can be determined as follows:

$$0 = (B - A) \tag{3.14}$$

Where constant *A* can be determined directly from the Equation,

$$A = 1 \tag{3.15}$$

Therefore, *B* is:

$$0 = (B - 1) \tag{3.16}$$

$$B = 1 \tag{3.17}$$

Equation 3.8 is integrated using the partial fraction equation and substituted with constant *A* and *B*:

$$\int_{K_0}^{K} \left(\frac{1}{K} + \frac{1}{(1-K)}\right) dK = \mu_{max} \int_{0}^{t} (dt) \tag{3.18}$$

Since initial *t* is *t* = 0, therefore:

$$\ln|K|_{K_0}^{K} - \ln|1-K|_{K_0}^{K} = \mu_{max}(t)_0^t \tag{3.19}$$

$$\ln\left(\frac{|K|}{|1-K|}\right)_{K_0}^{K} = \mu_{max}(t-0) \tag{3.20}$$

$$\ln\left(\frac{|K|}{|1-K|}\right) - \ln\left(\frac{|K_0|}{|1-K_0|}\right) = \mu_{max}t \tag{3.21}$$

$$\ln\left(\frac{|K||1-K_0|}{|K_0||1-K|}\right) = \mu_{max}t \tag{3.22}$$

Solve and rearrange Equation 3.22:

$$\frac{(K)(1-K_0)}{(K_0)(1-K)} = e^{\mu_{max}t} \tag{3.23}$$

$$\frac{(K)}{(1-K)} - \left(\frac{K_0}{1-K_0}\right)e^{\mu_{max}t} \tag{3.24}$$

$$K = (1-K)\left(\frac{K_0}{1-K_0}\right)e^{\mu_{max}t} \tag{3.25}$$

$$K = \left(\frac{K_0}{1-K_0}\right)e^{\mu_{max}t} - \left(\frac{K(K_0)}{1-K_0}\right)e^{\mu_{max}t} \tag{3.26}$$

$$K + \left(\frac{K(K_0)}{1-K_0}\right)e^{\mu_{max}t} = \left(\frac{K_0}{1-K_0}\right)e^{\mu_{max}t} \tag{3.27}$$

$$K + \left(1 + \left(\frac{(K_0)}{1-K_0}\right)e^{\mu_{max}t}\right) = \left(\frac{K_0}{1-K_0}\right)e^{\mu_{max}t} \tag{3.28}$$

$$K = \frac{\left(\frac{K_0}{1-K_0}\right)e^{\mu_{max}t}}{1 + \left(\frac{K_0}{1-K_0}\right)e^{\mu_{max}t}} \tag{3.29}$$

$$K = \frac{K_0(e^{\mu_{max}t})}{(1-K_0) + K_0(e^{\mu_{max}t})} \tag{3.30}$$

From Equation 3.30, two variables, K and K_0 and since $K = \frac{X}{X_{max}}$, K_0 is equal as:

$$K_0 = \frac{X}{X_{max}} \tag{3.31}$$

Therefore:

$$\frac{X}{X_{max}} = \frac{\frac{X_0}{X_{max}}(e^{\mu_{max}t})}{\left(1 - \frac{X_0}{X_{max}}\right) + \frac{X_0}{X_{max}}(e^{\mu_{max}t})} \tag{3.32}$$

Rearrange:

$$\frac{X}{X_{max}} = \left(\frac{1}{X_{max}}\right)\frac{X_0(e^{\mu_{max}t})}{1 - \left(\frac{X_0}{X_{max}}\right)(1 - e^{\mu_{max}t})} \tag{3.33}$$

$$X = \frac{X_0(e^{\mu_{max}t})}{1 - \left(\frac{X_0}{X_{max}}\right)(1 - e^{\mu_{max}t})} \tag{3.33}$$

Finally, the logistic equation is written as follow:

$$X = \frac{X_0(e^{\mu_{max}t})}{1 - \left(\frac{X_0}{X_{max}}\right)(1 - e^{\mu_{max}t})} \tag{3.34}$$

3.13.2 Kinetic of Glucose Utilization

The kinetic study of glucose utilization is calculated using a hybrid Leudeking-Piret logistic model. The modified Leudeking-Piret (MLP) equation is added with new variables, *m* and *n*, and can be written as:

$$-\frac{dS}{dt} = m\left(\frac{dX}{dt}\right) + n(X) \tag{3.35}$$

Where m is the glucose quantity required for cell growth, and n is the amount of glucose for activity unrelated to growth. When Equation 3.45 is compared with Equation 3.34,

variables $m = 1/Y_G$ and $n = m_s$. By inserting the variables dX/dt and X from the logistic growth model into Equation 3.35:

$$-\frac{dS}{dt} = m\left(\mu_{max}(X)\left(1 - \frac{X}{X_{max}}\right)\right) + n\left(\frac{X_0(e^{\mu_{max}t})}{1 - \left(\frac{X_0}{X_{max}}\right)(1 - e^{\mu_{max}t})}\right) \quad (3.36)$$

Then, when the equation is rearranged:

$$-dS = m\left(\mu_{max}(X)\left(1 - \frac{X}{X_{max}}\right)\right)dt + n\left(\frac{X_0(e^{\mu_{max}t})}{1 - \left(\frac{X_0}{X_{max}}\right)(1 - e^{\mu_{max}t})}\right)dt \quad (3.37)$$

Using the initial condition $t = 0$ ($X = X_0$ and $P = P_0$), Equation 3.36 will be integrated and resulted as:

$$-\int_{S_0}^{S} dS = \int_0^t m\left[\mu_{max}(X)\left(1 - \frac{X}{X_{max}}\right)\right]dt + \int_0^t n\left[\frac{X_0(e^{\mu_{max}t})}{1 - \left(\frac{X_0}{X_{max}}\right)(1 - e^{\mu_{max}t})}\right]dt \quad (3.38)$$

$$-(S)_{S_0}^{S} = m\left[\frac{X_0(e^{\mu_{max}t})}{1 - \left(\frac{X_0}{X_{max}}\right)(1 - e^{\mu_{max}t})}\right]_0^t + n\left[\frac{X_{max}\ln\left(X_{max} - X_0 + X_0(e^{\mu_{max}t})\right)}{\mu_{max}}\right]_0^t \quad (3.39)$$

$$-(S - S_0) = m\left[\frac{X_0(e^{\mu_{max}t})}{1 - \left(\frac{X_0}{X_{max}}\right)(1 - e^{\mu_{max}t})} - X_0\right] + n\left[\frac{X_{max}\ln\left(X_{max} - X_0 + X_0(e^{\mu_{max}t})\right)}{\mu_{max}} - \frac{X_{max}\ln\left(X_{max} - X_0 + X_0(e^{\mu_{max}0})\right)}{\mu_{max}}\right] \tag{3.40}$$

$$S - S_0 = -m\left[\frac{X_0(e^{\mu_{max}t})}{1 - \left(\frac{X_0}{X_{max}}\right)(1 - e^{\mu_{max}t})} - X_0\right] - n\left[\frac{X_{max}\ln\left(X_{max} - X_0 + X_0(e^{\mu_{max}t})\right)}{\mu_{max}} - \frac{X_{max}\ln\left(X_{max} - X_0 + X_0(1)\right)}{\mu_{max}}\right] \tag{3.41}$$

$$S - S_0 = -m\left[\frac{X_0(e^{\mu_{max}t})}{1 - \left(\frac{X_0}{X_{max}}\right)(1 - e^{\mu_{max}t})} - X_0\right] - n\left[\frac{X_{max}\ln\left(X_{max} - X_0 + X_0(e^{\mu_{max}t})\right)}{\mu_{max}} - \frac{X_{max}\ln(X_{max})}{\mu_{max}}\right] \tag{3.42}$$

$$S - S_0 = -m\left[\frac{X_0(e^{\mu_{max}t})}{1 - \left(\frac{X_0}{X_{max}}\right)(1 - e^{\mu_{max}t})} - X_0\right] - n\left[\frac{X_{max}\ln\left(X_{max} - X_0 + X_0(e^{\mu_{max}t})\right)}{\mu_{max}} - \frac{X_{max}\ln(X_{max})}{\mu_{max}}\right] \tag{3.43}$$

$$S - S_0 = -m\left[\frac{X_0(e^{\mu_{max}t})}{1 - \left(\frac{X_0}{X_{max}}\right)(1 - e^{\mu_{max}t})} - X_0\right] - n\left[\ln\left(\frac{X_{max} - X_0 + X_0(e^{\mu_{max}t})}{X_{max}}\right)\left(\frac{X_{max}}{\mu_{max}}\right)\right] \tag{3.44}$$

Substitute $m = \frac{1}{Y_G}$ and $n = m_s$ to simplify the equation to obtain the final equation for MLP:

$$S - S_0 = -\frac{1}{Y_G}\left[\frac{X_0(e^{\mu_{max}t})}{1 - \left(\frac{X_0}{X_{max}}\right)(1 - e^{\mu_{max}t})} - X_0\right] - m_s\left[\ln\left(1 - \left(\frac{X_0}{X_{max}}\right)(1 - e^{\mu_{max}t})\right)\left(\frac{X_{max}}{\mu_{max}}\right)\right] \quad (3.45)$$

3.13.3 Kinetic of Protein Production

Leudeking-Piret model is also used for the kinetics of protein production. The equations have a constituent of coefficients to express the products and categorize into growth or non-growth associated. The Leudeking-Piret model's general equation is expressed as:

$$\frac{dP}{dt} = \alpha\left(\frac{dX}{dt}\right) + \beta X \quad (3.46)$$

Where *dP/dt* is the rate of protein production (g L^{-1} day^{-1}), *dX/dt* is the rate of biomass production (g L^{-1} day^{-1}), α is the coefficient for growth associated product (g g^{-1}), β is the coefficient for non-growth associated product (g g^{-1} day^{-1}) and *X* is the biomass concentration (g L^{-1}).

The variables *dX/dt* and *X* in equation and are substituted into Equation 3.46 due to the LP model integrated with a logistic model, which yields to:

$$\frac{dP}{dt} = \alpha\left[\mu_{max}(X)\left(1 - \frac{X}{X_{max}}\right)\right] + \beta\left[\frac{X_0(e^{\mu_{max}t})}{1 - \left(\frac{X_0}{X_{max}}\right)(1 - (e^{\mu_{max}t}))}\right] \quad (3.47)$$

Reorganized the equation to:

$$dP = \alpha\left[\mu_{max}(X)\left(1 - \frac{X}{X_{max}}\right)\right]dt + \beta\left[\frac{X_0(e^{\mu_{max}t})}{1 - \left(\frac{X_0}{X_{max}}\right)\left(1 - (e^{\mu_{max}t})\right)}\right]dt \quad (3.48)$$

Incorporate Equation with initial conditions where $t = 0$ ($X = X_0$ and $P = P_0$):

$$\int_{P_0}^{P} dP = \int_0^t \alpha\left[\mu_{max}(X)\left(1 - \frac{X}{X_{max}}\right)\right]dt + \int_0^t \beta\left[\frac{X_0(e^{\mu_{max}t})}{1 - \left(\frac{X_0}{X_{max}}\right)\left(1 - (e^{\mu_{max}t})\right)}\right]dt \quad (3.49)$$

$$(P)_{P_0}^{P} = \alpha\left[\frac{X_0(e^{\mu_{max}t})}{1 - \left(\frac{X_0}{X_{max}}\right)\left(1 - (e^{\mu_{max}t})\right)}\right]_0^t + \beta\left[\frac{X_{max}\ln\left(X_{max} - X_0 + X_0(e^{\mu_{max}t})\right)}{\mu_{max}}\right]_0^t \quad (3.50)$$

$$P - P_0 = \alpha\left[\frac{X_0(e^{\mu_{max}t})}{1 - \left(\frac{X_0}{X_{max}}\right)\left(1 - (e^{\mu_{max}t})\right)} - \frac{X_0(e^{\mu_{max}t})}{1 - \left(\frac{X_0}{X_{max}}\right)\left(1 - (e^{\mu_{max}0})\right)}\right] + \beta\left[\frac{X_{max}\ln\left(X_{max} - X_0 + X_0(e^{\mu_{max}t})\right)}{\mu_{max}} - \frac{X_{max}\ln\left(X_{max} - X_0 + X_0(e^{\mu_{max}0})\right)}{\mu_{max}}\right] \quad (3.51)$$

$$P - P_0 = \alpha\left[\frac{X_0(e^{\mu_{max}t})}{1 - \left(\frac{X_0}{X_{max}}\right)\left(1 - (e^{\mu_{max}t})\right)} - X_0\right] + \beta\left[\frac{X_{max}\ln\left(X_{max} - X_0 + X_0(e^{\mu_{max}t})\right)}{\mu_{max}} - \frac{X_{max}\ln\left(X_{max} - X_0 + X_0(1)\right)}{\mu_{max}}\right] \quad (3.52)$$

$$P - P_0 = \alpha \left[\frac{X_0(e^{\mu_{max}t})}{1 - \left(\frac{X_0}{X_{max}}\right)\left(1 - (e^{\mu_{max}t})\right)} - X_0 \right] + \beta \left[\frac{X_{max} \ln\left(X_{max} - X_0 + X_0(e^{\mu_{max}t})\right)}{\mu_{max}} - \frac{X_{max} \ln(X_{max})}{\mu_{max}} \right] \quad (3.53)$$

$$P - P_0 = \alpha \left[\frac{X_0(e^{\mu_{max}t})}{1 - \left(\frac{X_0}{X_{max}}\right)\left(1 - (e^{\mu_{max}t})\right)} - X_0 \right] + \beta \left[\left(\frac{X_{max}}{\mu_{max}}\right) \ln\left(X_{max} - X_0 + X_0(e^{\mu_{max}t})\right) - \ln(X_{max}) \right] \quad (3.54)$$

$$P - P_0 = \alpha \left[\frac{X_0(e^{\mu_{max}t})}{1 - \left(\frac{X_0}{X_{max}}\right)\left(1 - (e^{\mu_{max}t})\right)} - X_0 \right] + \beta \left[\left(\frac{X_{max}}{\mu_{max}}\right) \ln\left(\frac{X_{max} - X_0 + X_0(e^{\mu_{max}t})}{X_{max}}\right) \right] \quad (3.55)$$

The equation is simplified to a final solution for LP model integrated with logistic model:

$$P - P_0 = \alpha \left[\frac{X_0(e^{\mu_{max}t})}{1 - \left(\frac{X_0}{X_{max}}\right)\left(1 - (e^{\mu_{max}t})\right)} - X_0 \right] + \beta \left[\left(\frac{X_{max}}{\mu_{max}}\right) \ln\left(1 - \left(\frac{X_0}{X_{max}}\right)(1 - e^{\mu_{max}t})\right) \right] \quad (3.56)$$

3.14 Statistical Analysis and Model Fitting

Data analysis for FFD was determined by the statistical software Minitab 18. The significance level of the full model term and adequacy checking of FFD was determined by the *F*-value and *p*-value acquired from Analysis of Variance (ANOVA). The accuracy and quality of the model were determined by R^2 and adj-R^2 coefficients. Fermentation profiles for shake flask and STR were plotted using Microsoft Excel, and

kinetic models were constructed on Polymath 6.0. Second order polynomial regression for AMX biodegradation percentage (AMX%) was generated using MATLAB R2023A.

CHAPTER 4
RESULTS AND DISCUSSION

4.1 Screening of Significant Parameters for AMX Biodegradation by *A. tamarii*

Experimental design of FFD is utilized to find the significant parameters and their unique interaction effects by reducing the number of experimental trials of the full factorial design (Shanmugam *et al.*, 2022). Table 4.1 shows the experimental response for the percentage biodegradation of amoxicillin (AMX%) fractional design matrix conducted with 24 experimental runs. In order to reduce the effects of experimental error, the experimental sequence (Std Order) was randomised by Minitab 18 software. Results indicate that the percentage of biodegradation of amoxicillin (AMX%) was in the range of 37.14% to 87.54%. The huge range is most likely due to combinations of high and low factor levels. Factors include initial pH, agitation speed, incubation time and inoculum size strongly influence amoxicillin degradation through fungal growth and enzyme activity. The interactions between the factors can influence the degradation conditions positively or negatively. Hence, producing a wide range of AMX%. Evaluation of significant factors on percentage biodegradation of amoxicillin (AMX%) using ANOVA at significance level $\alpha = 0.05$ via Minitab 18 software, with normal probability plot, Pareto chart, main effects and contour plot were included in the analysis.

Table 4.1
Design Matrix for 2^{4-1} fractional factorial design and percentage biodegradation of amoxicillin (AMX%) measured.

StdOrder	RunOrder	Blocks	Initial pH	Incubation time (hrs)	Agitation Speed (rpm)	Inoculum size (µL)	AMX%
9	1	1	4	24	120	100	51.26
21	2	1	4	24	200	1000	40.05
24	3	1	8	96	200	1000	55.30
1	4	1	4	24	120	100	40.63
13	5	1	4	24	200	1000	44.82
17	6	1	4	24	120	100	41.08
4	7	1	8	96	120	100	44.29
3	8	1	4	96	120	1000	87.54*
5	9	1	4	24	200	1000	54.30
14	10	1	8	24	200	100	51.63
10	11	1	8	24	120	1000	37.14
7	12	1	4	96	200	100	49.13
8	13	1	8	96	200	1000	44.82
16	14	1	8	96	200	1000	42.03
6	15	1	8	24	200	100	38.85
18	16	1	8	24	120	1000	44.98
20	17	1	8	96	120	100	54.52
12	18	1	8	96	120	100	50.43
23	19	1	4	96	200	100	47.36
22	20	1	8	24	200	100	57.19
19	21	1	4	96	120	1000	81.77*
11	22	1	4	96	120	1000	85.24*
15	23	1	4	96	200	100	39.43

*The values showed the highest achieved AMX% by *A. tamarii*

4.2 Full Regression Model Analysis for AMX Biodegradation Percentage (AMX%)

ANOVA analysed the full analysis of the regression model for AMX% at a significance level of $\alpha = 0.05$. According to Table 4.2, the value of $p<0.05$ indicates that the model terms are significant to the response of this experiment. The high F and low p-values of the main effects and the two-way interactions implied that the factors contribute significantly to the percentage biodegradation of amoxicillin (AMX%) response . The model F-value and p-value were recorded at 15.33 and $p<0.05$, respectively. Thus, shows that the regression model is statistically significant. The R^2 obtained 0.8703, which indicates 87.0% of variations attributed to the percentage biodegradation of amoxicillin (AMX%) compared to 81.4% of R^2-adjusted. The difference between R^2 and R^2 (adj) values is 5.6%, which is considered not a dramatic

difference for a small sample size of reduced factorial design (Jankovic *et al.*, 2021). From the ANOVA, high R^2 values indicate a good fitting of experimental and prediction data, therefore suggesting that the regression model used in this study has high explanatory power (Bruno Siewe *et al.*, 2021). Based on both R^2, the overall analysis indicates a good agreement between the actual and predicted values.

Table 4.2
ANOVA of the regression model for percentage biodegradation of amoxicillin (AMX%)

Source	DF	Adj SS	Adj MS	F-Value	P-Value
Model	7	4069.4	581.34	15.33	0.000
Linear	4	1959.2	489.81	12.92	0.000
Initial pH	1	414.4	414.42	10.93	0.004
Incubation time	1	796.1	796.15	21.00	0.000
Agitation Speed	1	381.4	381.36	10.06	0.006
Inoculum size	1	367.3	367.31	9.69	0.007
2-Way Interactions	3	2110.1	703.37	18.55	0.000
Initial pH*Incubation time	1	403.7	403.69	10.65	0.005
Initial pH*Agitation Speed	1	695.4	695.42	18.34	0.001
Initial pH*Inoculum size	1	1011.0	1011.01	26.67	0.000
Error	16	606.6	37.91		
Total	23	4675.9			

R^2 = 87.0%
R^2-adjusted = 81.4%

Both R^2 and adjusted-R^2 are used to predict the accuracy of the current regression model of fungal biomass in antibiotic biodegradation studies. The difference between R^2 and adjusted-R^2 values from the current study denotes a good agreement between the actual and predicted values (Plonsky & Ghanbar, 2018; R. S. Singh *et al.*, 2020).

4.3 Pareto Chart of Standardized Effect for AMX Biodegradation Percentage (AMX%)

Figure 4.1 below displays the Pareto chart of standardized effects. This plot detects factors and interaction effects that are significant to the response (Antony, 2023). The vertical line in the chart shows the minimum statistically significant effect value for the 0.05 significance level. On the other hand, the length of the horizontal column corresponds to the degree of significance of the effects, respectively. If the factor or interaction surpasses the vertical line, it is deemed a significant effect toward the percentage biodegradation of amoxicillin (AMX%) or vice versa (Adio *et al.*, 2017; Razali *et al.*, 2021). According to the chart, all effects and interactions are significant. The sequence corresponds to results obtained from the regression model in Table 4.2 showing that the parameters are statistically significant ($p<0.05$), ranked in order of initial pH and inoculum size (Factor AD), incubation time (Factor B), initial pH and agitation speed (Factor AC), initial pH (Factor A), initial pH and incubation time (Factor AB), agitation speed (Factor C) and inoculum size (Factor D) being the least significant.

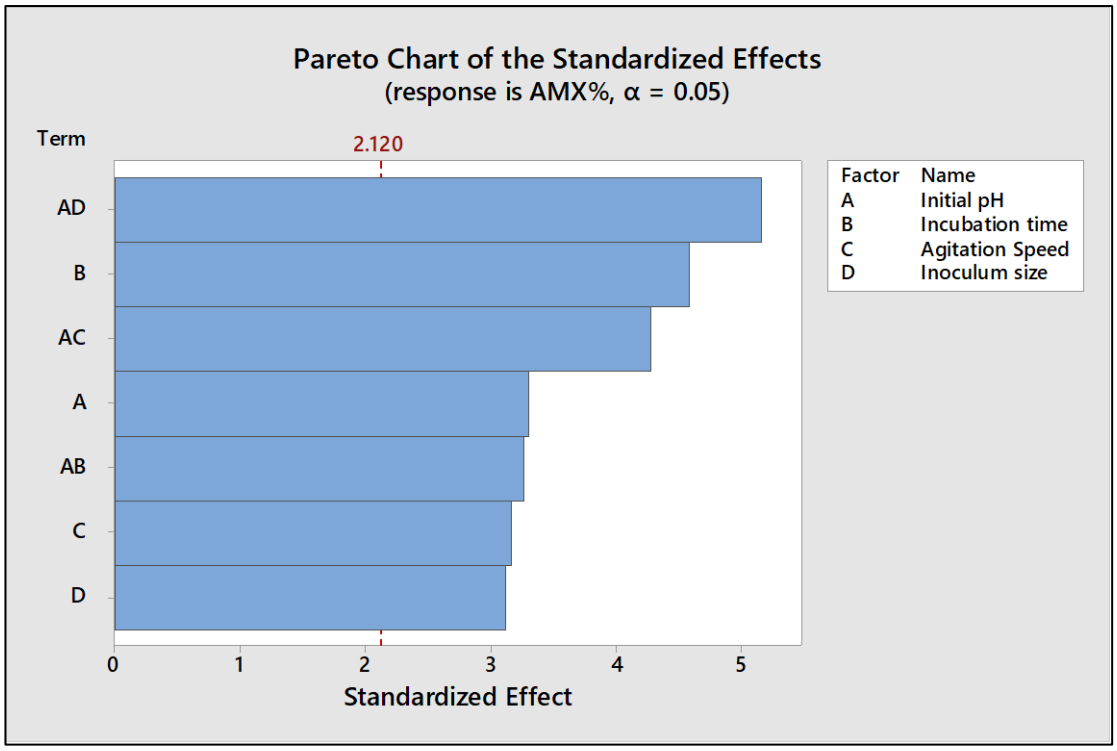

Figure 4.1. Pareto chart of the Standardized Effects for AMX%.

4.4 Main Effects Plot for Amoxicillin Biodegradation Percentage (AMX%) by *A. tamarii*

4.4.1 Incubation Time

Incubation time has the greatest influence towards AMX degradation. Table 4.2 shows that *F*-value and *p*-value of the main effect plot for incubation time at 21.00 and $p<0.05$, respectively, which indicates that incubation time is statistically significant. Figure 4.2 also displays a steep increasing slope from 24 hours to 96 hours inferring that those 96 hours of incubation time offer higher AMX% than 24 hours. Longer incubation time improves the biodegradation possibly due to enzyme activity and biosorption reaction (Hamad, 2020). Provided that the fungi have unlimited carbon sources during a long incubation period, the longer log phase may occur and simultaneously delay the presence of the stationary phase, followed by the declining phase (Yang *et al.*, 2012; Hamzah *et al.*, 2017). This resulted in more fungal biomass and better AMX biodegradation with increased incubation time. However, previous research also discovered that incubation time influences their desired reaction, and achieved maximum reaction after a specific amount of time (Barman *et al.*, 2015; Lahouar *et al.*, 2016; Melnichuk *et al.*, 2020). These studies suggest that a longer incubation period is not always ideal, especially when other parameters are not controlled. The activity of the enzymes may gradually decrease as time goes on with pH changes, which leads to inactivation and denaturation of the protein's 3D structure (Robinson, 2015). Therefore, having a specific incubation time with respect to an unlimited carbon source may provide maximal results for a specific process.

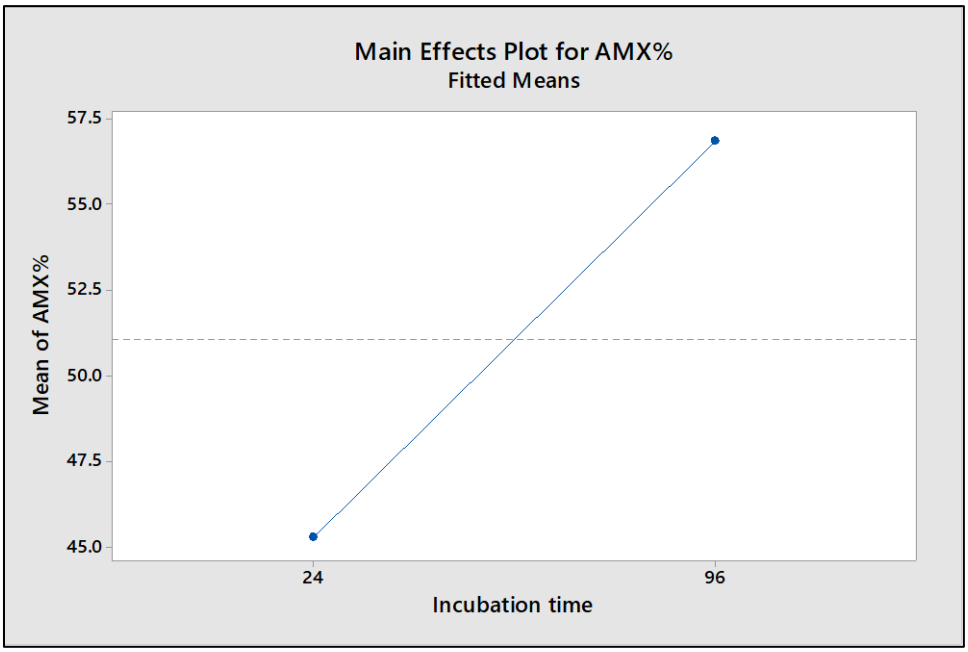

Figure 4.2. Main effects plot for incubation time.

4.4.2 Initial pH

Pareto chart displayed that pH is significant to the response. Table 4.2 shows that *F*-value of 10.93. with a *p*-value of $p<0.05$ indicating that pH is statistically significant towards the percentage biodegradation of AMX (AMX%). Figure 4.3 also displays a steep decreasing slope from pH 4.0 to 8.0 explaining that pH 4.0 offers maximum percentage biodegradation of AMX (AMX%) compared to pH 8.0. It has been known that pH influences fungal growth, spore germination, organic acid and enzyme production (Kosegarten *et al.*, 2017; Stevenson *et al.*, 2017; Akasaka *et al.*, 2018). Previous studies found that *A. tamarii* had maximum growth and bioactive compound production at low pH (Banjo *et al.*, 2019; Bose *et al.*, 2019; Batista *et al.*, 2020). Despite being able to grow over a wide pH, a high or low pH directly impacts the activity of enzymes secreted in the extracellular as optimal pH is significant for maximum activity (Markina-Iñarrairaegui *et al.*, 2020).

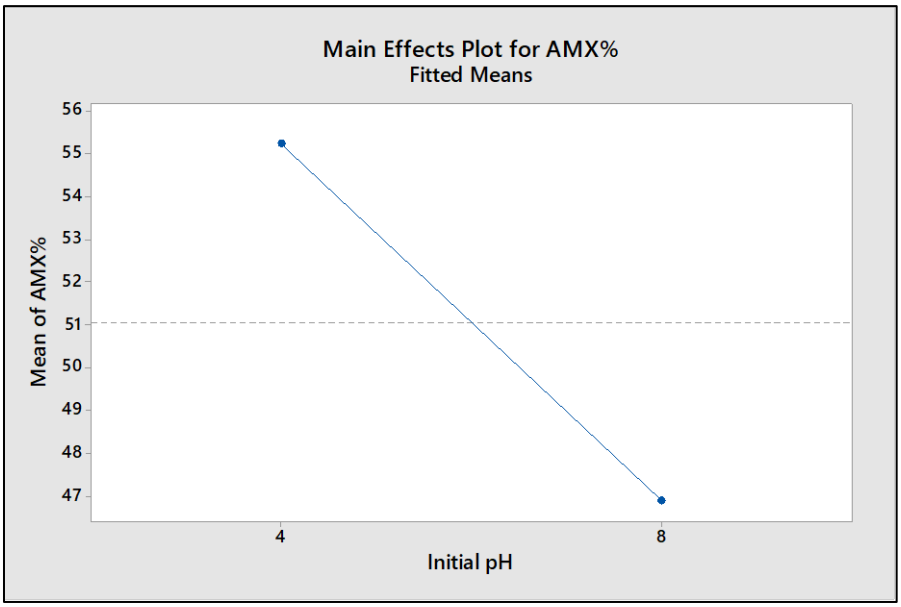

Figure 4.3. Main effects plot for pH.

4.4.3 Agitation Speed

Agitation speed significantly affects the response according to the respective F-value and p-value of 10.06 and $p<0.05$ (Figure 4.1 and Table 4.2). Figure 4.4 also displays a steep decreasing slope from 120 to 200 rpm, stating that 120 rpm offers an increased percentage biodegradation of AMX (AMX%) compared to 200 rpm. Previous research indicates that agitation speed influences the desired response (Miranti *et al.*, 2018; A'yuni & Ilmi, 2021). Different agitation speeds change the morphology and enzyme production of the fungi. At 0 rpm, the fungal floats on top of the surface medium forming a foam layer consisting of biomass entrapment at the surface of the medium (Elhussieny *et al.*, 2023). As the agitation speed increases, the fungal forms a spherical pellet and at high agitation speed, the pellet size decreases to smaller sizes and becomes dense due to high shear stress (Purwanto *et al.*, 2009; A'yuni & Ilmi, 2021). The optimal agitation speed may provide good dissolved oxygen and nutrient distribution for the fungi simultaneously improving their growth and biomass (Darah *et al.*, 2011; Kheirkhah *et al.*, 2023). Despite that, agitation may also induce shear stress, changes in morphology and possibly damage the cell structure (Ibrahim *et al.*, 2015; Banjo *et al.*, 2019; Buffo, Esperança, Béttega, *et al.*, 2020).

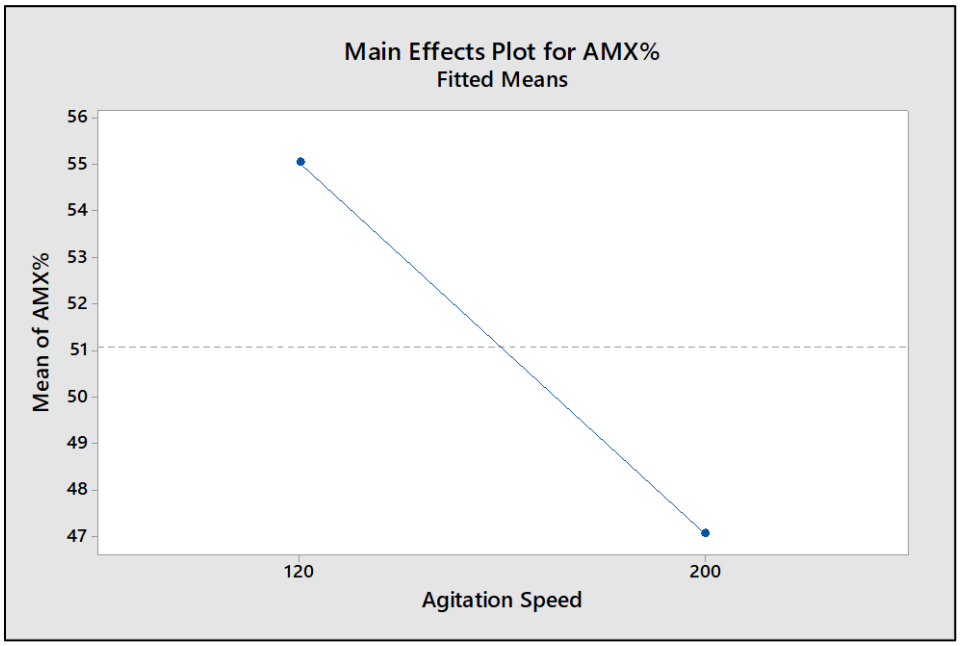

Figure 4.4. Main effects plot for agitation speed.

4.4.4 Inoculum Size

Inoculum size comes last compared to other parameters. However this factor continues to have a significant impact on the response of this experiment with *F*-values and *p*-values of 9.69 and $p<0.05$, respectively, as shown in Table 4.2. Based on Figure 4.5, a steep increasing slope from 100µL to 1000µL suggests that 1000µL of inoculum size offers a higher percentage of biodegradation compared to 100µL. An increase in inoculum size increases nutrient bioavailability and enzyme activity in the medium related to the process (van Kuijk *et al.*, 2016; Egbune *et al.*, 2023). Thus increasing the biodegradation of AMX by *A. tamarii.* On the other hand, according to previous literature, fermenting with a low inoculum size may cause insufficient cell biomass to utilize the available nutrients to conduct cellular growth (Dinarvand *et al.*, 2017). In addition, a further increase in inoculum size may cause an increase in the viscosity of the medium due to an increase in fungal growth, which affects the nutrient uptake of the cells (Adeoye *et al.*, 2015; Melnichuk *et al.*, 2020).

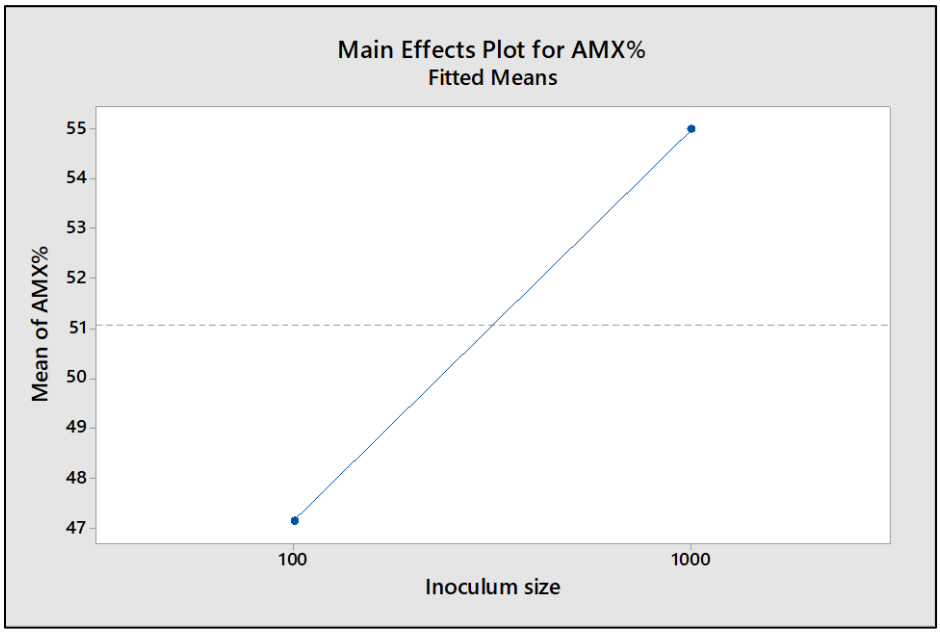

Figure 4.5. Main effects plot for inoculum size.

4.5 Contour plots of amoxicillin biodegradation percentage (AMX%) by *A. tamarii*

The contour plot is generated and visualized to study the interaction terms. The darker colours indicate a higher percentage of biodegradation of AMX (AMX%) values.

4.5.1 Inoculum Size and Initial pH

The interaction between inoculum size and initial pH has a significant effect on the response according to the Pareto chart in Figure 4.1 and ANOVA (Table 4.2), with the *F*-value of 26.67 with a *p*-value of $p<0.05$. Figure 4.6 displays that the maximum percentage biodegradation of AMX (AMX%) is achieved at the upper left of the plot, which is inoculum size at 1000µL and initial pH at 4.0. From the contour, the highest percentage biodegradation of AMX (AMX%) can be obtained when the inoculum size is increased and the pH level is decreased.

The interaction likely suggests that increasing the inoculum size of *A. tamarii* to its optimum increases the production of biomass and synthesis of extracellular enzymes, likely responsible for amoxicillin degradation (Adeyefa & Ebuehi, 2020). Simultaneously, a lower initial pH level is optimum to maximize enzymes and their catalytic activity as demonstrated in previous studies (Jalil & Ibrahim, 2021; Shi *et al.*, 2022; Mat Jalil *et al.*, 2023). Combining these two factors may have increased the

degradation of AMX as observed in the contour plot as high fungal biomass synthesize enzymes abundantly and function in their optimum environment.

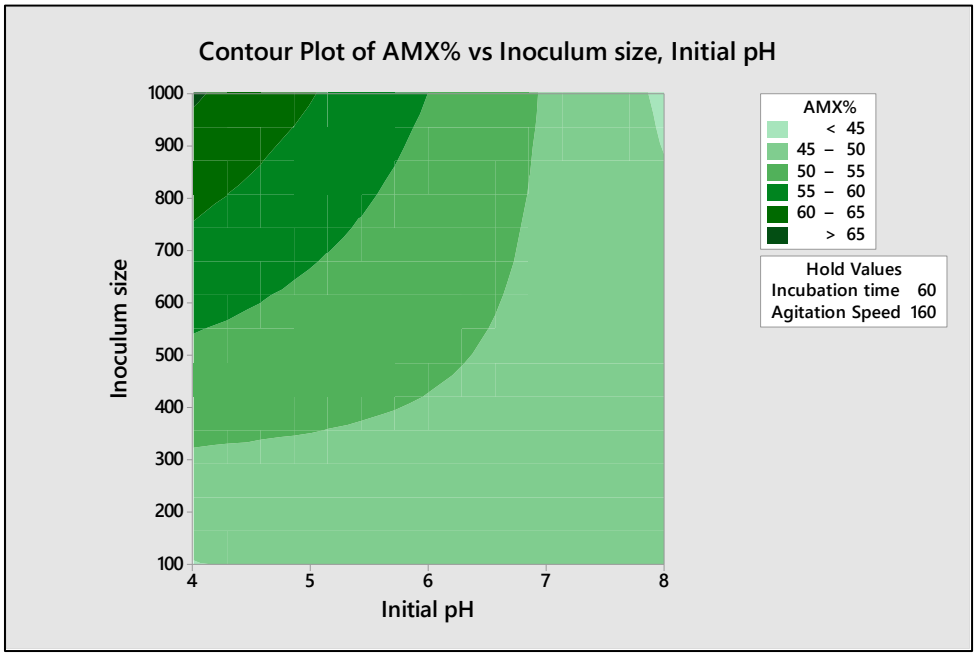

Figure 4.6. Contour plot for inoculum size and initial pH.

4.5.2 Agitation Speed and Initial pH

The interaction between agitation speed and pH significantly affects the response according to the Pareto chart in Figure 3.1 and Table 4.2, which showed an *F*-value of 18.34 with a *p*-value less than 0.05. Maximum percentage biodegradation of AMX (AMX%) is achieved at the bottom left of the plot with agitation speed at 120 rpm and initial pH at 4.0, as shown in Figure 3.7. The contour plot shows that when agitation speed and initial pH increase, the percentage biodegradation of AMX (AMX%) is negatively impacted.

Increasing the agitation speed leads to an increase in shear stress, potentially harming the fungi hyphae and enzyme production (Banjo *et al.*, 2019). Low agitation speed at 120 rpm suggests that the nutrient and oxygen distribution is sufficient, coupled with mildly acidic pH that may enhance the activity of enzymes for AMX biodegradation (Shi *et al.*, 2022). Thus, optimal AMX biodegradation occurs with gentle mixing and mildly acidic conditions that are favorable for fungal growth and enzyme activity.

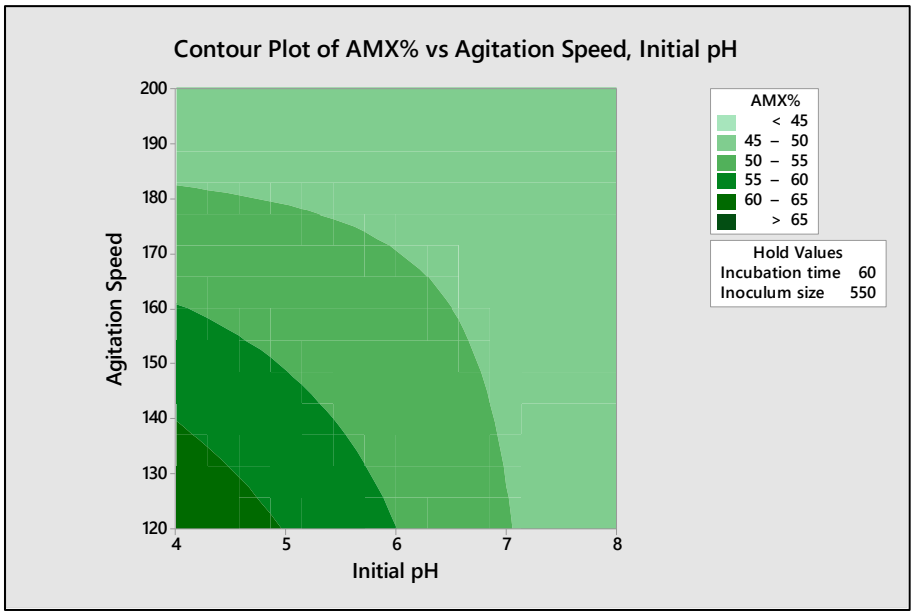

Figure 4.7. Contour plot for agitation speed and initial pH.

4.5.3 Incubation Time and Initial pH

The interaction between incubation time and pH significantly affects the response according to the Pareto chart in Figure 3.1. The chart is supported by Table 4.2, which shows an *F*-value of 10.65 with a *p*-value less than 0.05. According to Figure 4.8, the maximum percentage biodegradation of AMX (AMX%) is achieved at the upper left of the plot with an incubation time of 96 hrs and an initial pH of 4.0. The contour plot demonstrates that the percentage biodegradation of AMX (AMX%) is at its highest when incubation time increases while initial pH decreases.

Longer incubation time helps the fungi to receive sufficient nutrients and produce the necessary extracellular enzymes involved in AMX biodegradation (Yang *et al.*, 2012). Additionally, acidity of pH 4.0 offers optimal environment for enzyme activity, contributing to high degradation efficiency (Shi *et al.*, 2022) The synergy between the extended incubation time and acidic environment likely provided sufficient time to consume available nutrients in the medium and prolonged enzymatic activity for effective AMX biodegradation.

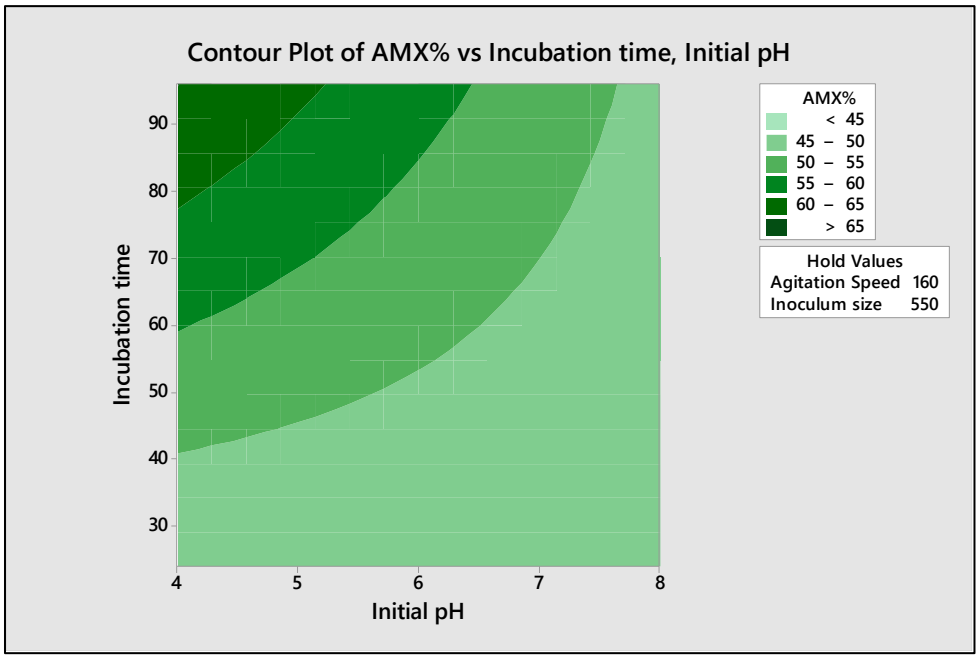

Figure 4.8. Contour plot for incubation time and pH.

4.6 Regression Model for Percentage Biodegradation of AMX (AMX%).

Table 4.3 presents the estimated effects and regression coefficients (Coef) including the standard deviation (SD_{coef}), t-statistics (T) and probability (P) values, for the main effects and second-order interaction terms. The regression equation is generated from the least squares method by the Minitab software.

Regression Equation in Uncoded Units

$$AMX\% = 85.4 - 5.46\ Initial\ pH + 0.502\ Incubation\ time - 0.5034\ Agitation\ Speed + 0.005196\ Inoculum\ size - 0.0570\ Initial\ pH * Incubatio\ time + 0.0673\ pH * Agitation\ Speed - 0.00721\ Initial\ pH * Inoculum\ size$$

Table 4.3
Estimated effects and coefficients of the regression model for percentage biodegradation of AMX (AMX%).

Term	Effect	Coef	SE Coef	*T*-Value	*p*-Value	VIF
Constant		51.06	1.26	40.63	0.000	
Initial pH	-8.31	-4.16	1.26	-3.31	0.004	1.00
Incubation time	11.52	5.76	1.26	4.58	0.000	1.00
Agitation Speed	-7.97	-3.99	1.26	-3.17	0.006	1.00
Inoculum size	7.82	3.91	1.26	3.11	0.007	1.00
Initial pH*Incubation time	-8.20	-4.10	1.26	-3.26	0.005	1.00
Initial pH*Agitation Speed	10.77	5.38	1.26	4.28	0.001	1.00
Initial pH*Inoculum size	-12.98	-6.49	1.26	-5.16	0.000	1.00

The model equation reveals that the four main effects and three interaction effects significantly influence the percentage biodegradation of AMX (AMX%) response. The positive coefficients for incubation time, inoculum size, and initial pH*agitation speed indicate their favorable influence on the response, on the other hand, the negative coefficient for initial pH, agitation speed, initial pH*incubation time, and initial pH*inoculum size reflects an antagonistic effect. This indicates that the high level of incubation time, inoculum size, and initial pH*agitation speed enhances the percentage biodegradation of AMX (AMX%), while high level of initial pH, agitation speed, initial pH*incubation time, and initial pH*inoculum size tends to deteriorate it.

4.7 Model Adequacy Checking

In order to ensure the validity and reliability of the FFD analysis, model adequacy was validated by using normal probability plot with standardized residuals as a tool for analysis (Sony & Marriapan, 2021). The normal probability plot is used as it is an effective and straightforward procedure. Figure 4.9 shows a normal probability plot of standardized residual. The plot displays that all points are close to the reference line and fall within the interval of -2 and +2 of standardized residual, suggesting no outliers. This also indicates that the plot is normally distributed. Furthermore, the model proposed is adequate and can be used for further calculations (Montgomery, 2017).

Contrastly, a study have found that the use of fractional factorial instead of full factorial may contribute to the presence of outliers (Shabbir *et al.*, 2019).

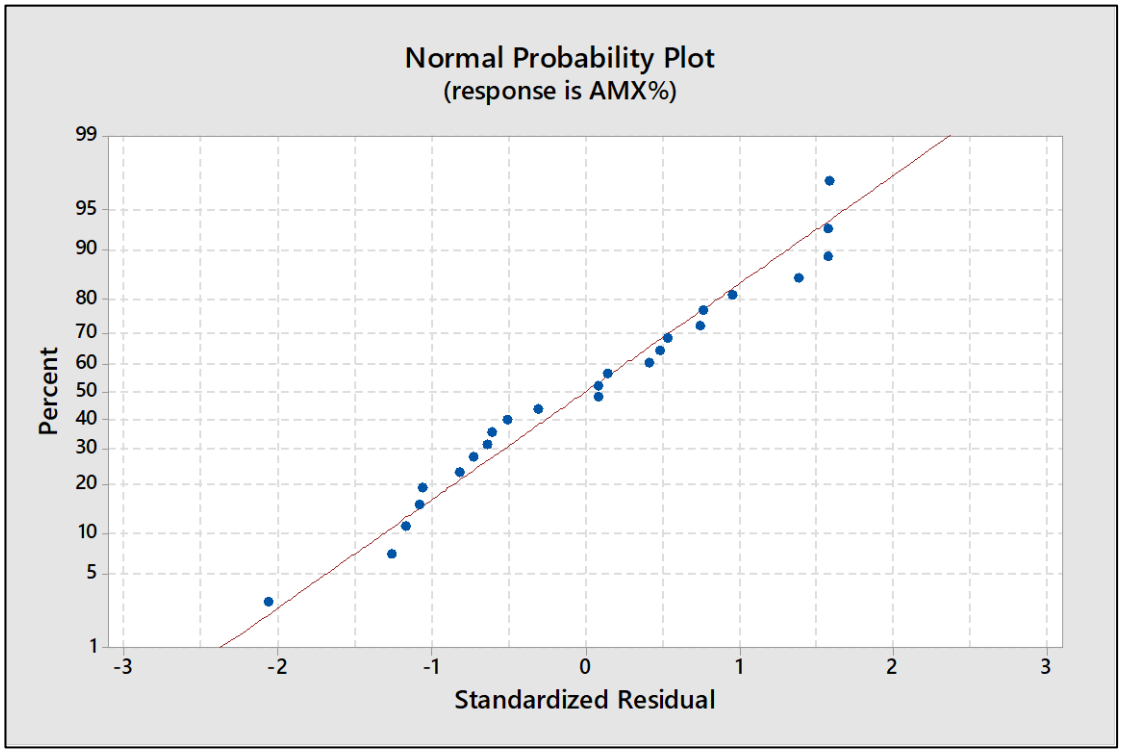

Figure 4.9. Normal probability plot of standardized residuals.

4.8 Response Optimizer for Significant Parameters

In Figure 4.10, the response optimizer plot for maximum percentage biodegradation of AMX (AMX%) by *A. tamarii* was generated by Minitab software. The plot produced a combination set of optimal parameters: initial pH 4, agitation speed of 120 rpm, incubation time of 96 hrs and inoculum size of 1000 µL. Based on these optimized parameters, the model predicts an 84.85% biodegradation of AMX (AMX%) using *A. tamarii*.

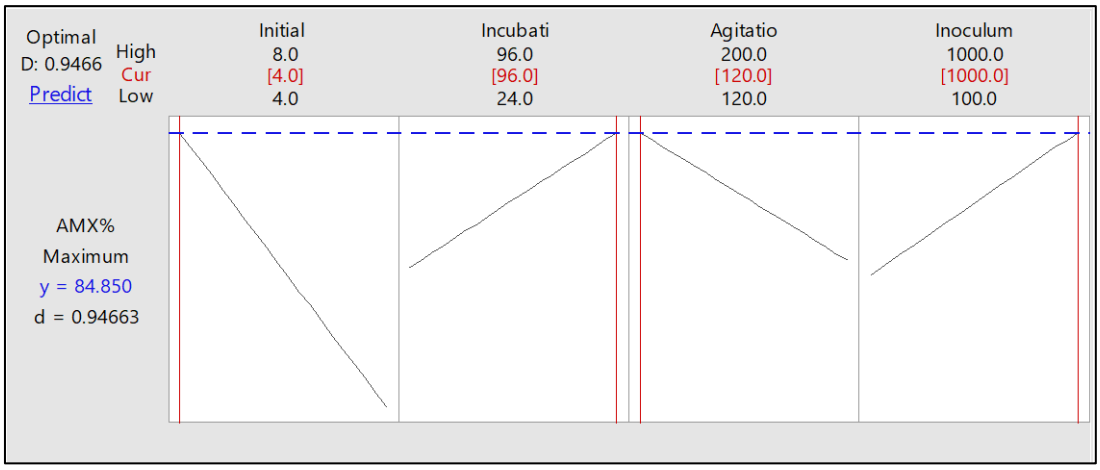

Figure 4.10. Response Optimizer for Percentage Biodegradation of AMX (AMX%).

Achieving a specific set of conditions would be favourable for the microorganisms and their enzymes to achieve optimal degradation. Our current study shows that initial pH 4.0, agitation speed of 120 rpm, incubation time of 96 hrs and inoculum size of 1000 µL achieved a significant biodegradation towards AMX. A research by Cai *et al.* (2023) discovered that *Trichoderma pubescens* from activated sludge has a removal efficiency of >98% in 24 hours. In the alkaline environment, the *T. pubescens* degraded AMX by uncoupling the hydroxyl group on the lactam ring and assisted with hydrolysis. According to Lueangjaroenkit *et al.* (2019), the fungi were able to deactivate amoxicillin by 100% within 5 days using purified manganese peroxidase (MnP_2) synthesized and excreted by a white rot fungi called *Trametes polyzona.* The enzymes were optimal at pH 4.5 and stable at a pH range from 4.0 to 8.0. A report found that *B. subtilis* were able to degrade 93.94% of amoxicillin with optimized parameters, which were 10.38 days incubation time, initial bacteria concentration of 5.57 $\log_{10}$ CFU mL^{-1} and final pH range from 5.0 to 7.5 (Al-Gheethi *et al.*, 2019). It was suggested that the β-lactamase enzyme degrades amoxicillin in an acidic environment, pH 3.0 and above. The enzyme cleaves the lactam group only, transforming amoxicillin into amoxicillin penicillanic acid. The product will then hydrate to amoxicillin penamaldic acid and degraded to amoxicillin penicillamine and amoxicillin penaldic. The amoxicillin penaldic will then lose CO_2 to generate penicillioldehyde (Al-Gheethi *et al.*, 2019). Present study demonstrates that high percentage of AMX biodegradation was achieved using fungus within a shorter timeframe (96 hours), and under initial acidic conditions of pH 4.0. Therefore, our study proved that *A. tamarii* is useful for bioremediation purposes after optimised. Further

analysis must be conducted to identify its degradation pathways and the enzymes responsible to conclude its application in large scale and on-site utilization.

4.9 Validation Experiment of Response Optimizer

Degradation was conducted using the optimized conditions (initial pH 4.0, 120 rpm, 96 hrs and 1000 µL). In the validation experiment, a triplicate run was carried out. The percentage biodegradation of AMX (AMX%) recorded from the triplicate run yielded a mean of 81.18±2.5% (mean±SD). Based on the prediction value by the software from the response optimizer, which suggested an 84.85% biodegradation percentage, the validation run fell around the range of the predicted value. This is due to a less than 5% difference between the predicted and actual values. The 95% confidence interval (CI) was also carried out for the triplicate data to validate further. The CI was (74.27%, 88.09%) which suggested that the true degradation percentage falls within the range. The predicted value of 84.85% falls within the interval range, indicating consistency with the experimental results. Results showed that the conditions were one of the best yet in achieving optimum percentage biodegradation of AMX (AMX%) using *A. tamarii*. Hence, the FFD utilized in this study is successful as it improved the process by enhancing the biodegradation of AMX by *A. tamarii* in shake flask.

4.10 Fermentation Profiles of *A. tamarii* in shake flasks

Submerged fermentation of *A. tamarii* with and without the presence of AMX is studied in aspects of fungal biomass, glucose utilization and protein production. The fermentation was carried out for 10 days using optimized parameters obtained from FFD, with the kinetics constant was calculated. The conditions for growing the fungal were kept the same, which were an initial pH of 4.0, incubation of 240 hours, inoculum size of 1000 µL and agitation speed of 120 rpm.

4.10.1 Fungal Growth Profiles With and Without the Presence of AMX

Effect of AMX towards the growth of *A. tamarii* using submerged fermentation is evaluated.

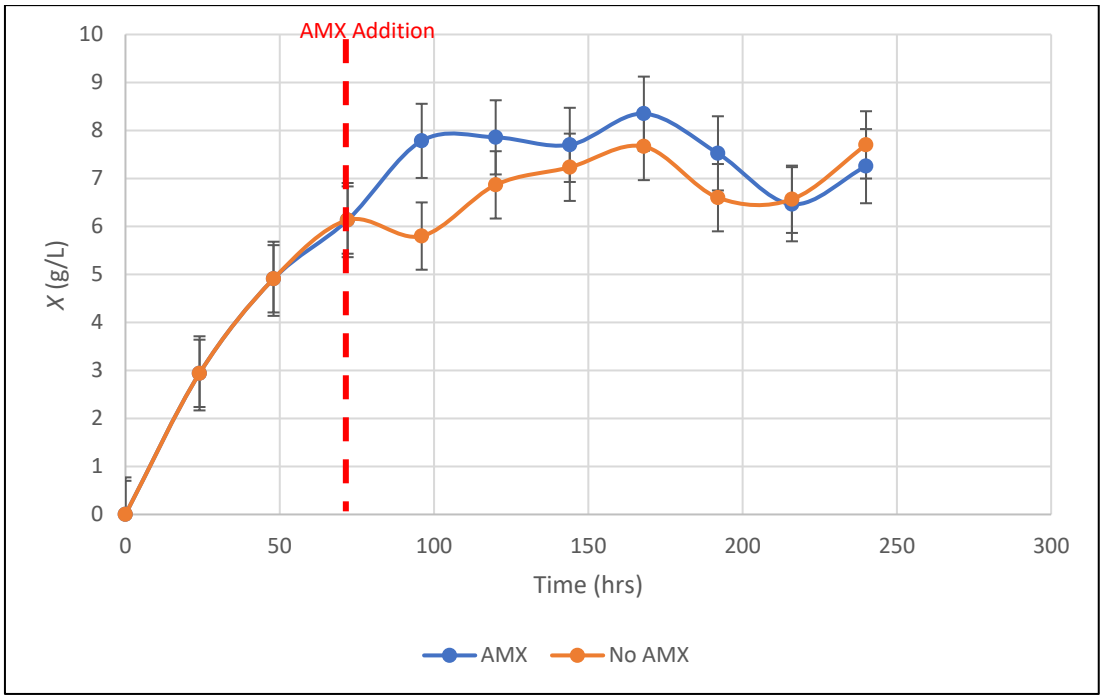

Figure 4.11. Fungal growth profile of *A. tamarii* in the presence and absence of AMX.

Figure 4.11 indicates that the fungal biomass showed similar growth patterns until 72 hours. After 72 hours, the biomass with the presence of AMX grew slightly higher than without AMX. *A. tamarii* reached maximum growth of 8.35 g/L at 168 hours in the presence of AMX. On the other hand, it grew to a maximum growth of 7.7 g/L in the absence of AMX at 240 hrs. ANOVA was conducted to determine whether there is a statistical difference between presence and absence of AMX across eleven incubation times (0-240 hrs). The *p*-value was higher than the significance level (α = 0.05). Therefore, the null hypothesis cannot be rejected. This concludes that no statistical significant difference was observed between the mean biomass in the presence and absence of AMX. Results showed that not only *is A. tamarii* greatly resistant to antimicrobial activity by AMX, but it may also contribute to its growth. A study also found that the effect of β-lactam antibiotic on white rot fungus *Verticillium leptobactrum* was insignificant towards its growth (Kumar *et al.*, 2013). Other than that, for *Aspergillus* species, degradation commonly leads to gaining nutrients for growth. This species exhibit the ability to secrete enzymes according to the available carbon sources to maximise their growth (Kowalczyk *et al.*, 2014).

4.10.2 Glucose Utilization Profiles With and Without the Presence of AMX

The comparison between the consumption of glucose by *A. tamarii* with and without the presence of AMX is evaluated. Glucose is the main carbon source for growth, which is a simple sugar, to provide as the primary source of energy for the cells. Chen *et al.* (2023) reported that β-lactam antibiotic degradation was improved when glucose was used as a co-metabolic substrate. Glucose or D-glucose can be phosphorylated to D-glucose-6-phosphate to undergo the pentose phosphate pathway or transformed to D-fructose-6-phosphate and enter glycolysis (Khosravi *et al.*, 2015).

According to Figure 3.12, glucose was consumed at a similar rate until 72 hours. After AMX was spiked in the shake flask, glucose consumption was slightly reduced compared to without AMX at 96 and 120 hrs. However, further incubation showed that shake flasks with AMX have a slightly higher amount of glucose consumed compared to those without AMX. This pattern mirrors the fungal growth profile demonstrated in Figure 4.11, where *A. tamarii* in the presence of AMX eventually achieved higher biomass.

In order to determine whether there is a statistical difference between presence and absence of AMX across eleven incubation times (0-240 hrs), ANOVA was conducted. The *p*-value exceeded the significance level ($\alpha = 0.05$), so the null hypothesis could not be rejected. This suggests no statistically significant difference in glucose consumption between the two conditions. This complements with a research which found that ciprofloxacin antibiotic degradation using activated sludge increased when the carbon source concentration (i.e. glucose) was increased (Nguyen *et al.*, 2018). According to research by Peng *et al.* (2020), the microbial consortium culture was positively improved in terms of relative abundance when glucose was mixed with tetracycline hydrochloride compared to pure glucose culture. A study also found that the maximum degradation of sulfamethoxazole obtained was due to organic substances found in swine manure leachate medium, including glucose. This supports co-metabolism of the antibiotic, therefore improving the degradation of sulfamethoxazole by anaerobic microorganisms (Xu *et al.*, 2011; Wang *et al.*, 2021). These findings highlight that degradation of antibiotics by microbial cultures is affected by glucose consumption and does not inhibit their growth. It can be concluded similarly for *A. tamarii*'s glucose metabolism unaffected by the presence of AMX, especially at the tested concentration.

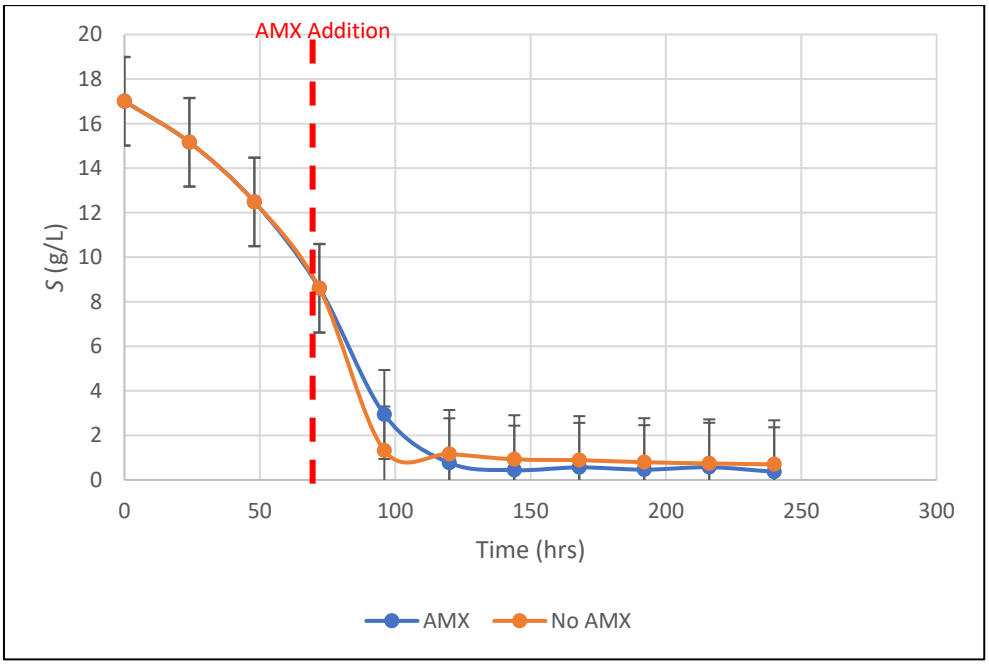

Figure 4.12. Glucose utilization profile of *A. tamarii* in the presence and absence of AMX.

4.10.3 Protein Production Profiles With and Without the Presence of AMX

The protein production as shown in Figure 4.13, indicates that both with AMX and without AMX have slightly similar patterns. Both had peak production occurring at the 96th hour of incubation. The peaks may suggest that the optimal phase for protein synthesis under both conditions is at the 96th hour which indicates the fungal's exponential phase as shown in glucose utilization (Figure 4.12) and fungal growth (Figure 4.11) of *A. tamarii*. During this phase, cells undergo primary metabolic pathways and produce metabolites such as amino acids, enzymes, proteins and organic acids, which are significant to cell growth (Walker & White, 2017; Gupta & Gupta, 2021). Despite that, it can be observed that shake flasks without AMX produced slightly more protein yield than shake flasks with AMX especially from 72 hours to 120 hours of incubation. This may imply a minor inhibitory effect of AMX on protein synthesis. However, the difference in protein production in both fermentations can be concluded as insignificant as the difference is not large enough to assume its impact on overall protein production.

An ANOVA test was performed to assess whether there is a statistical difference between the presence and absence of AMX across eleven incubation times (0-240 hrs). The null hypothesis was not rejected since the p-value was greater than the

significance level ($\alpha = 0.05$). This implies that the difference was statistically insignificant. Furthermore, the decrease in protein concentration after 192 hours is most likely influenced by the limiting substrate available in the medium, as glucose was almost depleted, as seen in Figure 4.12. As the main carbon source diminishes, the cells enter a stationary or death phase and any metabolic activity is reduced. Thus, protein production is reduced as well. Current findings may conclude that the presence of AMX has a negligible effect on the protein yield since both conditions reached peak production at the same hour.

Collectively, these findings showed a coordinated response by *A. tamarii* where growth, glucose consumption and protein production are maintained despite the presence of AMX in the environment. This further supports the potential of the fungus to degrade β-lactam antibiotics for wastewater treatment.

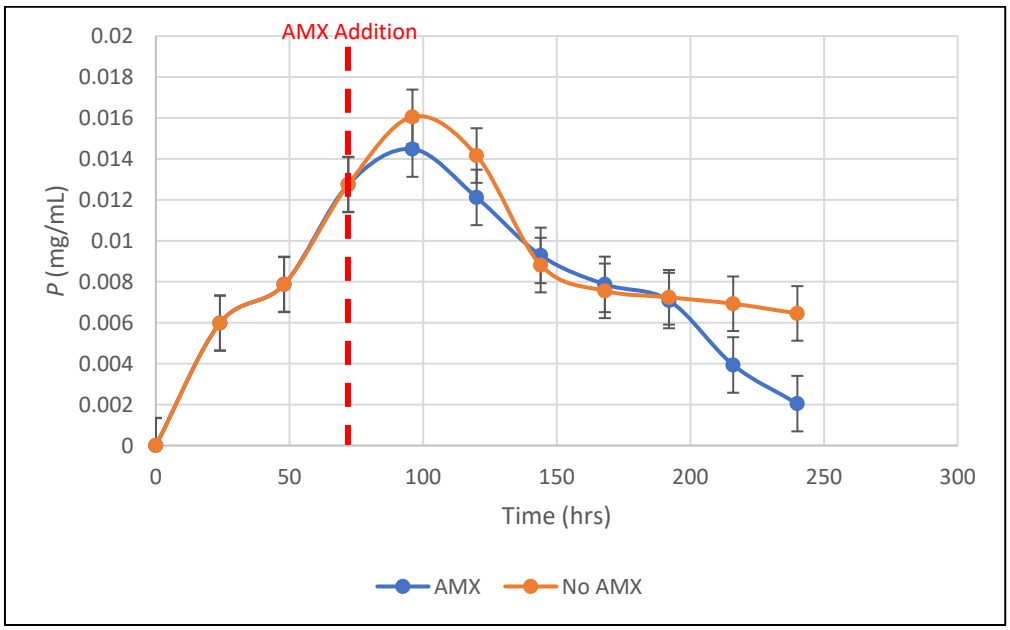

Figure 4.13. Protein production profile of *A. tamarii* in the presence and absence of AMX.

4.10.4 Kinetic Parameters Estimation

Experiments were conducted using batch fermentation to investigate the kinetic studies of amoxicillin (AMX) biodegradation by *A. tamarii* in the presence and absence of AMX. The kinetic parameters, including the rates of biomass formation (dX/dt), glucose utilization (dS/dt), and protein production (dP/dt), were determined by solving the corresponding differential equations through non-linear regression analysis as

shown in Table 4.4. The software Polymath 6.0 was employed to solve these non-linear equations and derive the kinetic parameters.

Table 4.4
Kinetic parameters of fungal growth, glucose consumption and protein production in the presence and absence of AMX

Kinetic Model	Parameters	Presence of AMX	Absence of AMX
Fungal Growth	X_0 (g L^{-1})	0.76 (± 0.67)	0.81 (± 0.97)
	X_{max} (g L^{-1})	7.54 (± 0.56)	6.95 (± 0.58)
	μ_{max} (day^{-1})	1.42 (± 0.58)	1.44 (± 0.87)
Glucose Consumption	Y_G (g g^{-1})	0.62 (± 0.19)	0.56 (± 0.20)
	m_s (g g^{-1} day^{-1})	0.11 (± 0.08)	0.12 (± 0.10)
Protein Production	α (g g^{-1})	0.003 (± 0.0003)	0.003 (± 0.0006)
	β (g g^{-1} day^{-1})	-2.507×10^{-4} ($\pm$ 5.33×10^{-5})	-2.026×10^{-4} ($\pm$ 8.97×10^{-5})

4.10.5 Kinetics of Fungal Growth

This study evaluated the kinetic parameters of fungal growth, maximum specific growth rate (μ_{max}) and maximum cell growth (X_{max}) for both the presence and absence of AMX in the fermentation flask using Verhulst-Pearl logistic growth model as presented in Table 4.4. The logistic growth model is a common and easily fitted model to microbial growth which makes it a widely used model (Goveas & Sajankila, 2020). The X_{max} values for both cultures were similar. Cultures with AMX had 7.54 g L^{-1} and 6.95 g L^{-1} for cultures without AMX. Abd Rahim and Saari (2018) investigated fermenting *A. oryzae* NSK in glucose and resulted in similar X_{max} values. The μ_{max} for culture containing AMX was 1.42 day^{-1} and 1.44 day^{-1} for culture in the absence of AMX, showing that the values are similar as well. The results indicate that AMX may have no inhibitory effect towards the growth of *A. tamarii*. Conversely, it was reported by Mohamad *et al.* (2024), that the growth of *A. tamarii* was reduced significantly when administering Nitrofurazone (0.529 g L^{-1}) compared to culture without Nitrofurazone (0.327 g L^{-1}), indicating antifungal properties towards the fungus. This may suggest that *A. tamarii* exhibits specific resistance towards AMX (categorized in β-lactam antibiotics), but not against Nitrofurazone. Previous research has investigated the effect of AMX on *A. flavus* and found that the antibiotic was ineffective in retarding the fungi's growth when administered below the concentration of 4000 µg/mL and below (Day *et al.*, 2009). This aligns with the current study, with the *A. tamarii* culture spiked

with an AMX concentration of 100 μg/mL (<4000 μg/mL). Furthermore, this is possibly due to the ability of the fungi to synthesize enzymes which can degrade AMX, but in low concentrations. Ji *et al.* (2021) reported in which found that *A. niger* exhibit minimal β-lactamase activity (0.02 ± 0.01 U/g). Further studies must be conducted to demonstrate *A. tamarii* ability to synthesize relevant enzymes or possibly, resistance mechanisms towards AMX.

4.10.6 Kinetics of Glucose Utilization

The kinetic model for glucose consumption was derived from the Verhulst-Pearl logistic growth model. This model describes the population dynamics of growth in a closed habitat (Gatto *et al.*, 1988). According to the substrate consumption equation, biomass yield coefficient over a substrate, Y_G and maintenance coefficient, m_s for fermentation with AMX are 0.62 g g^{-1} and 0.11 g g^{-1} day^{-1}, respectively. On the other hand, the Y_G and m_s for fermentation without AMX are 0.56 g g^{-1} and 0.12 g g^{-1} day^{-1}, respectively. The close values in Y_G may imply that the fungus is consistently efficient when utilizing glucose for biomass growth, regardless of the presence of AMX. Glucose as substrate is recognized to promote high fungal growth due to its role as sole carbon source (Xie *et al.*, 2017; Wang *et al.*, 2020). The similar values of m_s may indicate that the energy required for cell maintenance functions is not affected by the presence of AMX. No significant increase in energy demand is observed to adapt to AMX, implying the antibiotic at this concentration does not induce stress. Pusztahelyi *et al.* (2011) found that various enzymes are synthesized for carbon metabolism, such as glycolysis, gluconeogenesis, and the pentose phosphate shunt when *A. nidulans* responds under stress. Energy is produced as a stress defense. In comparison with Mohamad *et al.* (2024)'s study, where nitrofurazone is spiked into *A. tamarii* culture, the value of Y_G (0.139 g g^{-1}) was lower. In comparison, m_s (0.239 g g^{-1} day^{-1}) was higher, which explains that cell maintenance is favored over cell growth due to inhibition of the antibiotic towards the fungus (Emri *et al.*, 2015). The type and strength of stress significantly affects the maintenance and growth of the fungus. Results obtained from μ_{max} and X_{max} are consistent to the Y_G and m_s. Both fermentation flasks in the presence and absence have similar values, suggesting AMX did not influence the consumption of glucose by *A. tamarii*.

4.10.7 Kinetics of Protein Production

Kinetics of protein synthesis was fitted into Leudeking-Piret equation which is commonly used for product formation. According to the equation's nonlinear regression analysis, the kinetic parameters obtained for protein formation for growth associated α and non-growth associated β for culture with the presence of AMX are 0.003 g g^{-1} and -2.507 x 10^{-4} g g^{-1} day^{-1}, respectively. The α and β parameters were also calculated for fermentation in the absence of AMX and have close values to culture with the presence of AMX. The values are 0.003 g g^{-1} and -2.026x10^{-4} g g^{-1} day^{-1}, respectively. The product formation is unrelated to growth, hence the value of non-growth associated β can be positive, negative or zero (Singh & Srivastava, 2014). The kinetic profile indicates that protein production is growth-associated due to positive values of α with respect to the non-growth associated coefficient β which is negative. It was observed in a previous study that nitrofurazone affects *A. tamarii*'s protein production, by inducing both growth and non-growth associated proteins (Mohammad *et al.*, 2018). Under stressful circumstances, the fungus may produce various enzymes such as catalases, superperoxidase dimutases and mitogen-activated protein kinase to overcome harsh environments, increasing its protein production (Abdel-Hadi *et al.*, 2012). It was also discovered that *Phanerochaete chrysosporium* had a higher coefficient β than α on ligninolytic enzyme production, proposing that these enzymes are produced only in the presence of lignin and not necessarily as a secondary product (Shi *et al.*, 2014). Furthermore, in relation to previous results of fungal growth and glucose consumption, the findings agree with each other. The presence of AMX did not affect the protein production by *A. tamarii* as well.

The findings suggest that the degradation of AMX is most likely induced by a primary metabolite produced by the fungus. Further analysis is needed to study the enzymes involved and the mechanism of biodegrading AMX.

4.10.8 Simulations of Kinetic Model

The kinetic models were simulated to describe the rate of fungal growth (dX/dt), rate of glucose utilization (dS/dt) and the rate of protein production (dP/dt) generated using Polymath 6.0 software. The parameters displayed in Table 4.4 were used to solve the differential equations. The curve for fermentation in both the presence and absence

of AMX was shown in Figure 4.14. The simulations and experimental data proved there was a considerable agreement. The coefficient correlation (R^2) for each kinetic model used in culture flasks in both the presence and absence of AMX is shown in Table 4.5.

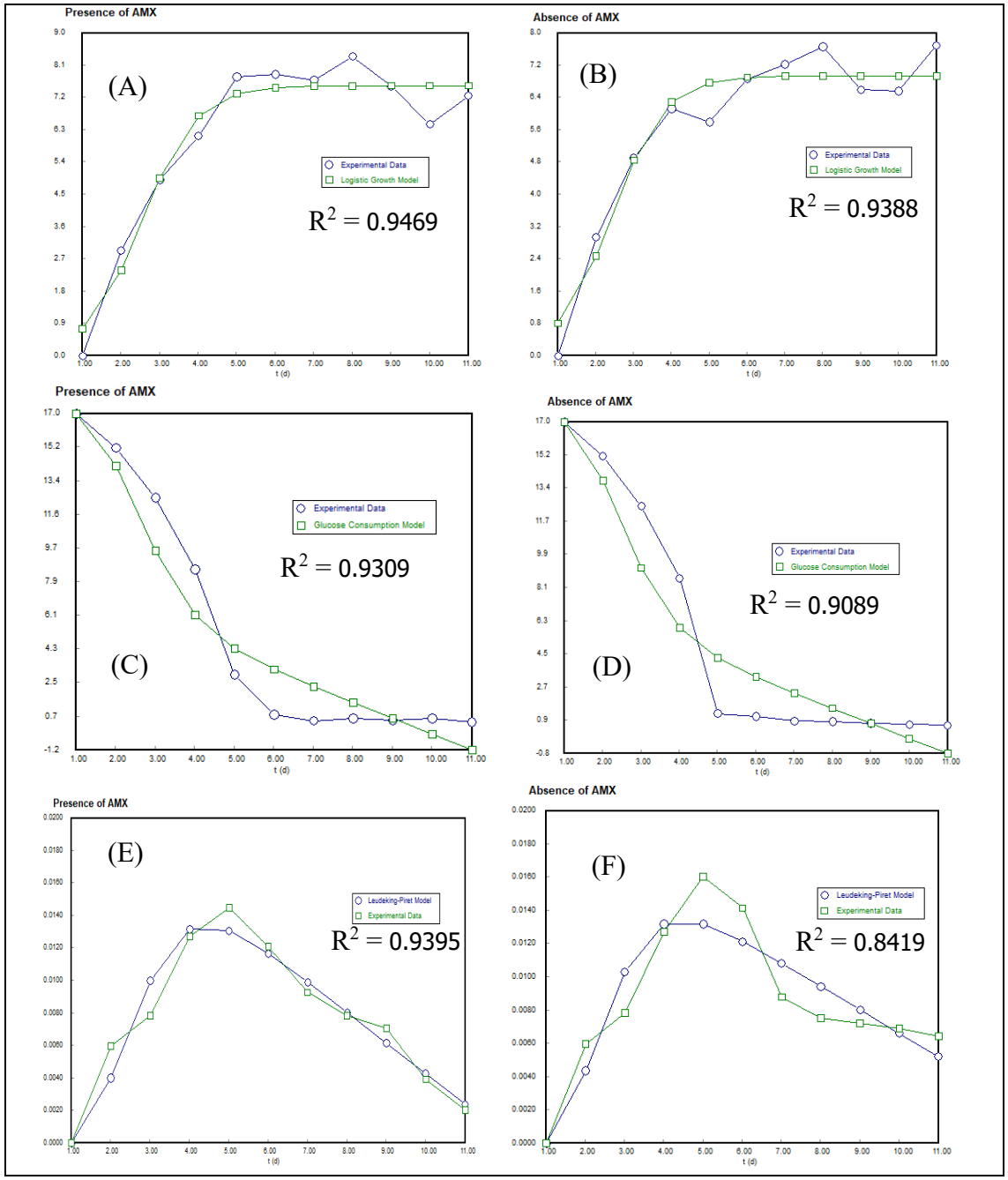

Figure 4.14. Kinetic model simulation for *A. tamarii* fermentation in the presence and absence of AMX: Logistic growth model (A, B), glucose consumption model (C, D) and Leudeking-Piret model (E, F).

Table 4.5
Correlation coefficient (R^2) for the simulation of experimental data in shake flasks for presence and absence of AMX

Model Simulation	R^2	
	Presence of AMX	Absence of AMX
Fungal growth $\frac{dX}{dt} = \mu_{max}(X)\left(1 - \frac{X}{X_{max}}\right)$	0.9469	0.9388
Glucose Utilization $-\frac{dS}{dt} = \frac{1}{Y_G}\left(\frac{dX}{dt}\right) + m_s(X)$	0.9309	0.9089
Protein Production $\frac{dP}{dt} = \alpha\left(\frac{dX}{dt}\right)$	0.9395	0.8419

Table 4.5 describes the R^2 of three kinetic models used in this study. All three models have good fit between simulated and experimental data. The logistic model for fungal growth has an R^2 of 0.9469 in the presence of AMX and 0.9388 in the absence of AMX. The glucose utilization model in the presence and absence of AMX resulted in an R^2 of 0.9309 and 0.9089, respectively. The Leudeking-Piret model for protein production in the presence of AMX exhibited a good fit as well, with an R^2 of 0.9395. In the absence of AMX, it showed decent R^2 values of 0.8419.

4.11 Fermentation of *A. tamarii* in Stirred-tank reactor (STR)

The fermentation of *A. tamarii* was carried out in a 3.8 L STR with a working volume of 2.0 L and was set at three different impeller speeds; 250, 500 and 770 rpm. Previous research has found that these impeller speeds produced maximum enzyme activity such as β-glucosidase, endoglucanase, xylanase, and endoinulinase (Abdella *et al.*, 2020; Buffo, Esperança, Farinas, *et al.*, 2020; Maumela *et al.*, 2021; GARES *et al.*, 2023). Obtaining the optimal agitation speed is significant for substrate consumption and production by cultures, which simultaneously affect the degradation of the desired compound. Impeller speed may provide good mixing, mass and heat transfer to the cell cultures which may improve the biomass concentration and simultaneously, produce shear forces which affect the morphology that can damage the structure of cell or inactivate activity of enzymes (Ibrahim *et al.*, 2015; Maiorano *et al.*, 2020; Iram *et al.*, 2022).

4.11.1 Glucose Utilization Profile with AMX in STR

The profile of glucose utilization was graphed for three respective impeller speeds. All three experimental fermentations were supplied with similar initial glucose concentrations. Figure 4.15 shows that the glucose concentration was reduced steadily for all three impeller speeds. The culture with an impeller speed of 250 rpm had 6.8 g/L of residual glucose concentration at the end of fermentation. Using an impeller speed of 500 rpm, the *A. tamarii* had a glucose residual concentration of 14.34 g/L at day 7. Lastly, residual glucose concentration was 3.94 g/L for an impeller speed of 770 rpm during the final day of fermentation. The results showed that *A. tamarii* consumed glucose the most when fermented at 770 rpm and the least at 500 rpm. This aligns with a previous study which found that higher impeller rates would provide better mixing of substrate and dissolved oxygen, which improves the cell growth and substrate consumption (Mitrović *et al.*, 2017). Table 4.6 displays the relationship between impeller speed and glucose consumption at two points of time: 72 and 168 hours. The 72-hour point is critical as the AMX is spiked into the bioreactor at that specific time. Therefore, it is important to observe the glucose consumption of *A. tamarii* when exposed to AMX. At 250 rpm, the rate of decrease in glucose consumption is 0.105 g/L/hrs. Glucose consumption at 550 rpm decreased at 0.137 g/L/hrs and 0.092 g/L/hrs at 770 rpm. Fermentation at 550 rpm may have a higher decrease rate compared to 770 rpm due to abundance of glucose residual. At 72 hrs in 770 rpm, the glucose residual concentration is already low (12.80 g/L), which became a limiting factor that may have hindered the growth of *A. tamarii* in STR. Possibly, the fungal could not support additional metabolic and degradation activities. For future studies, the AMX should be introduced at an earlier stage where glucose is available to maximise AMX degradation.

The study of fungal fermentation in bioreactors is challenging, and maintaining the consistency is proven to be difficult, especially when measuring the fermentation profiles as conducted in this study. Inconsistencies may occur due to uncontrolled growth of fungal mycelium which can affect the reactor operational conditions. For example, fungal growth on the wall of a bioreactor have been found to reduce the efficiency of the fungi to produce exopolysaccharides, a bioactive product with medicinal abilities (Supramani *et al.*, 2023). Experiments via bioreactor must adhere to strict, optimised and monitored parameters to achieve significant efficiency of any desired process as summarized in previous studies (Espinosa-Ortiz *et al.*, 2016;

Svobodová & Novotný, 2018; Petre *et al.*, 2021). In the worst-case scenario, the fungal mycelium grows on the surface of the reactor probes, causing them to become faulty.

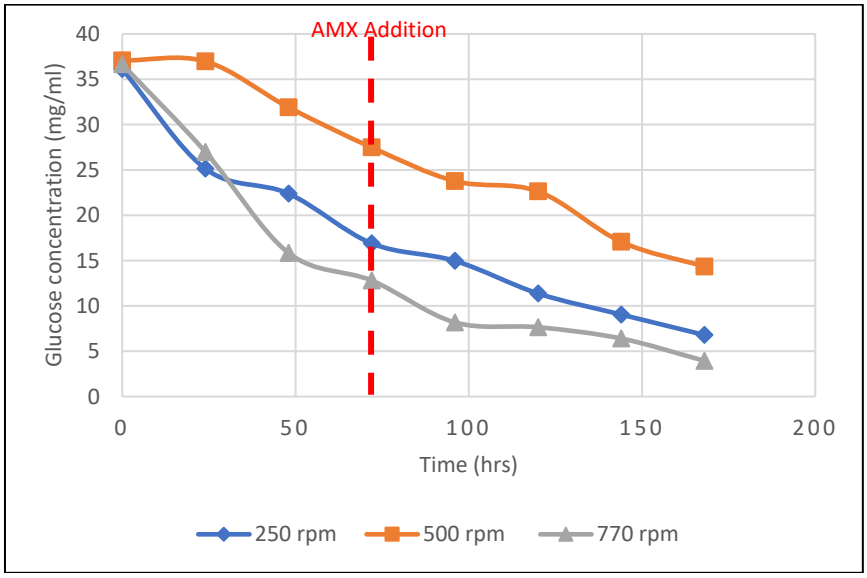

Figure 4.15. Glucose consumption profile by *A. tamarii* spiked with AMX in STR

Table 4.6
Glucose concentration decrease rate for 96 hrs (from 72nd hr to 168th hr)

Impeller Speed (rpm)	Residual glucose concentration (72 hours, g/L)	Residual glucose concentration (168 hours, g/L)	Decrease in residual glucose concentration (g/L)	Rate of glucose consumption (g/L/hrs)
250	16.89	6.80	10.09	0.105
500	27.48	14.34	13.14	0.137
770	12.80	3.95	8.85	0.092

4.11.2 Protein Production Profile With AMX in STR

It can be observed from the protein production profile in the Figure 4.16 that culturing *A. tamarii* using 250, 500 and 770 rpm produces protein in a similar hyperbolic pattern. However, it can be observed that fermentations at 250 and 500 rpm produce peak protein concentrations at the 72nd hour, which were 0.069 g/L and 0.047 g/L, respectively. The maximum protein concentration produced for 770 rpm was 0.071 g/L at the 96th hour, which was 24 hours later than that of 250 and 500 rpm cultures. According to Figure 4.16, fermentation at 500 rpm produced the most minor concentration of protein. Similar protein production was observed in 250 and 770 rpm cultures, although protein concentration dropped to a lower concentration for 770 rpm

than 250 rpm after reaching the maximum protein production. These findings complement the profiles in glucose utilization by *A. tamarii*. Similar protein production for *A. tamarii* reflects the similar glucose consumption in fermentation of 250 and 770 rpm. On the other hand, a 500 rpm culture with the most minor concentration of protein production has the least glucose utilization compared to 250 and 770 rpm cultures. The results suggest a link between nutrient availability and protein production. Table 4.7 displays the protein production rate of *A. tamarii* at 72 hours (Addition of AMX) and 168 hours. The most reduction occurred at 250 rpm (-0.0110 g/L/hr), followed by 500 rpm (-0.0103 g/L/hr) while 770 rpm showed the lowest reduction (-0.0049 g/L/hr). This is likely because the protein peak at 770 rpm occurs 24 hrs after the addition of AMX, while at 250 rpm, the peak occurred during the AMX addition.

The impeller speed has influenced the protein production of *A. tamarii*, with 770 rpm having the highest maximum protein production compared to 250 and 500 rpm. Fenice *et al.* (2012) found in their study that enzymes produced by *Lecanicillium muscariuum* exhibit the lowest activity at 500 rpm compared to lower impeller speeds. It was suggested that assays performed at 400 rpm cause the culture medium to become highly viscous. This limiting negatively influences oxygen mixing and transfer of the medium by decreasing the fluid flow, thus limiting the activity of microorganisms (Garcia-Ochoa & Gomez, 2009). Previous research also found that the maximum activity of extracellular fructosyltransferase (30 U dm^{-3}) by *A. oryzae* was obtained at 800 rpm compared to 400 rpm. The culture medium at 800 rpm had lower viscosity and formed smaller fungal pellets thus, improving nutrient distribution to the cells (Maiorano *et al.*, 2020). These findings align with current research on glucose consumption, proposing that 770 rpm provides a favorable environment for *A. tamarii* to produce protein and utilize available substrate.

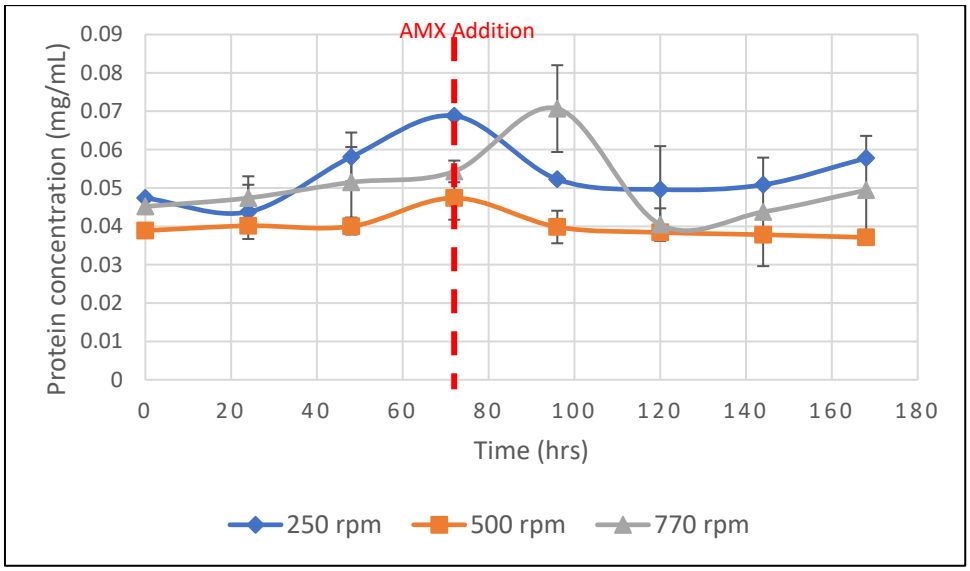

Figure 4.16. Protein production profile by *A. tamarii* spiked with AMX in STR

Table 4.7
Protein production rate for 96 hrs (from 72nd hr to 168th hr)

Impeller Speed (rpm)	Protein concentration (72 hours, g/L)	Protein concentration (168 hours, g/L)	Rate of Protein production (g/L/hrs)
250	0.0688	0.0578	-0.0110
500	0.0474	0.0371	-0.0103
770	0.0543	0.0494	-0.0049

4.11.3 AMX Degradation Profile at Different Impeller Speed in STR

The biodegradation of AMX (AMX%) in STR was measured at a 24 hour incubation interval . The second-order polynomial regression for amoxicillin degradation percentage shows significant patterns of behavior for 250, 500 and 770 rpm settings as shown in Figure 4.17. The high R^2 value of 0.98 for 250 rpm explains that the second-order polynomial equation is fitted well with the data. The negative coefficient for the x^2 term is -0.00118 and this proposes that the degradation rate decreases over time, which is logical for biological processes. This explanation is endorsed by glucose consumption and protein production at 250 rpm; as the substrate concentration decreases, protein production decreases, resulting in slower degradation rates. Despite that, the significant positive linear coefficient (0.436) shows the strong initial biodegradation in the earlier time points. Degradation tends to slow down after an initial rapid phase (Huang *et al.*, 2016; Yang *et al.*, 2016; Chinaglia *et al.*, 2018). At 500 rpm, the R^2 value (0.86) is the lowest compared to other impeller speeds. The data

seem to fit less to the polynomial model, possibly due to the degradation pattern being more variable at this impeller speed. Various additional factors like the hydrodynamics of the reactor, could affect the system and reduce the degradation efficiency. The x^2 term of 0.00076 is a positive coefficient, which indicates a slight increase in biodegradation rate. However, a relatively small linear coefficient of 0.268 suggests that initial degradation is slower at 500 rpm than at 250 rpm. The findings suggest that 500 rpm offers intermediate mixing and oxygen transfer as *A. tamarii* were unable to optimize the substrate for AMX degradation fully. Lastly, at 770 rpm, a strong fit can be observed in the second-order polynomial equation with an R^2 value of 0.94. The x^2 term shows a relatively higher positive coefficient with a value of 0.00123 implying that degradation accelerates faster than other speeds. Higher agitation speed may offer better substrate mixing and oxygen transfer but may be detrimental to the cells and enzymes due to shear stress (Mitrović *et al.*, 2017; Shu *et al.*, 2019; Deniz *et al.*, 2021). Nevertheless, the smaller linear coefficient (0.132) demonstrates a more gradual initial degradation phase. The rapid depletion of glucose by 72 hrs may have limited the biodegradation of amoxicillin after 72 hours of incubation as the cells were put under a substrate-limited environment. Further degradation may have been assisted by biosorption of the fungi biomass as cell walls possess significant amounts of glycoproteins, chitin and glycans that can interact with pollutants through various chemical reactions. The biodegradation profiles of three impeller speeds are explained effectively by the second-order polynomial regression model. The high R^2 values for 250 and 770 rpm imply a predictable and crystal clear pattern for AMX biodegradation, while a more complex pattern for 500 rpm is due to the lower R^2 value. Optimizing impeller speed is significant to ensure maximum substrate mixing while minimizing shear stress by the fungi to biodegrade AMX and other pharmaceutical pollutants effectively.

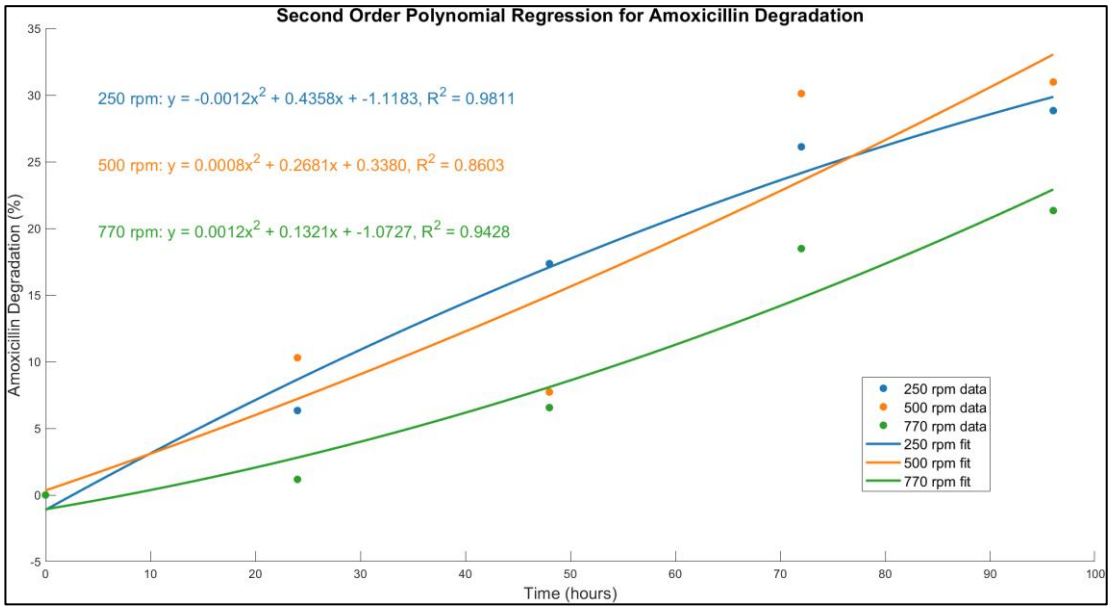

Figure 4.17. Second-order polynomial regression for amoxicillin degradation by *A. tamarii* in STR.

CHAPTER 5
CONCLUSION

FFD was conducted to identify significant factors affecting AMX% by *A. tamarii*. A 2^{4-1} FFD halved the number of experimental runs to 24, including triplicates. The design has resulted that all parameters; initial pH, agitation speed, incubation time and inoculum size are significant to the response in the order of incubation time > initial pH > agitation speed > inoculum size. Furthermore, a reduced regression model for AMX% was calculated, showing its R^2 (87.03%) and R^2(adj) (81.36%). The R^2 value obtained is high, indicating that the model is good and acceptable for estimating the response for the process studied. The process was improved using the conditions (pH 4, 120 rpm, 96 hrs and 1000 µL) and achieved maximum AMX%, which was 81.18±2.5% (Mean±SD).

Fermentation profiles of *A. tamarii* in shake flasks with and without the presence of AMX were evaluated along with kinetics of fungal growth, glucose consumption and protein production. The incubation parameters were used as in FFD. Fermentation profiles suggest that the presence of AMX had little to no effect on the growth, glucose consumption and protein production of *A. tamarii.* Kinetic models showed good agreement between the simulated and experimental data.

AMX degradation was also experimented with using STR with different impeller speeds. Fermentation profiles were analyzed except for fungal biomass due to cost and time restrictions. The current study suggests that *A. tamarii* is most efficient when incubated at 770 rpm impeller speed. At 770 rpm, the residual glucose concentration is at its lowest (3.94 g/L) and yields maximum protein production of 0.071 g/L compared to 250 and 500 rpm. The AMX degradation percentage was fitted in the second-order polynomial regression and showed a high R^2 value for 250 and 770 rpm, with values of 0.98 and 0.94, respectively.

The findings displayed that *A. tamarii* has excellent potential for applications in wastewater treatment like amoxicillin. Further study on the enzymes responsible for AMX biodegradation must be carried out to optimize their activity. Specific enzymes such as β-lactamase, laccases, and peroxidases, which are found in fungal degradation of pollutants, need to be identified and characterized. In addition, detailed pathways for AMX degradation must be investigated to identify intermediates compounds produced

during biodegradation. Some intermediates especially those resulting from β-lactam ring cleavage, may retain antimicrobial activity or pose environmental danger. Upscaling the degradation process into a bioreactor must be conducted with strict and controlled parameters to ensure efficient and predictable biodegradation by *A. tamarii*.

REFERENCES

A'yuni, H., & Ilmi, M. (2021). Lipase production from *Aspergillus aculeatus* Ms. 11 in broth medium with variation of agitation speed. AIP Conference Proceedings,

Abbas, A., Barkhouse, A., Hackenberger, D., & Wright, G. D. (2024). Antibiotic resistance: A key microbial survival mechanism that threatens public health. *Cell Host & Microbe*, *32*(6), 837-851.

Abd Hamid, A. H. H., Zulkifle, N. T., Mahat, M. M., Safian, M. F., & Ariffin, Z. Z. (2023). *Aspergillus tamarii* isolate 58 and *Lichtheimia ramosa* strain R: A potential amoxicillin biodegrader. *Journal of Applied Pharmaceutical Science*, *13*(10), 149-156.

Abd Rahim, M. H., & Saari, N. (2018). Evaluation of a Malaysian soy sauce koji strain *Aspergillus oryzae* NSK for c-aminobutyric acid (GABA) production using different native sugars.

Abdel-Azeem, A. M., Salem, F. M., Abdel-Azeem, M. A., Nafady, N. A., Mohesien, M. T., & Soliman, E. A. (2016). Chapter 1 - Biodiversity of the Genus *Aspergillus* in Different Habitats. In V. K. Gupta (Ed.), *New and Future Developments in Microbial Biotechnology and Bioengineering* (pp. 3-28). Elsevier.

Abdel-Hadi, A., Schmidt-Heydt, M., Parra, R., Geisen, R., & Magan, N. (2012). A systems approach to model the relationship between aflatoxin gene cluster expression, environmental factors, growth and toxin production by *Aspergillus flavus*. *Journal of the Royal Society Interface*, *9*(69), 757-767.

Abdella, A., Segato, F., & Wilkins, M. R. (2020). Optimization of process parameters and fermentation strategy for xylanase production in a stirred tank reactor using a mutant *Aspergillus nidulans* strain. *Biotechnology Reports*, *26*, e00457.

Adamus-Białek, W., Wawszczak, M., Arabski, M., Majchrzak, M., Gulba, M., Jarych, D., Parniewski, P., & Głuszek, S. (2019). Ciprofloxacin, amoxicillin, and aminoglycosides stimulate genetic and phenotypic changes in uropathogenic *Escherichia coli* strains. *Virulence*, *10*(1), 260-276.

Ademakinwa, A. N., Ayinla, Z. A., & Agunbiade, M. O. (2025). Characterization of a purified novel *Aureobasidium pullulans* NAC8 lipase and covalent-

immobilization for use in the biodegradation of oil-contaminated wastewater. *International Journal of Biological Macromolecules*, *304*, 140781.

Adeoye, A., Lateef, A., & Gueguim-Kana, E. (2015). Optimization of citric acid production using a mutant strain of *Aspergillus niger* on cassava peel substrate. *Biocatalysis and Agricultural Biotechnology*, *4*(4), 568-574.

Adeyefa, O., & Ebuehi, O. (2020). Isolation, identification and characterization of pectinase producers from agro wastes (*Citrus sinensis* and *Ananas comosus*). *World J Agric Soil Sci*, *4*(3), 1-6.

Adio, S. O., Omar, M. H., Asif, M., & Saleh, T. A. (2017). Arsenic and selenium removal from water using biosynthesized nanoscale zero-valent iron: a factorial design analysis. *Process Safety and Environmental Protection*, *107*, 518-527.

Ajayi, V. A., & Lateef, A. (2025). Optimization of production of detergent-compatible and thrombolytic protease by *Aspergillus flavus* AT grown on agrowastes using Taguchi technique cum nanoparticles supplementation. *Cleaner and Circular Bioeconomy*, *10*, 100144.

Akasaka, N., Kato, S., Kato, S., Hidese, R., Wagu, Y., Sakoda, H., & Fujiwara, S. (2018). Agmatine production by *Aspergillus oryzae* is elevated by low pH during solid-state cultivation. *Applied and Environmental Microbiology*, *84*(15), e00722-00718.

Al-Gheethi, A., Noman, E., Radin Mohamed, R. M. S., Ismail, N., Bin Abdullah, A. H., & Mohd Kassim, A. H. (2019). Optimizing of pharmaceutical active compounds biodegradability in secondary effluents by β-lactamase from *Bacillus subtilis* using central composite design. *Journal of Hazardous Materials*, *365*, 883-894.

Al-Hawash, A. B., Zhang, X., & Ma, F. (2019). Removal and biodegradation of different petroleum hydrocarbons using the filamentous fungus *Aspergillus sp.* RFC-1. *Microbiologyopen*, *8*(1), e00619.

Aldas-Vargas, A., van der Vooren, T., Rijnaarts, H. H. M., & Sutton, N. B. (2021). Biostimulation is a valuable tool to assess pesticide biodegradation capacity of groundwater microorganisms. *Chemosphere*, *280*, 130793.

Alidadi, H., Ghorbanian, A., Ghorbanian, M., Rahmanzadeh, E., Nemanifar, N., & Mehrabpour, M. (2018). Evaluation of amoxicillin antibiotic removal by electrocoagulation process from aqueous solutions: optimization through response surface methodology. *Desalination and Water Treatment*, *132*, 358-350.

Almquist, J., Cvijovic, M., Hatzimanikatis, V., Nielsen, J., & Jirstrand, M. (2014). Kinetic models in industrial biotechnology – Improving cell factory performance. *Metabolic Engineering*, *24*, 38-60.

Anandan, D., Marmer, W. N., & Dudley, R. L. (2007). Isolation, characterization and optimization of culture parameters for production of an alkaline protease isolated from *Aspergillus tamarii*. *Journal of Industrial Microbiology and Biotechnology*, *34*(5), 339-347.

Antony, J. (2023). 4 - A systematic methodology for design of experiments. In J. Antony (Ed.), *Design of Experiments for Engineers and Scientists (Third Edition)* (pp. 33-50). Elsevier.

Asghar, A., Lutze, H. V., Tuerk, J., & Schmidt, T. C. (2022). Influence of water matrix on the degradation of organic micropollutants by ozone based processes: A review on oxidant scavenging mechanism. *Journal of Hazardous Materials*, *429*, 128189.

Augsburger, N., Zaouri, N., Cheng, H., & Hong, P.-Y. (2021). The use of UV/H2O2 to facilitate removal of emerging contaminants in anaerobic membrane bioreactor effluents. *Environmental Research*, *198*, 110479.

Ausloos, M. (2011). Gompertz and Verhulst frameworks for growth and decay description. *arXiv preprint arXiv:1109.1269*.

Ayu, Y. S., & Kasiamdari, R. S. (2022). Screening and identification of fungi isolated from batik wastewaters for decolorization of Remazol Black B dye and batik effluent. *Journal of Degraded & Mining Lands Management*, *10*(1).

Baghapour, M. A., Shirdarreh, M. R., & Faramarzian, M. (2014). Degradation of amoxicillin by bacterial consortium in a submerged biological aerated filter: volumetric removal modeling. *Journal of Health Sciences & Surveillance System*, *2*(1), 15-25.

Balajee, S. A., Houbraken, J., Verweij, P. E., Hong, S. B., Yaghuchi, T., Varga, J., & Samson, R. A. (2007). *Aspergillus* species identification in the clinical setting. *Studies in Mycology*, *59*, 39-46.

Banjo, T., Kareem, S., Akinduti, P., Popoola, T., & Akinloye, O. (2019). Optimization and production of ascorbic acid by fusant cell of *Aspergillus flavus* and *Aspergillus tamarii*. *Journal of King Saud University - Science*, *31*(4), 931-936.

Banti, D. C., Mitrakas, M., & Samaras, P. (2021). Membrane fouling controlled by adjustment of biological treatment parameters in step-aerating MBR. *Membranes*, *11*(8), 553.

Barman, S., Sit, N., Badwaik, L. S., & Deka, S. C. (2015). Pectinase production by *Aspergillus niger* using banana (*Musa balbisiana*) peel as substrate and its effect on clarification of banana juice. *Journal of food science and technology*, *52*, 3579-3589.

Batista, J. M. S., Brandão-Costa, R. M. P., Carneiro da Cunha, M. N., Rodrigues, H. O. S., & Porto, A. L. F. (2020). Purification and biochemical characterization of an extracellular fructosyltransferase-rich extract produced by *Aspergillus tamarii* Kita UCP1279. *Biocatalysis and Agricultural Biotechnology*, *26*, 101647.

Bedaiwy, M. Y., Awadalla, O. A., Abou-Zeid, A. M., & Hamada, H. T. (2016). Optimal conditions for production of L-asparaginase from *Aspergillus tamarii*. *Egypt. J. Exper. Biol.(Botany)*, *12*(2), 229-237.

Benguenab, A., & Chibani, A. (2021). Biodegradation of petroleum hydrocarbons by filamentous fungi *(Aspergillus ustus* and *Purpureocillium lilacinum*) isolated from used engine oil contaminated soil. *Acta Ecologica Sinica*, *41*(5), 416-423.

Betts, J. I., & Baganz, F. (2006). Miniature bioreactors: current practices and future opportunities. *Microbial cell factories*, *5*(1), 21.

Bhattacharya, R., & Mazumder, D. (2021). Simultaneous nitrification and denitrification in moving bed bioreactor and other biological systems. *Bioprocess and Biosystems Engineering*, *44*(4), 635-652.

Bibashi, E., de Hoog, G. S., Pavlidis, T. E., Symeonidis, N., Sakantamis, A., & Walther, G. (2013). Wound infection caused by *Lichtheimia ramosa* due to a car accident. *Medical Mycology Case Reports*, *2*, 7-10.

Bielen, A., Šimatović, A., Kosić-Vukšić, J., Senta, I., Ahel, M., Babić, S., Jurina, T., González Plaza, J. J., Milaković, M., & Udiković-Kolić, N. (2017). Negative environmental impacts of antibiotic-contaminated effluents from pharmaceutical industries. *Water Research*, *126*, 79-87.

Bose, P., Gowrie, S. U., & Chathurdevi, G. (2019). Optimization of Culture Conditions for Growth and Production of Bioactive Metabolites by Endophytic Fungus-*Aspergillus tamarii*. *International Journal of Pharmacy and Biological Sciences*, *9*(2), 469-478.

Broccoli, A., Anselmi, S., Cavallo, A., Ferrari, V., Prevedelli, D., Pastorino, P., & Renzi, M. (2021). Ecotoxicological effects of new generation pollutants (nanoparticles, amoxicillin and white musk) on freshwater and marine phytoplankton species. *Chemosphere*, *279*, 130623.

Bruno Siewe, F., Kudre, T. G., & Narayan, B. (2021). Optimisation of ultrasound-assisted enzymatic extraction conditions of umami compounds from fish by-products using the combination of fractional factorial design and central composite design. *Food Chemistry*, *334*, 127498.

Bryskier, A. (2010). CHAPTER 22 - Macrolides. In R. G. Finch, D. Greenwood, S. R. Norrby, & R. J. Whitley (Eds.), *Antibiotic and Chemotherapy (Ninth Edition)* (pp. 276-289). W.B. Saunders.

Buffo, M. M., Esperança, M. N., Béttega, R., Farinas, C. S., & Badino, A. C. (2020). Oxygen transfer and fragmentation of *Aspergillus niger* pellets in stirred tank and concentric-duct airlift bioreactors. *Industrial Biotechnology*, *16*(2), 67-74.

Buffo, M. M., Esperança, M. N., Farinas, C. S., & Badino, A. C. (2020). Relation between pellet fragmentation kinetics and cellulolytic enzymes production by *Aspergillus niger* in conventional bioreactor with different impellers. *Enzyme and Microbial Technology*, *139*, 109587.

Bush, K. (2010). CHAPTER 14 - β-Lactam antibiotics: penicillins. In R. G. Finch, D. Greenwood, S. R. Norrby, & R. J. Whitley (Eds.), *Antibiotic and Chemotherapy (Ninth Edition)* (pp. 200-225). W.B. Saunders.

Busto, R. V., Roberts, J., Hunter, C., Escudero, A., Helwig, K., & Coelho, L. H. G. (2020). Mechanistic and ecotoxicological studies of amoxicillin removal through anaerobic degradation systems. *Ecotoxicology and Environmental Safety*, *192*, 110207.

Cai, Y., Yu, H., Ren, L., Ou, Y., Jiang, S., Chai, Y., Chen, A., Yan, B., Zhang, J., & Yan, Z. (2023). Treatment of amoxicillin-containing wastewater by *Trichoderma* strains selected from activated sludge. *Science of The Total Environment*, *867*, 161565.

Carvalho, J. F. d., & Moraes, J. E. F. d. (2021). Treatment of simulated industrial pharmaceutical wastewater containing amoxicillin antibiotic via advanced oxidation processes. *Environmental technology*, *42*(26), 4145-4157.

Cela-Dablanca, R., Barreiro, A., López, L. R., Santás-Miguel, V., Arias-Estévez, M., Núñez-Delgado, A., Álvarez-Rodríguez, E., & Fernández-Sanjurjo, M. J.

(2022). Relevance of sorption in bio-reduction of amoxicillin taking place in forest and crop soils. *Environmental Research*, *208*, 112753.

Chen, F., Ma, J., Zhu, Y., Li, X., Yu, H., & Sun, Y. (2022). Biodegradation performance and anti-fouling mechanism of an ICME/electro-biocarriers-MBR system in livestock wastewater (antibiotic-containing) treatment. *Journal of Hazardous Materials*, *426*, 128064.

Chen, H., Wang, Z., Huang, Y., Wei, J., Guo, G., & Miao, L. (2023). Anaerobic co-metabolic degradation of ceftriaxone sodium: Performance and mechanism. *Journal of Cleaner Production*, *394*, 136388.

Cheng, D. L., Ngo, H. H., Guo, W. S., Liu, Y. W., Zhou, J. L., Chang, S. W., Nguyen, D. D., Bui, X. T., & Zhang, X. B. (2018). Bioprocessing for elimination antibiotics and hormones from swine wastewater. *Science of The Total Environment*, *621*, 1664-1682.

Cherian, T., Ragavendran, C., Vijayan, S., Kurien, S., & Peijnenburg, W. J. G. M. (2023). A review on the fate, human health and environmental impacts, as well as regulation of antibiotics used in aquaculture. *Environmental Advances*, *13*, 100411.

Chinaglia, S., Tosin, M., & Degli-Innocenti, F. (2018). Biodegradation rate of biodegradable plastics at molecular level. *Polymer Degradation and Stability*, *147*, 237-244.

Chopra, I. (2010). CHAPTER 30 - Tetracyclines. In R. G. Finch, D. Greenwood, S. R. Norrby, & R. J. Whitley (Eds.), *Antibiotic and Chemotherapy (Ninth Edition)* (pp. 344-355). W.B. Saunders.

Chowdhury, J., Mandal, T. K., & Mondal, S. (2020). Genotoxic impact of emerging contaminant amoxicillin residue on zebra fish (*Danio rerio*) embryos. *Heliyon*, *6*(11), e05379.

Clardy, J., Fischbach, M. A., & Currie, C. R. (2009). The natural history of antibiotics. *Current Biology*, *19*(11), R437-R441.

Colla, L. M., Primaz, A. L., Benedetti, S., Loss, R. A., Lima, M. d., Reinehr, C. O., Bertolin, T. E., & Costa, J. A. V. (2016). Surface response methodology for the optimization of lipase production under submerged fermentation by filamentous fungi. *brazilian journal of microbiology*, *47*, 461-467.

Darah, I., Sumathi, G., Jain, K., & Lim, S. (2011). Influence of agitation speed on tannase production and morphology of *Aspergillus niger* FETL FT3 in

submerged fermentation. *Applied biochemistry and biotechnology*, *165*, 1682-1690.

Das, A., Bhattacharya, S., Shivakumar, S., Shakya, S., & Sogane, S. S. (2017). Coconut oil induced production of a surfactant-compatible lipase from *Aspergillus tamarii* under submerged fermentation. *Journal of Basic Microbiology*, *57*(2), 114-120.

Day, S., Lalitha, P., Haug, S., Fothergill, A. W., Cevallos, V., Vijayakumar, R., Prajna, N. V., Acharya, N. R., McLeod, S. D., & Lietman, T. M. (2009). Activity of antibiotics against *Fusarium* and *Aspergillus*. *British journal of ophthalmology*, *93*(1), 116-119.

de Sousa, F. A., de Morais, C. R., Vieira, J. S., Maranho, L. S., Machado, F. L., Pereira, S., Barbosa, L. C., Coelho, H. E., Campos, C. F., & Bonetti, A. M. (2019). Genotoxicity and carcinogenicity of ivermectin and amoxicillin *in vivo* systems. *Environmental Toxicology and Pharmacology*, *70*, 103196.

Delavar, M. A., & Wang, J. (2022). Chapter 7 - Bioreactor concepts, types, and modeling. In M. A. Delavar & J. Wang (Eds.), *Advanced Methods and Mathematical Modeling of Biofilms* (pp. 195-245). Academic Press.

Deniz, I., Demir, T., Oncel, S. S., Hames, E. E., & Vardar-Sukan, F. (2021). Effect of agitation and aeration on keratinase production in bioreactors using bioprocess engineering aspects. *The Protein Journal*, *40*, 388-395.

Derakhsheshpoor, R., Homayoonfal, M., Akbari, A., & Mehrnia, M. R. (2013). Amoxicillin separation from pharmaceutical wastewater by high permeability polysulfone nanofiltration membrane. *Journal of Environmental Health Science and Engineering*, *11*, 1-10.

Dewil, R., Mantzavinos, D., Poulios, I., & Rodrigo, M. A. (2017). New perspectives for Advanced Oxidation Processes. *Journal of Environmental Management*, *195*, 93-99.

Dhiman, P., Arora, N., Thanikachalam, P. V., & Monga, V. (2019). Recent advances in the synthetic and medicinal perspective of quinolones: A review. *Bioorganic Chemistry*, *92*, 103291.

Dinarvand, M., Rezaee, M., & Foroughi, M. (2017). Optimizing culture conditions for production of intra and extracellular inulinase and invertase from *Aspergillus niger* ATCC 20611 by response surface methodology (RSM). *brazilian journal of microbiology*, *48*, 427-441.

Dinos, G. P. (2017). The macrolide antibiotic renaissance. *British journal of pharmacology*, *174*(18), 2967-2983.

Dogan, S., & Kidak, R. (2016). A plug flow reactor model for UV-based oxidation of amoxicillin. *Desalination and Water Treatment*, *57*(29), 13586-13599.

Doi, Y., & Chambers, H. F. (2015). 20 - Penicillins and β-Lactamase Inhibitors. In J. E. Bennett, R. Dolin, & M. J. Blaser (Eds.), *Mandell, Douglas, and Bennett's Principles and Practice of Infectious Diseases (Eighth Edition)* (pp. 263-277.e263). W.B. Saunders.

Dowling, P. M., Prescott, J. F., & Baptiste, K. E. (2025). *Antimicrobial therapy in veterinary medicine*. Wiley Online Library.

Durakovic, B. (2017). Design of experiments application, concepts, examples: State of the art. *Periodicals of Engineering and Natural Sciences*, *5*(3).

Durand, G. A., Raoult, D., & Dubourg, G. (2019). Antibiotic discovery: history, methods and perspectives. *International Journal of Antimicrobial Agents*, *53*(4), 371-382.

Ebele, A. J., Oluseyi, T., Drage, D. S., Harrad, S., & Abdallah, M. A.-E. (2020). Occurrence, seasonal variation and human exposure to pharmaceuticals and personal care products in surface water, groundwater and drinking water in Lagos State, Nigeria. *Emerging Contaminants*, *6*, 124-132.

Egbune, E. O., Anigboro, A. A., Edeche, G., Edo, G. I., Onoharigho, F. O., Emakpor, O. L., Ozgor, E., Akhayere, E., & Tonukari, N. J. (2023). Effect of inoculum size on solid state fermentation of cassava (*Manito esculenta* Crantz). *Chemistry Africa*, *6*(6), 2911-2917.

El-Gamal, M. I., Brahim, I., Hisham, N., Aladdin, R., Mohammed, H., & Bahaaeldin, A. (2017). Recent updates of carbapenem antibiotics. *European Journal of Medicinal Chemistry*, *131*, 185-195.

El-Gindy, A. A., Saad, R. R., & Fawzi, E. M. (2015). Purification of β-xylosidase from *Aspergillus tamarii* using ground oats and a possible application on the fermented hydrolysate by *Pichia stipitis*. *Annals of Microbiology*, *65*(2), 965-974.

El-Sharkawy, R. M., Swelim, M. A., & Hamdy, G. B. (2022). *Aspergillus tamarii* mediated green synthesis of magnetic chitosan beads for sustainable remediation of wastewater contaminants. *Scientific reports*, *12*(1), 1-15.

Elander, R. (2003). Industrial production of β-lactam antibiotics. *Applied microbiology and biotechnology*, *61*(5), 385-392.

Elhussieny, N. I., El-Refai, H. A., Mohamed, S. S., Shetaia, Y. M., Amin, H. A., & Klöck, G. (2023). *Rhizopus stolonifer* biomass catalytic transesterification capability: optimization of cultivation conditions. *Microbial cell factories*, *22*(1), 154.

Elizalde Velazquez, A., Gómez-Oliván, L., Martínez, M., Islas-Flores, H., Dublan, O., & SanJuan-Reyes, N. (2016). Amoxicillin in the Aquatic Environment, Its Fate and Environmental Risk. In.

Emri, T., Szarvas, V., Orosz, E., Antal, K., Park, H., Han, K.-H., Yu, J.-H., & Pócsi, I. (2015). Core oxidative stress response in *Aspergillus nidulans*. *BMC genomics*, *16*, 1-19.

Espinosa-Ortiz, E. J., Rene, E. R., Pakshirajan, K., van Hullebusch, E. D., & Lens, P. N. L. (2016). Fungal pelleted reactors in wastewater treatment: Applications and perspectives. *Chemical Engineering Journal*, *283*, 553-571.

Essawy, A. A., Alsohaimi, I. H., Alhumaimess, M. S., Hassan, H. M. A., & Kamel, M. M. (2020). Green synthesis of spongy Nano-ZnO productive of hydroxyl radicals for unconventional solar-driven photocatalytic remediation of antibiotic enriched wastewater. *Journal of Environmental Management*, *271*, 110961.

Favier, L., Ungureanu, C. V., Simion, A. I., Bahrim, G., & Vial, C. (2021). Enhancing the biodegradation efficiency of a emergent refractory water pollutant by a bacterial isolate through a statistical process optimization approach. *Process Safety and Environmental Protection*, *148*, 1133-1145.

Fayyaz, I., Saddick, S., Mahmood, R. T., Asad, M. J., Hussain, M. A., Hu, J., Awais, M., Khan, M. I., & Saydaxmetova, S. (2025). Biodegradation of Azo and disperse dyes by *Trametes versicolor*: Process optimization and MnP enzyme dynamics. *Results in Engineering*, *25*, 103980.

Feng, S., Guo, W., Ding, A., Parsa, S. M., Pan, J., Cheng, D., Tung, T. V., & Ngo, H. H. (2025). Enzyme sources in wastewater treatment: Their influence on enzymatic bioremediation and large-scale applications. *Chemical Engineering Journal*, *510*, 161891.

Feng, S., Ngo, H. H., Guo, W., Chang, S. W., Nguyen, D. D., Cheng, D., Varjani, S., Lei, Z., & Liu, Y. (2021). Roles and applications of enzymes for resistant

pollutants removal in wastewater treatment. *Bioresource technology*, *335*, 125278.

Fenice, M., Barghini, P., Selbmann, L., & Federici, F. (2012). Combined effects of agitation and aeration on the chitinolytic enzymes production by the Antarctic fungus *Lecanicillium muscarium* CCFEE 5003. *Microbial cell factories*, *11*, 1-11.

Fernandes, P., Pereira, D., Watkins, P. B., & Bertrand, D. (2019). Differentiating the pharmacodynamics and toxicology of macrolide and ketolide antibiotics: Miniperspective. *Journal of Medicinal Chemistry*, *63*(12), 6462-6473.

Ferreira, G., Boer, C. G., & Peralta, R. M. (1999). Production of xylanolytic enzymes by *Aspergillus tamarii* in solid state fermentation. *FEMS Microbiology Letters*, *173*(2), 335-339.

Ferreira, J. A., Varjani, S., & Taherzadeh, M. J. (2020). A Critical Review on the Ubiquitous Role of Filamentous Fungi in Pollution Mitigation. *Current Pollution Reports*, *6*(4), 295-309.

Freitas, L. D., & Radis-Baptista, G. (2021). Pharmaceutical Pollution and Disposal of Expired, Unused, and Unwanted Medicines in the Brazilian Context. *Journal of Xenobiotics*, *11*(2), 61-76.

Fu, L., Huang, T., Wang, S., Wang, X., Su, L., Li, C., & Zhao, Y. (2017). Toxicity of 13 different antibiotics towards freshwater green algae *Pseudokirchneriella subcapitata* and their modes of action. *Chemosphere*, *168*, 217-222.

Fukuda, I. M., Pinto, C. F. F., Moreira, C. d. S., Saviano, A. M., & Lourenço, F. R. (2018). Design of experiments (DoE) applied to pharmaceutical and analytical quality by design (QbD). *Brazilian journal of pharmaceutical sciences*, *54*.

Garcia-Ochoa, F., & Gomez, E. (2009). Bioreactor scale-up and oxygen transfer rate in microbial processes: An overview. *Biotechnology Advances*, *27*(2), 153-176.

GARES, M., Serge, H., KASSEM AL SAYED, M., ALLOUN, W., & KACEM CHAOUCHE, N. (2023). The study of the industrial aptitude of *Aspergillus fumigatus* strain for xylanase production. *Egyptian Journal of Chemistry*, *66*(10), 163-177.

Gatto, M., Muratori, S., & Rinaldi, S. (1988). A functional interpretation of the logistic equation. *Ecological Modelling*, *42*(2), 155-159.

Gibson, P. S., Bexkens, E., Zuber, S., Cowley, L. A., & Veening, J.-W. (2022). The acquisition of clinically relevant amoxicillin resistance in *Streptococcus*

pneumoniae requires ordered horizontal gene transfer of four loci. *PLoS Pathogens*, *18*(7), e1010727.

Gidijala, L., Kiel, J. A. K. W., Bovenberg, R. A. L., Van Der Klei, I. J., & Berg, M. A. V. D. (2010). Biosynthesis of active pharmaceuticals: β-lactam biosynthesis in filamentous fungi. *Biotechnology and Genetic Engineering Reviews*, *27*(1), 1-32.

Gonçalves, F. A., Leite, R. S. R., Rodrigues, A., Argandoña, E. J. S., & Fonseca, G. G. (2013). Isolation, identification and characterization of a novel high level β-glucosidase-producing *Lichtheimia ramosa* strain. *Biocatalysis and Agricultural Biotechnology*, *2*(4), 377-384.

Goveas, L. C., & Sajankila, S. P. (2020). Effect of yeast extract supplementation on halotolerant biosurfactant production kinetics coupled with degradation of petroleum crude oil by *Acinetobacter baumannii* OCB1 in marine environment. *Bioresource Technology Reports*, *11*, 100447.

Gozlan, I., Rotstein, A., & Avisar, D. (2013). Amoxicillin-degradation products formed under controlled environmental conditions: Identification and determination in the aquatic environment. *Chemosphere*, *91*(7), 985-992.

Guncum, E., Bakirel, T., Anlas, C., Isiklan, N., Ustun Alkan, F., Charehsaz, M., & Aydin, A. (2021). The screening of the safety profile of polymeric based amoxicillin nanoparticles in various test systems. *Toxicology Letters*, *348*, 1-9.

Gunst, R. F., & Mason, R. L. (2009). Fractional factorial design. *Wiley Interdisciplinary Reviews: Computational Statistics*, *1*(2), 234-244.

Gupta, R., & Gupta, N. (2021). *Fundamentals of bacterial physiology and metabolism*. Springer.

Hamad, M. T. M. H. (2020). Biodegradation of diazinon by fungal strain *Apergillus niger* MK640786 using response surface methodology. *Environmental Technology & Innovation*, *18*, 100691.

Hamzah, A., Manikan, V., & Abd Aziz, N. A. F. (2017). Biodegradation of tapis crude oil using consortium of bacteria and fungi: Optimization of crude oil concentration and duration of incubation by response surface methodology. *Sains Malaysiana*, *46*(1), 43-50.

Homa, M., Manikandan, P., Szekeres, A., Kiss, N., Kocsubé, S., Kredics, L., Alshehri, B., Dukhyil, A. A. B., Revathi, R., Narendran, V., Vágvölgyi, C., Shobana, C. S., & Papp, T. (2019). Characterization of *Aspergillus tamarii* Strains From

Human Keratomycoses: Molecular Identification, Antifungal Susceptibility Patterns and Cyclopiazonic Acid Producing Abilities. *Front Microbiol*, *10*, 2249.

Homayoonfal, M., & Mehrnia, M. R. (2014). Amoxicillin separation from pharmaceutical solution by pH sensitive nanofiltration membranes. *Separation and Purification Technology*, *130*, 74-83.

Honfoga, J. N. B., Nascimento, P. A., Ferreira, A. N., da Silva, E. C., Bauer, L. C., Teixeira, J. M., Santana, N. B., & Bonomo, R. C. F. (2025). Production and characterization of L-asparaginase by *Aspergillus niger*: A sustainable use of pitaya (*Hylocereus spp*.) by-products. *Sustainable Chemistry for the Environment*, *10*, 100255.

Howard, A., Reza, N., Green, P. L., Yin, M., Duffy, E., Mwandumba, H. C., Gerada, A., & Hope, W. (2025). Artificial intelligence and infectious diseases: tackling antimicrobial resistance, from personalised care to antibiotic discovery. *The Lancet Infectious Diseases*.

Hu, Y., Lei, D., Wu, D., Xia, J., Zhou, W., & Cui, C. (2022). Residual β-lactam antibiotics and ecotoxicity to *Vibrio fischeri*, *Daphnia magna* of pharmaceutical wastewater in the treatment process. *Journal of Hazardous Materials*, *425*, 127840.

Huang, X., Zhang, X., Feng, F., & Xu, X. (2016). Biodegradation of tetracycline by the yeast strain *Trichosporon mycotoxinivorans* XPY-10. *Preparative Biochemistry and Biotechnology*, *46*(1), 15-22.

Hutchings, M. I., Truman, A. W., & Wilkinson, B. (2019). Antibiotics: past, present and future. *Current Opinion in Microbiology*, *51*, 72-80.

Ibrahim, D., Weloosamy, H., & Lim, S.-H. (2015). Effect of agitation speed on the morphology of *Aspergillus niger* HFD5A-1 hyphae and its pectinase production in submerged fermentation. *World Journal of Biological Chemistry*, *6*(3), 265.

Inyinbor, A. A., Bello, O. S., Fadiji, A. E., & Inyinbor, H. E. (2018). Threats from antibiotics: A serious environmental concern. *Journal of Environmental Chemical Engineering*, *6*(1), 784-793.

Iram, A., Cekmecelioglu, D., & Demirci, A. (2022). The effect of Dilution, Aeration, and Agitation on Fungal Cellulase and Xylanase Production by DDGS-based Fermentation Media in Stirred Tank Bioreactors. 2022 ASABE Annual International Meeting,

İstifli, E. S., & Topaktaş, M. (2010). Cytogenetic genotoxicity of amoxicillin. *Environmental and molecular mutagenesis*, *51*(3), 222-228.

Jain, M., Kumar, S. S., & Goswami, L. (2022). Aerobic and anaerobic bioreactor systems for wastewater treatment. In *Techno-economics and life cycle assessment of bioreactors* (pp. 13-22). Elsevier.

Jalil, M., & Ibrahim, D. (2021). Partial purification and characterization of pectinase produced by *Aspergillus niger* LFP-1 grown on pomelo peels as a substrate. Trop Life Sci Res 32 (1): 1–22. In

Jankovic, A., Chaudhary, G., & Goia, F. (2021). Designing the design of experiments (DOE) – An investigation on the influence of different factorial designs on the characterization of complex systems. *Energy and Buildings*, *250*, 111298.

Ji, J., Gao, T., Salama, E.-S., El-Dalatony, M. M., Peng, L., Gong, Y., Liu, P., & Li, X. (2021). Using *Aspergillus niger* whole-cell biocatalyst mycelial aerobic granular sludge to treat pharmaceutical wastewater containing β-lactam antibiotics. *Chemical Engineering Journal*, *412*, 128665.

K Chaurasia, P., L Bharati, S., Sharma, M., K Singh, S., SS Yadav, R., & Yadava, S. (2015). Fungal laccases and their biotechnological significances in the current perspective: a review. *Current Organic Chemistry*, *19*(19), 1916-1934.

Kamaruddin, F. F., Musa, M., Mahat, M. M., Ariffin, S. H. Z., Safian, M. F., & Ariffin, Z. Z. (2022). Biodegradation of doxycycline hyclate by local *Purpureocillium lilacinum* strain PlHN17 and *Trichoderma asperellum* isolate Tullur: monitoring by antimicrobial activity. *Jordan J Biol Sci*, *15*(3), 457-461.

Kardos, N., & Demain, A. L. (2011). Penicillin: the medicine with the greatest impact on therapeutic outcomes. *Applied microbiology and biotechnology*, *92*, 677-687.

Kealey, C., Creaven, C., Murphy, C., & Brady, C. (2017). New approaches to antibiotic discovery. *Biotechnology Letters*, *39*, 805-817.

Keshri, V., Panda, A., Levasseur, A., Rolain, J.-M., Pontarotti, P., & Raoult, D. (2018). Phylogenomic analysis of β-lactamase in archaea and bacteria enables the identification of putative new members. *Genome Biology and Evolution*, *10*(4), 1106-1114.

Khanpour-Alikelayeh, E., Partovinia, A., Talebi, A., & Kermanian, H. (2020). Investigation of *Bacillus licheniformis* in the biodegradation of Iranian heavy crude oil: A two-stage sequential approach containing factor-screening and optimization. *Ecotoxicology and Environmental Safety*, *205*, 111103.

Kheirkhah, T., Neubauer, P., & Junne, S. (2023). Controlling *Aspergillus niger* morphology in a low shear-force environment in a rocking-motion bioreactor. *Biochemical Engineering Journal*, *195*, 108905.

Khosravi, C., Benocci, T., Battaglia, E., Benoit, I., & de Vries, R. P. (2015). Chapter One - Sugar Catabolism in *Aspergillus* and Other Fungi Related to the Utilization of Plant Biomass. In S. Sariaslani & G. M. Gadd (Eds.), *Advances in applied microbiology* (Vol. 90, pp. 1-28). Academic Press.

Klein, E. Y., Van Boeckel, T. P., Martinez, E. M., Pant, S., Gandra, S., Levin, S. A., Goossens, H., & Laxminarayan, R. (2018). Global increase and geographic convergence in antibiotic consumption between 2000 and 2015. *Proceedings of the National Academy of Sciences*, *115*(15), E3463-E3470.

Kohanski, M. A., Dwyer, D. J., & Collins, J. J. (2010). How antibiotics kill bacteria: from targets to networks. *Nat Rev Microbiol*, *8*(6), 423-435.

Kosegarten, C. E., Ramírez-Corona, N., Mani-López, E., Palou, E., & López-Malo, A. (2017). Description of *Aspergillus flavus* growth under the influence of different factors (water activity, incubation temperature, protein and fat concentration, pH, and cinnamon essential oil concentration) by kinetic, probability of growth, and time-to-detection models. *International journal of food microbiology*, *240*, 115-123.

Kowalczyk, J. E., Benoit, I., & de Vries, R. P. (2014). Chapter Two - Regulation of Plant Biomass Utilization in *Aspergillus*. In S. Sariaslani & G. M. Gadd (Eds.), *Advances in applied microbiology* (Vol. 88, pp. 31-56). Academic Press.

Krátký, M. (2024). Novel Sulfonamide Derivatives as a Tool to Combat Methicillin-Resistant *Staphylococcus Aureus*. *Future Medicinal Chemistry*, *16*(6), 545-562.

Kumar, R. R., Park, B. J., Jeong, H. R., Lee, J. T., & Cho, J. Y. (2013). Biodegradation of B-lactam antibiotic ampicillin by white rot fungi from aqueous solutions. *Journal of Pure and Applied Microbiology*, *7*(4), 3163-3169.

Kwon, J. H. (2017). 141 - Macrolides, Ketolides, Lincosamides and Streptogramins. In J. Cohen, W. G. Powderly, & S. M. Opal (Eds.), *Infectious Diseases (Fourth Edition)* (pp. 1217-1229.e1211). Elsevier.

Lahouar, A., Marin, S., Crespo-Sempere, A., Saïd, S., & Sanchis, V. (2016). Effects of temperature, water activity and incubation time on fungal growth and aflatoxin B1 production by toxinogenic *Aspergillus flavus* isolates on sorghum seeds. *Revista Argentina de Microbiología*, *48*(1), 78-85.

Lalchhandama, K. (2021). History of penicillin. *WikiJournal of Medicine*, *8*(1), 1-16.

Lawal, O. A., Aborisade, A. T., Akomolafe, O. M., & Lawal, O. T. (2025). Effective degradation of spent engine oil (SEO) by *Aspergillus tamarii* and *Aspergillus terreus* isolated from SEO-contaminated soil. *Chemistry and Ecology*, *41*(9), 1232-1250.

Leggett, J. E. (2017). 143 - Aminoglycosides. In J. Cohen, W. G. Powderly, & S. M. Opal (Eds.), *Infectious Diseases (Fourth Edition)* (pp. 1233-1238.e1231). Elsevier.

Lei, K., Zhu, Y., Chen, W., Pan, H.-Y., Cao, Y.-X., Zhang, X., Guo, B.-B., Sweetman, A., Lin, C.-Y., Ouyang, W., He, M.-C., & Liu, X.-T. (2019). Spatial and seasonal variations of antibiotics in river waters in the Haihe River Catchment in China and ecotoxicological risk assessment. *Environment International*, *130*, 104919.

Lewis, K. (2020). The science of antibiotic discovery. *Cell*, *181*(1), 29-45.

Li, C., Zhou, J., Du, G., Chen, J., Takahashi, S., & Liu, S. (2020). Developing *Aspergillus niger* as a cell factory for food enzyme production. *Biotechnology Advances*, *44*, 107630.

Li, W., Zhou, R., Zhou, R., Weerasinghe, J., Zhang, T., Gissibl, A., Cullen, P. J., Speight, R., & Ostrikov, K. (2022). Insights into amoxicillin degradation in water by non-thermal plasmas. *Chemosphere*, *291*, 132757.

Ligon, B. L. (2004). Penicillin: its discovery and early development. Seminars in pediatric infectious diseases,

Lima, L. M., Silva, B. N. M. d., Barbosa, G., & Barreiro, E. J. (2020). β-lactam antibiotics: An overview from a medicinal chemistry perspective. *European Journal of Medicinal Chemistry*, *208*, 112829.

Liu, H., Wang, L., Wei, S., Wu, Y., Zheng, Y., Yuan, F., & Hou, J. (2022). Study on photocatalytic degradation of amoxicillin in wastewater by Bi2WO6/nano-ZnO. *Optical Materials*, *123*, 111835.

Llarrull, L. I., Testero, S. A., Fisher, J. F., & Mobashery, S. (2010). The future of the β-lactams. *Current Opinion in Microbiology*, *13*(5), 551-557.

Lobritz, M. A., Andrews, I. W., Braff, D., Porter, C. B. M., Gutierrez, A., Furuta, Y., Cortes, L. B. G., Ferrante, T., Bening, S. C., Wong, F., Gruber, C., Bakerlee, C. W., Lambert, G., Walker, G. C., Dwyer, D. J., & Collins, J. J. (2022). Increased

energy demand from anabolic-catabolic processes drives β-lactam antibiotic lethality. *Cell Chemical Biology*, *29*(2), 276-286.e274.

Lueangjaroenkit, P., Teerapatsakul, C., Sakka, K., Sakka, M., Kimura, T., Kunitake, E., & Chitradon, L. (2019). Two Manganese Peroxidases and a Laccase of *Trametes polyzona* KU-RNW027 with Novel Properties for Dye and Pharmaceutical Product Degradation in Redox Mediator-Free System. *Mycobiology*, *47*(2), 217-229.

Lukacs, G., & Ohno, M. (2012). Recent progress in the chemical synthesis of antibiotics.

Ma, Y.-M., Liang, X.-A., Zhang, H.-C., & Liu, R. (2016). Cytotoxic and Antibiotic Cyclic Pentapeptide from an Endophytic *Aspergillus tamarii* of *Ficus carica*. *Journal of Agricultural and Food Chemistry*, *64*(19), 3789-3793.

Ma, Y., Ling, T.-j., Su, X.-q., Jiang, B., Nian, B., Chen, L.-j., Liu, M.-l., Zhang, Z.-y., Wang, D.-p., Mu, Y.-y., Jiao, W.-w., Liu, Q.-t., Pan, Y.-h., & Zhao, M. (2021). Integrated proteomics and metabolomics analysis of tea leaves fermented by *Aspergillus niger*, *Aspergillus tamarii* and *Aspergillus fumigatus*. *Food Chemistry*, *334*, 127560.

MacLean, R. C., & San Millan, A. (2019). The evolution of antibiotic resistance. *Science*, *365*(6458), 1082-1083.

Maiorano, A. E., da Silva, E. S., Perna, R. F., Ottoni, C. A., Piccoli, R. A. M., Fernandez, R. C., Maresma, B. G., & de Andrade Rodrigues, M. F. (2020). Effect of agitation speed and aeration rate on fructosyltransferase production of *Aspergillus oryzae* IPT-301 in stirred tank bioreactor. *Biotechnology Letters*, *42*(12), 2619-2629.

Mancuso, G., Midiri, A., Gerace, E., & Biondo, C. (2021). Bacterial antibiotic resistance: The most critical pathogens. *Pathogens*, *10*(10), 1310.

Markina-Iñarrairaegui, A., Spielvogel, A., Etxebeste, O., Ugalde, U., & Espeso, E. A. (2020). Tolerance to alkaline ambient pH in *Aspergillus nidulans* depends on the activity of ENA proteins. *Scientific reports*, *10*(1), 14325.

Mast, Y., & Wohlleben, W. (2014). *Streptogramins* – Two are better than one! *International Journal of Medical Microbiology*, *304*(1), 44-50.

Mat Jalil, M. T., Zakaria, N. A., Salikin, N. H., & Ibrahim, D. (2023). Assessment of cultivation parameters influencing pectinase production by *Aspergillus niger*

LFP-1 in submerged fermentation. *Journal of Genetic Engineering and Biotechnology*, *21*(1), 45.

Maumela, P., Rose, S., van Rensburg, E., Chimphango, A. F. A., & Görgens, J. F. (2021). Bioprocess optimisation for high cell density endoinulinase production from recombinant *Aspergillus niger*. *Applied biochemistry and biotechnology*, *193*(10), 3271-3286.

Meghwanshi, G. K., Kaur, N., Verma, S., Dabi, N. K., Vashishtha, A., Charan, P., Purohit, P., Bhandari, H., Bhojak, N., & Kumar, R. (2020). Enzymes for pharmaceutical and therapeutic applications. *Biotechnology and Applied Biochemistry*, *67*(4), 586-601.

Melnichuk, N., Braia, M. J., Anselmi, P. A., Meini, M.-R., & Romanini, D. (2020). Valorization of two agroindustrial wastes to produce alpha-amylase enzyme from *Aspergillus oryzae* by solid-state fermentation. *Waste Management*, *106*, 155-161.

Mir-Tutusaus, J. A., Baccar, R., Caminal, G., & Sarrà, M. (2018). Can white-rot fungi be a real wastewater treatment alternative for organic micropollutants removal? A review. *Water Research*, *138*, 137-151.

Miranti, A., Arbianti, R., & Utami, T. S. (2018). Effect of pH, temperature and medium agitation rate in production of AA, DHA, EPA from *Aspergillus oryzae* with submerged fermentation. IOP Conference Series: Earth and Environmental Science,

Mitra, S., & Murthy, G. S. (2022). Bioreactor control systems in the biopharmaceutical industry: a critical perspective. *Systems microbiology and biomanufacturing*, *2*(1), 91-112.

Mitrović, I. Ž., Grahovac, J. A., Dodić, J. M., Grahovac, M. S., Dodić, S. N., Vučurović, D. G., & Vlajkov, V. R. (2017). Effect of agitation rate on the production of antifungal metabolites by *Streptomyces hygroscopicus* in a lab-scale bioreactor. *Acta Periodica Technologica*(48), 231-244.

Mohamad, N. A., Zamri, M. Z., Saat, M. N., & Ariffin, Z. Z. (2024). Nitrofurazone biodegradation kinetics by batch fermentation of *Aspergillus tamarii*. *Asia-Pacific Journal of Molecular Biology and Biotechnology*, *32*, 98-109.

Mohammad, N., Safian, M., Ariffin, S., & Ariffin, Z. (2018). Biotransformation of nitrofurans antibiotics by *Aspergillus* species-residual antibacterial activity. *Malaysian Journal of Biochemistry & Molecular Biology*, *2*, 28-33.

Mohammadi, M., Gheibi, M., Fathollahi-Fard, A. M., Eftekhari, M., Kian, Z., & Tian, G. (2021). A hybrid computational intelligence approach for bioremediation of amoxicillin based on fungus activities from soil resources and aflatoxin B1 controls. *Journal of Environmental Management*, *299*, 113594.

Mohan, R., Subramanian, R., Muthiah, S., & Natarajan, S. (2019). Enhancement of α-amylase production in pelleted *Aspergillus tamarii* through optimization for desizing of cotton fabric. *Journal of Environmental Biology*, *40*(5), 1084-1093.

Mohr, K. I. (2016). History of antibiotics research. *How to overcome the antibiotic crisis: facts, challenges, technologies and future perspectives*, 237-272.

Monaghan, T. I., Baker, J. A., Robinson, G. K., & Shepherd, M. (2021). Parallel bioreactor system for accessible and reproducible anaerobic culture. *Access Microbiology*, *3*(4), 000225.

Monclaro, A. V., Petrović, D. M., Alves, G. S., Costa, M. M., Midorikawa, G. E., Miller, R. N., Filho, E. X., Eijsink, V. G., & Várnai, A. (2020). Characterization of two family AA9 LPMOs from *Aspergillus tamarii* with distinct activities on xyloglucan reveals structural differences linked to cleavage specificity. *PLoS One*, *15*(7), e0235642.

Mondal, S., & Malakar, S. (2020). Synthesis of sulfonamide and their synthetic and therapeutic applications: Recent advances. *Tetrahedron*, *76*(48), 131662.

Montgomery, D. C. (2017). *Design and analysis of experiments* (9 ed.). John wiley & sons.

Mu, Y., Kang, H., Song, X., Cao, C., Sun-Waterhouse, D., Waterhouse, G. I. N., Zhao, M., & Su, G. (2025). Soybean protein isolate hydrolysate addition during fermentation of soybean meal with *Aspergillus oryzae* enhances the release of umami components in subsequent hydrolysis process. *Food Bioscience*, *71*, 107105.

Mulinari, J., Ambrosi, A., Feng, Y., He, Z., Huang, X., Li, Q., Di Luccio, M., Hotza, D., & Oliveira, J. V. (2023). Polydopamine-assisted one-step immobilization of lipase on α-alumina membrane for fouling control in the treatment of oily wastewater. *Chemical Engineering Journal*, *459*, 141516.

Munir, M., Abdullah, R., Haq, I., Kaleem, A., Iqtedar, M., & Ashraf, S. (2020). Purification, characterization, kinetics and thermodynamic analysis of polygalacturonase from *Aspergillus tamarii* for industrial applications. *Revista Mexicana de Ingeniería Química*, *19*(Sup. 1), 293-304.

Murthy, G. S., Johnston, D. B., Rausch, K. D., Tumbleson, M., & Singh, V. (2012). Design and evaluation of an optimal controller for simultaneous saccharification and fermentation process. *Applied biochemistry and biotechnology*, *166*(1), 87-111.

Muthukumar Sathya, P., Mohan, H., Park, J.-H., Seralathan, K.-K., & Oh, B.-T. (2023). Applied potential assisted biodegradation of amoxicillin (AMX) using bacterial consortium isolated from a waste dump site. *Chemosphere*, *343*, 140230.

N. Politis, S., Colombo, P., Colombo, G., & M. Rekkas, D. (2017). Design of experiments (DoE) in pharmaceutical development. *Drug development and industrial pharmacy*, *43*(6), 889-901.

Najafpour, G. D. (2007). CHAPTER 6 - Bioreactor Design. In G. D. Najafpour (Ed.), *Biochemical Engineering and Biotechnology* (pp. 142-169). Elsevier.

Narayanan, C. M., & Narayan, V. (2019). Biological wastewater treatment and bioreactor design: a review. *Sustainable Environment Research*, *29*(1), 33.

Nguyen, L. N., Nghiem, L. D., & Oh, S. (2018). Aerobic biotransformation of the antibiotic ciprofloxacin by *Bradyrhizobium sp.* isolated from activated sludge. *Chemosphere*, *211*, 600-607.

Noormohamadi, H. R., Fat'hi, M. R., Ghaedi, M., & Ghezelbash, G. R. (2019). Potentiality of white-rot fungi in biosorption of nickel and cadmium: Modeling optimization and kinetics study. *Chemosphere*, *216*, 124-130.

Nuñez, S., Garelli, F., & De Battista, H. (2016). Product-based sliding mode observer for biomass and growth rate estimation in Luedeking–Piret like processes. *Chemical Engineering Research and Design*, *105*, 24-30.

Obotey Ezugbe, E., & Rathilal, S. (2020). Membrane technologies in wastewater treatment: a review. *Membranes*, *10*(5), 89.

Ong, G. H., Kee, W. K., Ahmed, R. D. A. H., Ying, J. K. n. Z., Rui, W. R., Er, L. K., & Tanee, T. (2024). Degradation of Polypropylene Using Fungal Enzyme As A Sustainable Approach To Management Plastic Waste. *Malaysian Applied Biology*, *53*(2), 93-100.

Oulebsir, A., Chaabane, T., Tounsi, H., Omine, K., Sivasankar, V., Flilissa, A., & Darchen, A. (2020). Treatment of artificial pharmaceutical wastewater containing amoxicillin by a sequential electrocoagulation with calcium salt followed by nanofiltration. *Journal of Environmental Chemical Engineering*, *8*(6), 104597.

Papich, M. G. (2013). Chapter 39 - Antimicrobial Drugs. In R. J. Washabau & M. J. Day (Eds.), *Canine and Feline Gastroenterology* (pp. 471-476). W.B. Saunders.

Papich, M. G. (2016). Amoxicillin. In M. G. Papich (Ed.), *Saunders Handbook of Veterinary Drugs (Fourth Edition)* (pp. 37-39). W.B. Saunders.

Park, S. R., Han, A. R., Ban, Y.-H., Yoo, Y. J., Kim, E. J., & Yoon, Y. J. (2010). Genetic engineering of macrolide biosynthesis: past advances, current state, and future prospects. *Applied microbiology and biotechnology*, *85*(5), 1227-1239.

Paul, R., Gerling, S., Berger, M., Blümlein, K., Jäckel, U., & Schuchardt, S. (2019). Occupational exposure to antibiotics in poultry feeding farms. *Annals of work exposures and health*, *63*(7), 821-827.

Peng, X., Cao, J., Xie, B., Duan, M., & Zhao, J. (2020). Evaluation of degradation behavior over tetracycline hydrochloride by microbial electrochemical technology: Performance, kinetics, and microbial communities. *Ecotoxicology and Environmental Safety*, *188*, 109869.

Pérez-Parada, A., Agüera, A., Gómez-Ramos, M. d. M., García-Reyes, J. F., Heinzen, H., & Fernández-Alba, A. R. (2011). Behavior of amoxicillin in wastewater and river water: identification of its main transformation products by liquid chromatography/electrospray quadrupole time-of-flight mass spectrometry. *Rapid Communications in Mass Spectrometry*, *25*(6), 731-742.

Petre, A., Ene, M., & Vamanu, E. (2021). Submerged Cultivation of *Inonotus obliquus* Mycelium Using Statistical Design of Experiments and Mathematical Modeling to Increase Biomass Yield. *Applied Sciences*, *11*(9), 4104.

Pichichero, M. E., & Zagursky, R. (2014). Penicillin and Cephalosporin allergy. *Annals of Allergy, Asthma & Immunology*, *112*(5), 404-412.

Pinto, A. P., Teixeira, D. M., Caldeira, A. T., & Rodrigues, S. C. (2020). Chapter 1 - Biodegradation of pesticides by adapted fungi. Potential use on biopurification systems? In M. N. V. Prasad (Ed.), *Agrochemicals Detection, Treatment and Remediation* (pp. 1-23). Butterworth-Heinemann.

Plonsky, L., & Ghanbar, H. (2018). Multiple regression in L2 research: A methodological synthesis and guide to interpreting R^2 values. *The Modern Language Journal*, *102*(4), 713-731.

Poznyak, T. I., Chairez Oria, I., & Poznyak, A. S. (2019). Chapter 11 - Biodegradation. In T. I. Poznyak, I. Chairez Oria, & A. S. Poznyak (Eds.), *Ozonation and Biodegradation in Environmental Engineering* (pp. 353-388). Elsevier.

Pratiwi, W., & Baihaqi, R. (2024). Ecotoxicity assessment of amoxicillin degradation product in aqueous media after photochemical process. IOP Conference Series: Earth and Environmental Science,

Praveena, S. M., Shaifuddin, S. N. M., Sukiman, S., Nasir, F. A. M., Hanafi, Z., Kamarudin, N., Ismail, T. H. T., & Aris, A. Z. (2018). Pharmaceuticals residues in selected tropical surface water bodies from Selangor (Malaysia): Occurrence and potential risk assessments. *Science of The Total Environment*, *642*, 230-240.

Premalatha, A., Vijayalakshmi, K., Shanmugavel, M., & Rajakumar, G. S. (2022). Optimization of culture conditions for enhanced production of extracellular α-amylase using solid state and submerged fermentation from *Aspergillus tamarii* MTCC5152. *Biotechnology and Applied Biochemistry*.

Purohit, T. J., Hanning, S. M., Amirapu, S., & Wu, Z. (2021). Rectal bioavailability of amoxicillin sodium in rabbits: Effects of suppository base and drug dose. *Journal of Controlled Release*, *338*, 858-869.

Purwanto, L., Ibrahim, D., & Sudrajat, H. (2009). Effect of agitation speed on morphological changes in *Aspergillus niger* hyphae during production of tannase. *World J Chem*, *4*(1), 34-38.

Pusztahelyi, T., Klement, É., Szajli, E., Klem, J., Miskei, M., Karányi, Z., Emri, T., Kovács, S., Orosz, G., Kovács, K. L., Medzihradszky, K. F., Prade, R. A., & Pócsi, I. (2011). Comparison of transcriptional and translational changes caused by long-term menadione exposure in *Aspergillus nidulans*. *Fungal Genetics and Biology*, *48*(2), 92-103.

Rahdar, S., & Ahmadi, S. (2019). The removal of amoxicillin with Zno nanoparticles in combination with US-H_2O_2 advanced oxidation processes from aqueous solutions. *Iranian Journal of Health Sciences*, *7*(1), 36-45.

Rajak, P., Ganguly, A., Dey, S., & Sen, K. (2025). Antibiotics in wastewater: Exploring the sources, links to antibiotic resistance, and strategies for their removal. *Cleaner Water*, *4*, 100110.

Rajaura, S., Chauhan, P., Chandra, H., & Bhardwaj, N. (2023). Aflatoxin B1 administration induces reactive oxygen species production and apoptosis of erythrocytes in mice. *Toxicon*, *221*, 106963.

Razali, S. A., Rasit, N., & Ooi, C. K. (2021). Statistical analysis of xylanase production from solid state fermentation of rice husk associated fungus *Aspergillus niger*. *Materials Today: Proceedings*, *39*, 1082-1087.

Robinson, P. K. (2015). Enzymes: principles and biotechnological applications. *Essays Biochem*, *59*, 1-41.

Robledo, A., Aguilera-Carbo, A. F., Prado-Barragan, A., Sepulveda-Torre, L., Rodríguez-Herrera, R., Contreras-Esquivel, J. C., & Aguilar, C. N. (2018). Kinetics of ellagic acid accumulation by solid-state fermentation. *Theoretical Models and Experimental Approaches in Physical Chemistry. Apple Academic Press, pp293-306*.

Robles-Morales, D., Reyes Cervantes, A., Díaz-Godínez, R., Tovar-Jiménez, X., Medina-Moreno, S., & Jiménez-González, A. (2021). Design and performance evaluation of a fungi-bacteria consortium to biodegrade organic matter at high concentration on synthetic slaughterhouse wastewater. *Water, Air, & Soil Pollution*, *232*(6), 223.

Rodriguez-Herrera, R., Puc, L. E. C., Sobrevilla, J. M. V., Luque, D., Cardona-Felix, C. S., Aguilar-González, C. N., & Flores-Gallegos, A. C. (2019). Chapter 36 - Enzymes in the Pharmaceutical Industry for β-Lactam Antibiotic Production. In M. Kuddus (Ed.), *Enzymes in Food Biotechnology* (pp. 627-643). Academic Press.

Roy, J. (2011). 10 - The top five most common or long-selling drugs. In J. Roy (Ed.), *An Introduction to Pharmaceutical Sciences* (pp. 231-296). Woodhead Publishing.

Saat, M. N., & Annuar, M. S. M. (2020). Statistical analysis of one-pot lipase-catalyzed esterification of ϵ-caprolactone with methyl-d-glucopyranoside and its extension. *Biocatalysis and Agricultural Biotechnology*, *23*, 101464.

Saat, M. N., Annuar, M. S. M., Alias, Z., Chuan, L. T., & Chisti, Y. (2014). Modeling of growth and laccase production by *Pycnoporus sanguineus*. *Bioprocess and Biosystems Engineering*, *37*, 765-775.

Salvo, F., De Sarro, A., Caputi, A. P., & Polimeni, G. (2009). Amoxicillin and amoxicillin plus clavulanate: a safety review. *Expert opinion on drug safety*, *8*(1), 111-118.

Sarahroodi, S., & Mikaili, P. (2012). Self-medication with antibiotics: a global challenge of our generation. *Pakistan journal of biological sciences: PJBS*, *15*(14), 707-708.

Saravanan, A., Jayasree, R., Kumar, P. S., Varjani, S., Hemavathy, R. V., Jeevanantham, S., & Yaashikaa, P. R. (2020). Production of pigment using

Aspergillus tamarii: New potentials for synthesizing natural metabolites. *Environmental Technology & Innovation*, *19*, 100967.

Sathya, P. M., Mohan, H., Park, J.-H., Seralathan, K.-K., & Oh, B.-T. (2023). Applied potential assisted biodegradation of amoxicillin (AMX) using bacterial consortium isolated from a waste dump site. *Chemosphere*, *343*, 140230.

Segura, Y., Martínez, F., & Melero, J. A. (2013). Effective pharmaceutical wastewater degradation by Fenton oxidation with zero-valent iron. *Applied Catalysis B: Environmental*, *136*, 64-69.

Seifollahi, Z., Abbasi, A., & Rahbar-Kelishami, A. (2019). Application of solvent extraction for the removal of amoxicillin drug residues in environmental waters. *Iranian Journal of Pharmaceutical Sciences*, *15*(4), 41-52.

Seiple, I. B., Zhang, Z., Jakubec, P., Langlois-Mercier, A., Wright, P. M., Hog, D. T., Yabu, K., Allu, S. R., Fukuzaki, T., & Carlsen, P. N. (2016). A platform for the discovery of new macrolide antibiotics. *Nature*, *533*(7603), 338-345.

Sezhian, U., & Bose, P. (2019). Optimization of Culture Conditions for Growth and Production of Bioactive Metabolites by Endophytic Fungus -*Aspergillus tamarii*. 469-478.

Shabbir, M. S., Siddiqi, A. F., Kassim, N. M., Mustafa, F., & Abbas, M. (2019). Analysis of exprimental designs with outliers. *Amazonia Investiga*, *8*(18), 53-68.

Shahtalebi, A., Sarrafzadeh, M., & MONTAZER, R. M. (2011). Application of nanofiltration membrane in the separation of amoxicillin from pharmaceutical wastewater.

Shanmugam, B. K., Vardhan, H., Raj, M. G., Kaza, M., Sah, R., & Hanumanthappa, H. (2022). Application of fractional factorial design for evaluating the separation performance of the screening machine. *International Journal of Coal Preparation and Utilization*, *42*(11), 3369-3379.

Shanmugavel, M., Vasantharaj, S., Yazhmozhi, A., Bhavsar, P., Aswin, P., Felshia, C., Mani, U., Ranganathan, B., & Gnanamani, A. (2018). A study on pectinases from *Aspergillus tamarii*: Toward greener approach for cotton bioscouring and phytopigments processing. *Biocatalysis and Agricultural Biotechnology*, *15*, 295-303.

Sharma, S., Kumar, K., & Chauhan, S. (2021). Role of electrolyte-drug interactions in solution behavior of antibiotic drug streptomycin sulphate: Density, speed of sound and viscosity studies. *Chemical Data Collections*, *34*, 100745.

Shaw, S. P. (2015). Chapter 176 - β-Lactam Antimicrobials. In D. C. Silverstein & K. Hopper (Eds.), *Small Animal Critical Care Medicine (Second Edition)* (pp. 928-929). W.B. Saunders.

Shi, J., Chinn, M. S., & Sharma-Shivappa, R. R. (2014). Interactions between fungal growth, substrate utilization, and enzyme production during solid substrate cultivation of *Phanerochaete chrysosporium* on cotton stalks. *Bioprocess and Biosystems Engineering*, *37*, 2463-2473.

Shi, X., Wu, D., Xu, Y., & Yu, X. (2022). Engineering the optimum pH of β-galactosidase from *Aspergillus oryzae* for efficient hydrolysis of lactose. *Journal of Dairy Science*, *105*(6), 4772-4782.

Shokrkar, H., Ebrahimi, S., & Zamani, M. (2018). A review of bioreactor technology used for enzymatic hydrolysis of cellulosic materials. *Cellulose*, *25*, 6279-6304.

Shu, L., Yang, M., Zhao, H., Li, T., Yang, L., Zou, X., & Li, Y. (2019). Process optimization in a stirred tank bioreactor based on CFD-Taguchi method: A case study. *Journal of Cleaner Production*, *230*, 1074-1084.

Siddiquee, S. (2018). Chapter 4 - Recent Advancements on the Role of Biologically Active Secondary Metabolites from *Aspergillus*. In V. K. Gupta & S. Rodriguez-Couto (Eds.), *New and Future Developments in Microbial Biotechnology and Bioengineering* (pp. 69-94). Elsevier.

Singh, R. K., Tripathi, R., Ranjan, A., & Srivastava, A. K. (2020). Chapter 9 - Fungi as potential candidates for bioremediation. In P. Singh, A. Kumar, & A. Borthakur (Eds.), *Abatement of Environmental Pollutants* (pp. 177-191). Elsevier.

Singh, R. S., Chauhan, K., Kaur, K., & Pandey, A. (2020). Statistical optimization of solid-state fermentation for the production of fungal inulinase from apple pomace. *Bioresource Technology Reports*, *9*, 100364.

Singh, Y., & Srivastava, S. (2014). Performance improvement of *Bacillus aryabhattai* ITBHU02 for high-throughput production of a tumor-inhibitory L-asparaginase using a kinetic model based approach. *Journal of Chemical Technology & Biotechnology*, *89*(1), 117-127.

Sodhi, K. K., Kumar, M., & Singh, D. K. (2021). Insight into the amoxicillin resistance, ecotoxicity, and remediation strategies. *Journal of Water Process Engineering*, *39*, 101858.

Sony, M., & Marriapan, V. (2021). A Methodological Approach to Assessment and Reporting of the Model Adequacy in Simulation Studies. *International Journal of Operations Research and Information Systems (IJORIS)*, *12*(4), 1-17.

Souza, F. S., da Silva, V. V., Rosin, C. K., Hainzenreder, L., Arenzon, A., & Féris, L. A. (2018). Comparison of different advanced oxidation processes for the removal of amoxicillin in aqueous solution. *Environmental technology*, *39*(5), 549-557.

Spížek, J., & Řezanka, T. (2017). Lincosamides: Chemical structure, biosynthesis, mechanism of action, resistance, and applications. *Biochem Pharmacol*, *133*, 20-28.

Stevenson, A., Hamill, P. G., Dijksterhuis, J., & Hallsworth, J. E. (2017). Water-, pH- and temperature relations of germination for the extreme xerophiles *Xeromyces bisporus* (FRR 0025), *Aspergillus penicillioides* (JH 06 THJ) and *Eurotium halophilicum* (FRR 2471). *Microbial biotechnology*, *10*(2), 330-340.

Sukmana, H., Bellahsen, N., Pantoja, F., & Hodur, C. (2021). Adsorption and coagulation in wastewater treatment–Review. *Progress in Agricultural Engineering Sciences*, *17*(1), 49-68.

Supramani, S., Rejab, N. A., Ilham, Z., Ahmad, R., Show, P.-L., Ibrahim, M. F., & Wan-Mohtar, W. A. A. Q. I. (2023). Performance of Biomass and Exopolysaccharide Production from the Medicinal Mushroom *Ganoderma lucidum* in a New Fabricated Air-L-Shaped Bioreactor (ALSB). *Processes*, *11*(3), 670.

Svobodová, K., & Novotný, Č. (2018). Bioreactors based on immobilized fungi: bioremediation under non-sterile conditions. *Applied microbiology and biotechnology*, *102*, 39-46.

Tchobanoglus, G., Burton, F., & Stensel, H. D. (2003). Wastewater engineering: treatment and reuse. *American Water Works Association. Journal*, *95*(5), 201.

Teh, C. Y., Budiman, P. M., Shak, K. P. Y., & Wu, T. Y. (2016). Recent advancement of coagulation–flocculation and its application in wastewater treatment. *Industrial & Engineering Chemistry Research*, *55*(16), 4363-4389.

Thakare, R., Kesharwani, P., Dasgupta, A., Srinivas, N., & Chopra, S. (2020). Chapter 1 - Antibiotics: past, present, and future. In P. Kesharwani, S. Chopra, & A. Dasgupta (Eds.), *Drug Discovery Targeting Drug-Resistant Bacteria* (pp. 1-8). Academic Press.

Tran, T. T., Nguyen, A. T., Quach, D. T., Pham, D. T.-H., Cao, N. M., Nguyen, U. T.-H., Dang, A. N.-T., Tran, M. A., Quach, L. H., & Tran, K. T. (2022). Emergence of amoxicillin resistance and identification of novel mutations of the pbp1A gene in *Helicobacter pylori* in Vietnam. *BMC microbiology*, *22*(1), 41.

Urban-Chmiel, R., Marek, A., Stępień-Pyśniak, D., Wieczorek, K., Dec, M., Nowaczek, A., & Osek, J. (2022). Antibiotic resistance in bacteria—A review. *Antibiotics*, *11*(8), 1079.

Van Boeckel, T. P., Brower, C., Gilbert, M., Grenfell, B. T., Levin, S. A., Robinson, T. P., Teillant, A., & Laxminarayan, R. (2015). Global trends in antimicrobial use in food animals. *Proceedings of the National Academy of Sciences*, *112*(18), 5649-5654.

van Kuijk, S. J., Sonnenberg, A. S., Baars, J. J., Hendriks, W. H., & Cone, J. W. (2016). The effect of particle size and amount of inoculum on fungal treatment of wheat straw and wood chips. *Journal of Animal Science and Biotechnology*, *7*, 1-9.

Vardanyan, R., & Hruby, V. (2016). Chapter 30 - Antibiotics. In R. Vardanyan & V. Hruby (Eds.), *Synthesis of Best-Seller Drugs* (pp. 573-643). Academic Press.

Verma, M., & Haritash, A. K. (2020). Photocatalytic degradation of Amoxicillin in pharmaceutical wastewater: A potential tool to manage residual antibiotics. *Environmental Technology & Innovation*, *20*, 101072.

Volk, T. J. (2013). Fungi. In S. A. Levin (Ed.), *Encyclopedia of Biodiversity (Second Edition)* (pp. 624-640). Academic Press.

Vulić, A., Lešić, T., Kudumija, N., Zadravec, M., Kiš, M., Vahčić, N., & Pleadin, J. (2021). The development of LC-MS/MS method of determination of cyclopiazonic acid in dry-fermented meat products. *Food Control*, *123*, 107814.

Wahyuni, E. T., Cahyono, R. N., Nora, M., Alharissa, E. Z., & Kunarti, E. S. (2024). Degradation of amoxicillin residue under visible light over TiO2 doped with Cr prepared from tannery wastewater. *Results in Chemistry*, *7*, 101302.

Wakai, S., Arazoe, T., Ogino, C., & Kondo, A. (2017). Future insights in fungal metabolic engineering. *Bioresource technology*, *245*, 1314-1326.

Walker, G. M., & White, N. A. (2017). Introduction to fungal physiology. *Fungi: biology and applications*, 1-35.

Wang, H., Yang, J., Yu, X., Zhao, G., Zhao, Q., Wang, N., Jiang, Y., Jiang, F., He, G., & Chen, Y. (2018). Exposure of adults to antibiotics in a Shanghai suburban area and health risk assessment: A biomonitoring-based study. *Environmental science & technology*, *52*(23), 13942-13950.

Wang, J., Hui, X., Liu, H., & Dai, X. (2024). Classification, characteristics, harmless treatment and safety assessment of antibiotic pharmaceutical wastewater (APWW): A comprehensive review. *Chemosphere*, *366*, 143504.

Wang, J., & Zhuan, R. (2020). Degradation of antibiotics by advanced oxidation processes: An overview. *Science of The Total Environment*, *701*, 135023.

Wang, S., Yuan, R., Chen, H., Wang, F., & Zhou, B. (2021). Anaerobic biodegradation of four sulfanilamide antibiotics: Kinetics, pathways and microbiological studies. *Journal of Hazardous Materials*, *416*, 125840.

Wang, Y., Chen, C., Zhou, D., Xiong, H., Zhou, Y., Dong, S., & Rittmann, B. E. (2019). Eliminating partial-transformation products and mitigating residual toxicity of amoxicillin through intimately coupled photocatalysis and biodegradation. *Chemosphere*, *237*, 124491.

Wang, Y., Yan, H., Neng, J., Gao, J., Yang, B., & Liu, Y. (2020). The Influence of NaCl and Glucose content on Growth and Ochratoxin A production by *Aspergillus ochraceus, Aspergillus carbonarius* and *Penicillium nordicum*. *Toxins*, *12*(8), 515.

Watkins, R. R., & Bonomo, R. A. (2017). 140 - β-Lactam Antibiotics. In J. Cohen, W. G. Powderly, & S. M. Opal (Eds.), *Infectious Diseases (Fourth Edition)* (pp. 1203-1216.e1202). Elsevier.

Weber, D. J., Tolkoff-Rubin, N. E., & Rubin, R. H. (1984). Amoxicillin and potassium clavulanate: an antibiotic combination. Mechanism of action, pharmacokinetics, antimicrobial spectrum, clinical efficacy and adverse effects. *Pharmacotherapy*, *4*(3), 122-136.

Wencewicz, T. A. (2019). Crossroads of Antibiotic Resistance and Biosynthesis. *Journal of Molecular Biology*, *431*(18), 3370-3399.

Wilke, M. S., Lovering, A. L., & Strynadka, N. C. J. (2005). β-Lactam antibiotic resistance: a current structural perspective. *Current Opinion in Microbiology*, *8*(5), 525-533.

Wu, S., Yu, X., Hu, Z., Zhang, L., & Chen, J. (2009). Optimizing aerobic biodegradation of dichloromethane using response surface methodology. *Journal of Environmental Sciences*, *21*(9), 1276-1283.

Xiang, W.-S., Wang, J.-D., Wang, X.-J., & Zhang, J. (2009). A novel macrolide compound from *Streptomyces bingchenggensis*: fermentation, isolation, structure elucidation and biological properties. *The Journal of Antibiotics*, *62*(4), 229-231.

Xiao, B., Lian, B., Sun, L., & Shao, W. (2012). Gene transcription response to weathering of K-bearing minerals by *Aspergillus fumigatus*. *Chemical Geology*, *306-307*, 1-9.

Xie, Y., Zhou, H., Liu, C., Zhang, J., Li, N., Zhao, Z., Sun, G., & Zhong, Y. (2017). A molasses habitat-derived fungus *Aspergillus tubingensis* XG21 with high β-fructofuranosidase activity and its potential use for fructooligosaccharides production. *AMB Express*, *7*, 1-9.

Xu, B., Mao, D., Luo, Y., & Xu, L. (2011). Sulfamethoxazole biodegradation and biotransformation in the water–sediment system of a natural river. *Bioresource technology*, *102*(14), 7069-7076.

Yakobi, S. H., & Nwodo, U. U. (2025). AI-driven modelling, antimicrobial discovery, and precision therapeutics for targeting bacterial persisters. *In Silico Research in Biomedicine*, *1*, 100062.

Yang, C.-W., Hsiao, W.-C., & Chang, B.-V. (2016). Biodegradation of sulfonamide antibiotics in sludge. *Chemosphere*, *150*, 559-565.

Yang, C.-W., Liu, C., & Chang, B.-V. (2020). Biodegradation of amoxicillin, tetracyclines and sulfonamides in wastewater sludge. *Water*, *12*(8), 2147.

Yang, S.-F., Lin, C.-F., Wu, C.-J., Ng, K.-K., Yu-Chen Lin, A., & Andy Hong, P.-K. (2012). Fate of sulfonamide antibiotics in contact with activated sludge – Sorption and biodegradation. *Water Research*, *46*(4), 1301-1308.

Yip, D. W., & Gerriets, V. (2020). Penicillin.

Yolmeh, M., & Jafari, S. M. (2017). Applications of response surface methodology in the food industry processes. *Food and Bioprocess Technology*, *10*(3), 413-433.

Yu, P., Low, M. Y., & Zhou, W. (2018). Design of experiments and regression modelling in food flavour and sensory analysis: A review. *Trends in Food Science & Technology*, *71*, 202-215.

Zain ul Arifeen, M., Ma, Y., Wu, T., Chu, C., Liu, X., Jiang, J., Li, D., Xue, Y.-R., & Liu, C.-H. (2022). Anaerobic biodegradation of polycyclic aromatic hydrocarbons (PAHs) by fungi isolated from anaerobic coal-associated sediments at 2.5 km below the seafloor. *Chemosphere*, *303*, 135062.

Zaragoza, O. (2017). Mycology. In *Reference Module in Life Sciences*. Elsevier.

Zhang, C., Zeng, J., Xiong, W., & Zeng, Z. (2020). Rapid determination of amoxicillin in porcine tissues by UPLC-MS/MS with internal standard. *Journal of Food Composition and Analysis*, *92*, 103578.

Zhang, H., Guan, W., Zhang, L., Guan, X., & Wang, S. (2020). Degradation of an Organic Dye by Bisulfite Catalytically Activated with Iron Manganese Oxides: The Role of Superoxide Radicals. *ACS Omega*, *5*(29), 18007-18012.

Zhang, J., Fan, P.-H., Lin, G.-M., Chang, W.-C., & Liu, H.-w. (2020). 2.14 - Recent Progress in Unusual Carbohydrate-Containing Natural Products Biosynthesis. In H.-W. Liu & T. P. Begley (Eds.), *Comprehensive Natural Products III* (pp. 336-392). Elsevier.

Zhong, J.-J. (2010). Recent advances in bioreactor engineering. *Korean Journal of Chemical Engineering*, *27*, 1035-1041.

Zhou, L.-J., Ying, G.-G., Liu, S., Zhang, R.-Q., Lai, H.-J., Chen, Z.-F., & Pan, C.-G. (2013). Excretion masses and environmental occurrence of antibiotics in typical swine and dairy cattle farms in China. *Science of The Total Environment*, *444*, 183-195.

APPENDICES

APPENDICES

APPENDIX 1

One-Way ANOVA for Fungal Growth Biomass With and Without the Presence of AMX Across 240 Hrs

Descriptive Statistics

Parameter	Without AMX	With AMX
Sample size (n)	11	11
Mean biomass	6.08	5.67
Variance	6.56	5.41

One-way ANOVA Summary

Source of Variation	Sum of Squares (SS)	Degrees of Freedom (df)	Mean Square (MS)	F-value	p-value
Between groups	2.22	1	2.22	0.154	0.699
Within groups	289.40	20	14.47	—	—
Total	291.62	21	—	—	—

Note: One-way ANOVA revealed no statistically significant difference in fungal biomass between fermentations with and without AMX ($p > 0.05$), indicating that the presence of AMX did not inhibit fungal growth under the experimental conditions.

APPENDIX 2

One-Way ANOVA for Fungal Glucose Utilization With and Without the Presence of AMX Across 240 Hrs

Descriptive Statistics

Parameter	Without AMX	With AMX
Sample size (n)	11	11
Mean biomass	5.395	5.252
Variance	46.53	47.87

One-way ANOVA Summary

Source of Variation	Sum of Squares (SS)	Degrees of Freedom (df)	Mean Square (MS)	F-value	p-value
Between groups	0.112	1	0.112	0.0024	0.96
Within groups	931.99	20	46.60	—	—
Total	932.10	21	—	—	—

Note: No statistically significant difference in glucose utilization was observed between fermentations with and without AMX ($p > 0.05$). The low coefficient of determination ($R^2 \approx 0.00012$) indicates that the presence of AMX contributed negligibly to the overall variability in glucose utilization

APPENDIX 3

One-Way ANOVA for Fungal Protein Production With and Without the Presence of AMX Across 240 Hrs

Descriptive Statistics

Parameter	Without AMX	With AMX
Sample size (n)	11	11
Mean protein concentration	0.00794	0.00926
Variance	0.00002	0.00002

One-way ANOVA Summary

Source of Variation	Sum of Squares (SS)	Degrees of Freedom (df)	Mean Square (MS)	F-value	p-value
Between groups	0.00001	1	0.00001	0.63	0.44
Within groups	0.00032	20	0.00002	—	—
Total	0.00033	21	—	—	—

Note: One-way ANOVA indicated no statistically significant difference in fungal protein production between fermentations conducted with and without AMX ($p > 0.05$). The results suggest that the presence of AMX did not adversely affect protein secretion under the experimental conditions.

AUTHOR'S PROFILE

Muhammad Zafri bin Zamri completed his MSc in Molecular Biology at the Faculty of Applied Sciences, Universiti Teknologi MARA. He received his bachelor's degree in Biomolecular Science at the Faculty of Applied Sciences, Universiti Teknologi MARA. His academic research primarily focused on bioremediation of antibiotic using fungus and its applications in healthcare and wastewater treatment industries. This reflected a deep interest in the practical applications of molecular science. Currently, he serves as a Sales Specialist within the scientific and laboratory industry, where he leverages his technical background to support advancements in research and diagnostics.

LIST OF PUBLICATIONS

Zamri, M. Z., Saat, M. N., Kamil, M. A. M., & Ariffin, Z. Z. (2025). Kinetic Studies in Shake Flask and Impact of Impeller Speed on Amoxicillin Biodegradation by *Aspergillus tamarii*. Jordan Journal of Biological Sciences, 18(3). https://doi.org/10.54319/jjbs/180309

Zamri, M. Z., Saat, M. N., Kamil, M. A. M., & Ariffin, Z. Z. (2025). Screening of factors influencing amoxicillin biodegradation by *Aspergillus tamarii* using fractional factorial design. Journal of Applied Pharmaceutical Science, 15(5), 232-241. http://doi.org/10.7324/JAPS.2025.192932